

i  
UNIVERSITY OF NAIROBI  
LIBRARY  
P. O. Box 30197  
NAIROBI

✓ The Foetal Membranes, Placenta and the gonadogenital organs of the female root-rat *Tachyoryctes splendens* (Ruppell): A morphological and morphometric study. 1)

By

NORBERT MAKORI, B.V.M. (NBI)  
Department of Veterinary Anatomy  
University of Nairobi.

A thesis submitted in part fulfillment for the degree of Master of Science (Veterinary Anatomy) in the University of Nairobi.

1992

DECLARATION

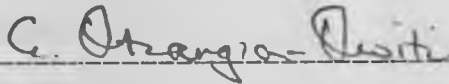
This thesis is my original work and has not been presented for a degree in any other University



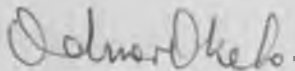
NORBERT MAKORI

Department of Veterinary Anatomy  
University of Nairobi, Kenya.

This thesis has been submitted for examination with our approval as University supervisors.



G.E. OTIANGA-OWITI, BVM, MSc, Ph.D.  
Senior Lecturer, Dept. of Vet. Anatomy.



D. ODUOR-OKELO, BVSc, DVM, MSc, Ph.D  
Professor of Veterinary Anatomy,  
Dept. of Vet. Anatomy.



C.N. WARUI, BVM, Ph.D  
Senior Lecturer, Dept. of Vet. Anatomy.

## TABLE OF CONTENTS

	PAGE
TITLE .....	(i)
DECLARATION.....	(ii)
TABLE OF CONTENTS.....	(iii)
LIST OF SYMBOLS.....	(vii)
SUMMARY.....	(viii)
ACKNOWLEDGEMENTS.....	(x)
MATERIALS PUBLISHED.....	(xi)
CHAPTER 1.....	1
1.0 GENERAL INTRODUCTION AND	
LITERATURE REVIEW.....	1
1.1. GENERAL INTRODUCTION.....	1
1.2. TAXONOMY.....	3
1.3. THE REPRODUCTIVE BIOLOGY.....	4
1.3.1. THE REPRODUCTIVE ORGANS.....	4
1.3.2. OVULATION AND BREEDING PATTERN.....	4
1.3.3. IMPLANTATION, THE FOETAL MEMBRANES	
AND PLACENTA.....	6
1.4. MORPHOMETRY OF THE PLACENTA.....	8
1.5. OBJECTIVES.....	10
CHAPTER 2.....	12
2.0. MATERIALS AND METHODS.....	12
2.1. BIOLOGICAL MATERIALS AND METHODS.....	12
2.1.1. TISSUE FIXATION.....	13
2.1.1.1. FIXATION BY IMMERSION.....	13

2.1.1.2. FIXATION BY PERFUSION.....	13
2.1.1.3. TISSUE SAMPLING AND PROCESSING FOR MORPHOLOGICAL STUDIES.....	14
2.2. QUANTITATIVE MATERIALS AND METHODS.....	15
2.2.1. STRUCTURAL BASIS OF MORPHOMETRY OF THE PLACENTA.....	15
2.2.2. TISSUE SAMPLING AND PROCESSING FOR MORPHOMETRY.....	16
2.2.3. STEREOLOGICAL ANALYSIS.....	17
2.2.3.1. ANALYSIS AT THE FIRST LEVEL OF SAMPLING.....	17
2.2.3.2. ANALYSIS AT THE SECOND LEVEL OF SAMPLING.....	18
2.2.3.3. THE PLACENTA OXYGEN DIFFUSING CAPACITY.....	20
2.2.4. MEASUREMENT OF TISSUE SHRINKAGE.....	20
2.2.5. DATA HANDLING.....	21
2.3. STEREOLOGICAL METHODS.....	21
2.3.1. POINT COUNTING MORPHOMETRY AS AN ESTIMATOR FOR VOLUME DENSITY.....	21
2.3.2. INTERSECTION COUNTING MORPHOMETRY AS AN ESTIMATOR FOR SURFACE DENSITY.....	23
2.3.3. INTERCEPT LENGTH AS AN ESTIMATOR FOR HARMONIC MEAN THICKNESS.....	23
2.3.4. STEREOLOGICAL ESTIMATION OF THE OXYGEN DIFFUSING CAPACITY.....	24
2.3.5. PHYSICOCHEMICAL QUANTITY ESTIMATION.....	26
CHAPTER 3.....	27
3.0. RESULTS.....	27
3.1. GENERAL REMARKS.....	27

3.2. MICROSCOPIC OBSERVATIONS.....	28
3.2.1. THE OVARY IN THE NON-GRAVID ROOT-RAT.....	28
3.2.2. THE OVARY OF PREGNANT ROOT-RATS.....	29
3.2.3. THE PREGNANT UTERUS.....	30
3.2.4. IMPLANTATION.....	31
3.2.5. EXPANSION STAGE.....	32
3.2.6. DEVELOPMENT OF THE PLACENTA.....	33
3.2.7. THE DEFINITIVE PLACENTA.....	34
3.2.7.1. ULTRASTRUCTURE OF THE PLACENTA.....	36
3.2.8. THE DECIDUA.....	38
3.2.9. THE FOETO-MATERNAL CIRCULATION WITHIN THE LABYRINTH.....	39
3.3. THE YOLK SAC, AMNION, AND ALLANTOIS.....	40
3.4. THE HAEMOPHAGOUS-LIKE ORGAN.....	41
3.5. QUANTITATIVE OBSERVATIONS.....	42
3.5.1. THE MATERNAL AND FOETAL BODY WEIGHTS AND THE VOLUME OF THE PLACENTA.....	42
3.5.2. STEREOLOGICAL PARAMETERS OF THE PLACENTA.....	42
CHAPTER 4.....	45
4.0. DISCUSSION AND PHYLOGENETIC CLASSIFICATION.....	45
4.1. THE OVARY.....	45
4.2. OVULATION AND BREEDING PATTERN.....	47
4.3 IMPLANTATION.....	49
4.4. THE AMNION.....	52
4.5. THE ALLANTOIS.....	53
4.6. THE YOLK SAC AND REICHERT'S MEMBRANE.....	53
4.7. THE PLACENTA MORPHOLOGY.....	55

4.8. THE DECIDUA.....59

4.9. THE HAEMOPHAGOUS ORGAN.....61

4.10. MORPHOMETRY OF THE PLACENTA.....63

4.11. PHYLOGENETIC CLASSIFICATION.....66

APPENDIX 1.....70

BIBLIOGRAPHY.....73

## SYMBOLS USED IN MORPHOMETRY

$A_a$ :	Areal density
$I_a$ :	number of intersection points
$L_c$ :	length of test system
$M$ :	final microscopic magnification
$n$ :	number of profiles or quantities
$P_a$ :	number of points falling on a profile of a particular test component
$P_t$ :	total number of points on the test system
$P_p$ :	point density
$S_a$ :	surface area
$S_{va}$ :	surface density
$V_a$ :	absolute volume of a component
$V_v$ :	Volume density
$I/L$ :	reciprocals of the intercepts
$\tau_h$ :	Harmonic mean thickness
$K$ :	Krogh's diffusion coefficient

## SUMMARY

The foetal membranes, placenta and some of the gonadogenital organs of the root-rat (*Tachyoryctes splendens*) were fixed and examined by routine histological and ultrastructural methods. Specimens of the late term placenta were fixed and used for a morphometric analysis. The root-rat ovulates more than one egg and this usually occurs from both ovaries. There is apparently a high incidence of foetal resorption in these rodents leading mostly to a single embryo growing to full term. Twinning does occur occasionally in these rodents. Implantation of the blastocyst is antimesometrial and the embryonic disc is mesometrially oriented. The mode of implantation is eccentric and secondarily interstitial. Like in most other rodents there is a primary decidual reaction involving the uterine stroma at the site of implantation. Amniogenesis is by cavitation with a temporary open epamniotic cavity. Inversion of the yolk sac is complete but the disappearance of the parietal segment occurs relatively late. With the complete breakdown of both the capsular and parietal deciduas, the yolk sac wall at the margins of the placenta becomes bathed in a pool of maternal blood and tissue debris resembling the haemophagous organ. The yolk sac villi bordering the placental disc are well vascularized. The allantoic vesicle is persistent up to the limb bud stage.

The definitive chorioallantoic placenta is haemochorial with the interhaemal membrane showing a distinct arrangement of three layers of trophoblast between the maternal blood spaces and the foetal capillary endothelium (haemotrichorial). The outer layer of trophoblast enclosing the maternal blood space is cellular while the next two layers are syncytial. The outer layer of trophoblast is rich in granular endoplasmic reticulum whereas this organelle is less abundant in subsequent layers. The placenta shows conspicuous endodermal sinuses or placental pits (of Duval).

Using a morphometric model of oxygen diffusion it was demonstrated that the overall weight specific diffusing capacity of the root-rat late-term placenta ( $4.73 \text{ cm}^3 \text{ min}^{-1} \text{ mmHg}^{-1} \text{ kg}^{-1}$ ) is two and half times that of man ( $1.86 \text{ cm}^3 \text{ min}^{-1} \text{ mmHg}^{-1} \text{ kg}^{-1}$ ). The root-rat also shows a marked irregularity and compensatory thinning of the interhaemal membrane leading to a low harmonic mean thickness. It is suggested that the low harmonic mean thickness and the high oxygen diffusing capacity may probably be a structural and functional adaptation of the root-rat placenta to the hypoxic-hypercarbic conditions occurring in the burrows where these rodents live.

Even though the root-rat shares a few foetal membrane development features with the *Geomys*, most of the morphological and developmental characteristics of the foetal membranes and placenta of the root-rat suggest that this rodent is closely related to the myomorphs

The observations made in this study suggest that the root-rat should be placed in its own minor family (Tachyoryctoidae) in the

## ACKNOWLEDGEMENTS

I am grateful for the financial support given by the Deans' Committee of the University of Nairobi (Grant No. 500-655-190) without which this work would not have been accomplished.

I wish to express my sincere appreciation to Dr. G.E. Otianga-Owiti, Prof. Oduor-Okelo, and Dr. C.N Warui for their advice and supervision during the period of this study.

I also wish to thank those who provided the necessary technical assistance in histology, electron microscopy, and photography, Messrs. J. Mavulu, J.M. Gachoka, P.K. Kiguru, and S Ochieng of the Department of Vet. Anatomy; M.M. Chintawi of the International Centre of Insect Physiology and Ecology; J.M. Musyoka for trapping the root-rats.

My appreciation to the entire Masese family for their support and to my wife Joyce, daughter Kemunto and son Masese for their love and encouragement.

## MATERIALS PUBLISHED

1. Makori, N., Oduor-Okelo, D. and Otianga-Owiti, G. (1991).  
Morphogenesis of the Foetal Membranes and Placenta of  
the root-rat ( *Tachyoryctes splendens* (Ruppell)). *Afri. J.  
Ecol.* Vol. 29, pp. 248 - 260.
2. Makori, N., Oduor-Okelo, D., Warui, C.N. and Otianga-Owiti, G.  
(1992). An ultrastructural and morphometric study of  
the late-term placenta of the root-rat ( *Tachyoryctes  
splendens* (Ruppell)). Proceedings of the 2nd  
International Conference on Advances in Reproductive  
Research in Man and Animals, National Museums of  
Kenya, Nairobi, Kenya.

## Chapter 1

### 1.0. GENERAL INTRODUCTION AND LITERATURE REVIEW ON THE REPRODUCTIVE BIOLOGY OF THE ROOT-RAT (*Tachyoryctes splendens* Ruppell)

#### 1.1 General Introduction

The rodent *Tachyoryctes* belongs to the family Rhizomyidae whose other members are *Rhizomys* and *Cannomys* (Missone, 1968; Kingdon, 1974; Walker, 1975). Missone (1968) recognized two species of *Tachyoryctes*, namely *T. splendens* found in most parts of Eastern Africa, and *T. macrocephalus* which is confined to Ethiopia. *T. splendens* is commonly known as the root-rat. It is an aggressive, solitary and fossorial rodent which lives in underground burrows but occasionally ventures above the ground at night to forage. The adult weighs about 180-250 g and resembles the American pocket gopher (*Geomyidae*) with a compact body, modified for burrowing life, short limbs and claws, and a short tail with little hair. The length of the head and body is about 120-260 mm, and that of the tail is 50-95 mm. This rodent has been found to cohabit the same ecosystem with the naked mole rat and *Heliophobius* in the East African region (Kingdon, 1974). In Kenya the root-rat is found in the southern half of the Rift Valley, Nyanza, Western, Central and Nairobi provinces.

Rodents are usually regarded as pests and disease carriers and have therefore attracted more attention in the areas of pest and disease control than in the area of their reproductive biology. This

has led to a paucity of knowledge on the reproductive biology of these animals which are unique and would offer clues on some of the complicated reproductive physiology mechanisms observed in members of the animal kingdom. The root-rat is no exception to this bias and like most rodents is mostly trapped for destruction rather than scientific investigation in its reproductive biology.

Roots and tubers are the main diet of the root-rat, but it is likely that they "graze" to some extent since fresh grass can sometimes be found in their stomachs (Jarvis, 1969a,b). In regions where root-rats occur, they usually damage food crops, particularly beans and peas, sweet potatoes, pyrethrum roots, and groundnuts

The root-rats have been used as a source of protein by man in most localities where they occur (Kingdon, 1974; Walker, 1975). In Buganda, Uganda, these rodents were highly regarded because they were believed to have a special value as charms. Despite this frequent interaction with man, the root-rats are not known to be disease transmitters.

Two main forms of *T. splendens* have been identified, the Western *ruandae* form (Rahm, 1969) found in Rwanda and Eastern Uganda, and the larger *ibeanus* form (Jarvis & Sale, 1971) found around Nairobi and most regions of Kenya. These two forms are regarded as subspecies of *T. splendens* because their anatomy is the same except for minor differences in skull structure (Kingdon, 1974). The fur of these rodents is thick and soft, the colour being brown with a dark-grey undercoat, but juveniles less than four months are black. Males are relatively larger and lighter in colour than the

females, and thus these rodents show some degree of sexual dimorphism.

Few studies have been made on the reproductive biology of the root-rat. Jarvis (1969a,b) examined the gross anatomy of the reproductive organs of male and female root-rats and found them similar to those of other myomorphs. Preliminary histological studies of the ovary and preputial glands have been made; however, detailed histological and ultrastructural studies on the reproductive organs, especially the pregnant uterus, foetal membranes and placenta of the root-rat are lacking.

## 1.2. Taxonomy

The classification of the order Rodentia is shown in Table I, and it is generally accepted that the root-rat belongs to the genus *Tachyoryctes* of the family *Rhizomyidae* in the suborder Myomorpha. This is based mainly on paleontological and osteological features (Simpson, 1945). It has been reported that the earliest Rhizomyid fossil recognized is *Tachyoryctoides* from the Asian Oligocene (Kingdon, 1974). Fossils of the living root-rat, *Tachyoryctes splendens*, have been reported from the Laetolil beds in northern Tanzania (Leaky, *et al.*, 1976).

The sub-family Tachyoryctinae has been placed in the families Spalacidae (Thomas, 1896; Tullberg, 1899; Weber, 1928) and Muridae (Winge, 1924; Ellerman, 1940) but today it is generally placed in the family Rhizomyidae (Simpson, 1945; Missone, 1968; Walker, 1975).

The genus *Tachyoryctes* has previously been split into fourteen species and eleven subspecies (Ellerman, 1941). However,

Missone(1968) has grouped all these into two main species namely *T. macrocephallus* (Ruppell) found in the highlands of Ethiopia, and *T. splendens* (Ruppell) which incorporates most of the species and subspecies.

### 1.3. The Reproductive Biology

#### 1.3.1. The reproductive organs

The female reproductive system of the root-rat as described by Jarvis (1969b) comprises a pair of ovaries and oviducts, two uterine horns, a cervix, and a vagina.

Based mainly on the observations made by Jarvis (1969a,b) the pregnant root-rats have a large number of seemingly active corpora lutea in the ovaries. There are instances when one ovary may contain up to ten corpora lutea for one healthy and one regressing embryo. The average number of corpora lutea, most of which are probably luteinized follicles, increase with embryo age. Most of the uteri examined show the presence of placental scars.

#### 1.3.2. Ovulation and breeding patterns

Ovulation involves the shedding of eggs from an ovary, and in mammals, the number of eggs ovulated usually exceeds the number born (Mossman & Duke, 1973). Some mammalian groups, and rodents in particular, have a tendency to superovulate, thus ensuring that one or two fertilized eggs will successfully implant. As an example the pronghorn antelope (*Antilocapra americana*)

ovulates five to eight eggs which are fertilized and of these at least one or two are implanted (O'Gara, 1969). However, in some species, there appears to occur an excessive form of superovulation. For example, the South African long-eared elephant shrew ovulates 50-60 eggs yet only two can be accommodated for implantation, while the plains viscacha ( *Lagostomus maximus* ) ovulates 300-800 eggs, seven to eight get fertilized and only two implant (Horst & Gillman, 1941; Weir, 1971b).

*Tachyoryctes splendens* is a superovulator but only one or two implanted eggs survive to term (Jarvis, 1969b; Jarvis & Sale, 1971). The root-rat is polyoestrous and has a potential to breed throughout the year (Jarvis 1969a,b). The root-rat, therefore, has been able to adapt its main breeding season to fit the local rainfall pattern. Ovulation probably occurs simultaneously in both the right and left ovaries.

Twinning occurs in the root-rats, but one born is the more frequent occurrence (Rahm, 1969; Jarvis, 1969b). The neonates are mainly confined to the burrow and totally dependent on the mother for food and protection until they are able to fend for themselves (Jarvis, 1969b). Rahm(1969) estimated the gestation period of the root-rat to be between 45-50 days. The only other myomorph rodent with a long gestation period of 46 days is the Australian rat, *Mesembryomys gouldii* (Crichton, 1969). Long gestation periods in rodents are mostly associated with the suborder Hystricomorpha (Weir, 1974).

Table I

A Classification of the order Rodentia ( after Simpson, 1945)

Class Mammalia

Order Rodentia

Suborder	Sciuromorpha	Myomorpha	Hystricomorpha
Families and Genera in the suborder	<p>1. Aplodontidae (Sewellels) -<i>Aplodontia</i> .</p>	<p>1. Cricetidae (Voles, mice &amp; rats) -<i>Meriones, Neotoma, Reithrodontomys, Peromyscus, Mesocricetus, Ondata, Microtus, Clethrionomys.</i></p>	<p>1. Hystricidae (old world porcupines)- <i>Hystrix, Thecurus, Atherurus.</i></p>
Families and Genera in the suborder	<p>2. Sciuridae (Squirrels, Chipmunk, marmots) -<i>Sciurus, Citellus, Cynomys, Marmota, Tamias, Eutamias, Funambulus, Glaucomys.</i></p>	<p>2. Muridae (Old World rats &amp; mice) -<i>Mus, Rattus</i></p>	<p>2. Erethizontidae (New World porcupines) <i>Erethizon, Coendou</i></p>
Families and Genera in the suborder	<p>3. Geomyidae (pocket gophers) -<i>Geomys</i></p>	<p>3. Spalacidae (blind mole rats)</p>	<p>3. Caviidae (guinea pigs, marmosets, guinea pigs, marmosets, guinea pigs, marmosets) -<i>cavia, Galea, Microcavia.</i></p>

	<p>4. Heteromyidae (pocket "mice", pocket rats, spring mice", "kangaroo" rats) - <i>Perognathous</i> <i>Microdipodops</i>; <i>Dipodomys</i>.</p>	<p>4. *Rhizomyidae (bamboo rats, root- rats). <i>Tachyoryctes</i></p>	<p>4. Hydrochoeridae (capybaras) <i>Hydrochoerus</i>, <i>Neochoerus</i>.</p>
Families and Genera in the suborder	<p>5. Anomaluridae (scally-tailed squirrels) <i>Anomalurus</i></p>	<p>5. Gliridae (dormice hazel mice) <i>Dryomys</i>, <i>Glirulus</i></p>	<p>5. Dinomyidae (long tailed pacas) <i>Dinomys</i></p>
	<p>5. Ctenodactylidae (gundis) - <i>Ctenodactylus</i></p>	<p>5. Platycanthomyidae (spiny dormice) - <i>Platycanthomys</i></p>	<p>6. Dasyproctidae (pacas, agoutis, acushis) <i>Dasyprocta</i>, <i>Myoprocta</i></p>
	<p>7. Pedetidae (springhass, or jumping "hare") - <i>Pedetes</i></p>	<p>7. Seleviniidae</p>	<p>7. Chinchillidae (viscachas, chinchillas) <i>chinchilla</i></p>
	<p>8. Castoridae (beavers) <i>castor</i></p>	<p>8. Zapodidae (jumping "mice" birch mice). <i>Zapus</i>, <i>Napaeozapus</i></p>	<p>8. Capromyidae (Lutias, nutrias) <i>Myocastor</i>.</p>

	9. Dipodidae (jerboas) <i>-Jaculus</i>	9. Octodontidae (degus) <i>-Octodon,</i> <i>Octodontomys.</i>
		10. Ctenomyidae (tucus tucus) <i>-ctenomys</i>
		11. Abrocomyidae (rat chinchillas) <i>-Abrocomys.</i>
		12. Echimyidae (spiny rats ) <i>-Proechimys.</i>
		13. Thryonomyidae (cane rats) <i>Thryonomys</i>
		14. Petromyidae (rock rats) <i>Petromys</i>
Families and Genera in the suborder		15. Bathyergidae (African mole rats) <i>Cryptomys,</i> <i>Bathyergus,</i> <i>Heterocephalus</i>

\* Genera under study.

### 1.3.3. Implantation, the foetal membranes, and placenta.

The process of implantation shows marked variation in different mammalian orders ranging from instances where the blastocyst remains in the uterine cavity i.e superficial implantation, to situations where the blastocyst implants by passing through the uterine epithelium and becoming completely cut off from the uterine lumen, that is interstitial implantation (Boyd & Hamilton, 1952). Interstitial implantation is quite apparent in the order Rodentia and in some primates, and less so in Insectivora and Chiroptera (Mossman, 1937, 1987). However, in most of the mammalian orders, superficial implantation is more common (Mossman, 1987). In the order Rodentia, the superficial form of implantation is commonly observed in the suborder Sciuromorpha (Mossman, 1987). A secondary type of interstitial implantation is found in the suborder Myomorpha, whereas complete (primary) interstitial implantation is more commonly found in the suborder Hystricomorpha (Mossman, 1937, 1987; Boyd & Hamilton, 1952; Roberts & Perry, 1974). The type of implantation has a close correlation with other embryonic developmental events, particularly the mode of amnion formation (Boyd & Hamilton, 1952). In superficial implantation, amniogenesis is by folds whereas in the interstitial type of implantation it occurs by cavitation.

The foetal membranes are formed from the zygote but they do not form part of the embryo itself and are shed or absorbed at birth (Boyd & Hamilton, 1952). The foetal membranes include the yolk

7

sac, the allantois, the amnion, and the chorion and other embryonic appendages (*e.g.* placenta). In most rodent suborders similarities have been noted in the major developmental events of these foetal membranes. The suborder Sciuromorpha, represented by the family Sciuridae, shows a late and incomplete inversion of the germ layers, a well developed, temporary choriovitelline placenta, a small allantoic sac and a placenta that is formed by invasion of chorioallantoic villi into the degenerating epithelial symplasma of the uterine glands. The interhaemal membrane is haemomonochorial (Mossman, 1937, 1987; Mossman & Weisfeldt, 1939). In the suborder Myomorpha, the major families Cricetidae and Muridae show the following features in their foetal membrane development: an early complete inversion of the yolk sac; amnion formation by cavitation; a small chorion completely incorporated into the labyrinthine haemochorial placenta; a persistent periplacental bilaminar omphalopleure; conspicuous placental pits on the foetal side of the placenta; and a haemotrichorial placenta (Mossman, 1937, 1987; Snell, 1941; Fischer & Floyd, 1972a,b; King & Hastings, 1977). In some minor families of myomorpha, particularly the Zapodidae and Dipodidae which are closely related to the family Rhizomyidae, there are clear differences in some details of the development of the foetal membranes and placenta from those of the major families (Muridae & Cricetidae). In Dipodidae (Jerboas) and Zapodidae (jumping mice) the blastocyst is relatively larger and the rudimentary epamniotic cavity is wider and more open (Mossman, 1987); yolk sac inversion is complete but occurs late, and the definitive haemochorial placenta shows the trophoblast of the

zona intima to consist entirely of giant cells (King & Mossman, 1974). The third suborder of the order rodentia, Hystricomorpha, also shows some basic features which differ from those of the other two suborders. These characteristics are derived mainly from studies on the family Caviidae (Mossman, 1937, 1987; Blandua, 1949; Davidoff, 1973; Kaufmann & Davidoff, 1977) and include a complete (primary) interstitial implantation, amniogenesis by cavitation with an epamniotic cavity, very early and complete inversion of the yolk sac, a small placenta (Trager), large villous inverted yolk sac, a prominently lobulated, labyrinthine haemochorial placenta; and no allantoic sac. The development of the rodent foetal membranes has therefore been widely studied; however, Mossman (1987) notes that information on the foetal membranes of the root-rat is lacking. Comprehensive studies have been made on the breeding season, litter size and burrowing patterns of these rodents, but as stated earlier the gross and histological anatomy of the reproductive organs has only been briefly examined (Jarvis, 1969a,b; Jarvis & Sale, 1971).

#### 1.4. Morphometry of the Placenta

The placenta which in the eutheria is essentially for metabolic exchange also performs other functions (Amoroso, 1952). As an organ for exchange, the placenta is designed anatomically to approximate the maternal and foetal circulations in order to allow diffusion of metabolites over a large surface area (Mayhew, *et al.*, 1984). It has been further observed by Mayhew, *et al.* (1984) that one vital aspect of the placenta is the ability to transfer oxygen to the

foetus by simple diffusion. The interhaemal barrier between maternal and foetal erythrocytes is neither uniform in composition nor in thickness (Mayhew, *et al.*, 1984). This barrier through which oxygen passes from maternal to foetal erythrocytes mainly consists of five tissue components arranged in series. These include: The maternal erythrocytes; the maternal blood plasma; the labyrinthine membrane (consisting of trophoblast, stroma, and foetal capillary endothelium); the foetal blood plasma, and the foetal erythrocytes. Each of these components partially hinders diffusion of oxygen.

The physiological oxygen diffusing capacity of the placenta has been estimated in a number of species including man, sheep, rabbits and dogs (Metcalf, *et al.*, 1967). Investigations on the placental morphometric oxygen diffusing capacity of the human placenta (Mayhew *et al.*, 1984) show that this value is higher than the physiological diffusing capacity. It appears that physiological estimates for oxygen diffusing capacity are lower than the morphometric estimates because values for the oxygen partial pressure gradient at the site of gaseous exchange are not easily obtained (Mayhew, *et al.*, 1984). On the other hand, all the parameters needed for estimating the morphometric diffusing capacity can easily be measured on tissue sections. Furthermore, the placental barrier is uneven in composition and thickness and measurements of physiological oxygen diffusing capacity of the placenta do not take this into account. In estimating the morphometric oxygen diffusing capacity of the placenta diffusion distances are expressed as harmonic means (rather than arithmetic

means) in order to attach greater functional importance to thinner regions (Weibel, 1970).

Morphometric studies on the placental diffusing capacity for oxygen are relatively few, especially for fossorial rodents. The laboratory white rat (Baur, 1977) and the guinea pig (Baur, 1977; Kaufman & Davidoff, 1977) placentae have been investigated and some morphometric parameters, especially the absolute volumes, surface areas and harmonic mean thickness have been measured. However, no estimation of the morphometric diffusing capacity of the placentae was made in these studies. Apparently, no investigations have been made on the morphometric characteristics of the definitive placenta of the root-rat. This rodent lives in hypoxic-hypercarbic atmospheric conditions (Chapman & Bennett, 1975). Therefore a morphometric study of the root-rat placenta could contribute to some knowledge on the factors which influence the functional capacity of the placenta as an organ for materno-foetal metabolic exchange.

### 1.5. Objectives of the present study

As pointed out in the literature review there is an apparent lack of information on the morphology of the reproductive organs, foetal membranes and placenta of the root-rat, *T. splendens*. The aim of this study is, therefore, to examine the histological and ultrastructural characteristics of the female reproductive system of the root-rat with emphasis on the morphogenesis of the foetal membranes and placenta. An attempt will be made to compare

these observations with those made on the more widely studied members of *Muridae*, *Sciuridae*, *Geomys*, *Dipodomys* and *Cavia*.

Furthermore, the root-rat lives in hypoxic hypercarbic conditions and may therefore have developed some structural modifications in the organs concerned with gaseous exchange, particularly the lungs and the placenta. To find out whether such structural changes have occurred in the placenta, stereological methods will be used to determine the oxygen diffusing capacity of the late term placenta.

## Chapter 2

### 2.0. MATERIALS AND METHODS

#### 2.1. Biological materials and methods

A total of 113 root-rats were captured during the study period (Table III). Thirty (30) adult female root-rats were separated and examined for morphology and foetal membrane development (Table III) and five (5) for placental morphometry (Table IV). The remaining 75 animals were killed for disposal. The animals were caught using noose-traps (Fig.1) by mole trappers in Nairobi and Ngong areas from November, 1990 to November, 1991. The root-rats were brought to the laboratory in wire-cages and sexed by examination of the external genital organs.

In preparation for dissection, each mole-rat was sufficiently anesthetized with either chloroform or sodium pentobarbitone, and then weighed. Prior to dissection, the root rats were killed with an overdose of sodium pentobarbitone. The abdominal cavity was opened along the ventral mid-line to expose the female reproductive organs. In pregnant animals the number of foetuses in each uterine horn was noted, the crown-rump-length of each foetus was measured and by means of the ageing methods adopted by Jarvis (1969 a & b), the approximate stage of gestation was estimated (Table II). Tissue fixation, processing and sampling methods depended on whether the specimens were to be used for morphological studies or morphometric analysis.

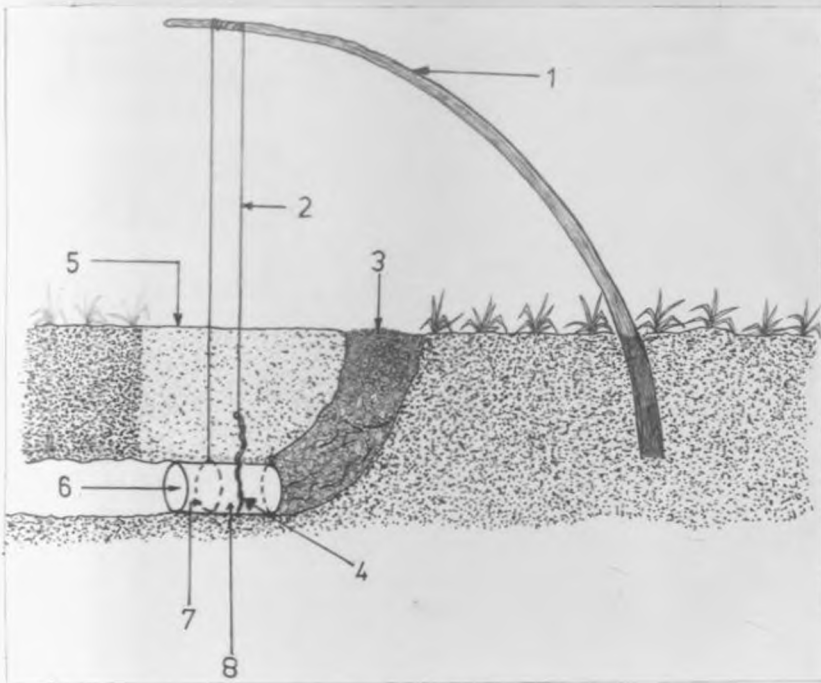


Figure 1. Schematic representation of the noose-trap used for catching the root-rats.

- 1, tensile stick firmly anchored in the ground
- 2, tightly stretched string attaching an aromatic root or tuber, e.g. carrot, to the tensile stick
- 3, leaves and soil loosely applied to cover the tunnel
- 4, aromatic plant root or tuber to attract the rodent and set off the trap on being cut
- 5, loose mound of soil
- 6 opening through which the root-rat enters the trap
- 7, loose noose made of wire that tightly holds the animal once the trap is triggered off
- 8, small diameter tin open at both ends

Table II. Some reproductive features of the Root-rat (*T. splendens*)

Root-rat No.	Weight (g)	Reproductive state and number of fetuses	Weight of locus/foetus (g)	Crown-rump-length in mm.	General remarks
1	150.56	early pregnancy right horn one foetus	0.42 (wt. of locus)	-	showed establishment of chorioallantoic placenta
2	190.00	early pregnancy right horn one foetus	0.38 (wt. of locus)	-	showed establishment of chorioallantoic placenta
3	195.02	very early pregnancy left horn	-	-	Blastocyst stage

Table II (cont'd)

4	205.89	mid-pregnancy right horn one foetus	2.5 (wt. of foetus)	33	Definitive placenta Complete inversion of germ layers
5	189.50	mid-pregnancy right horn one foetus	2.35 (wt. of foetus)	30	Definitive placenta Complete inversion of the germ layers
6	160.50	early pregnancy both horns one foetus in each horn	0.34;0.36 (wt. of loculi)	-	Expansion stage. Early allantois
7	173.50	early pregnancy both horns one foetus in each	0.5;0.5 (wt. of foetuses)	39;40	Mature placenta
8	180.83	early pregnancy both horns one foetus in each	0.75;0.72 (wt. of foetuses)	39;39	Mature placenta

Table II (cont'd)

9	129.89	early pregnancy one foetus left horn	0.20 (wt of loculi)	-	Expansion stage. Early allantois
10	177.00	late pregnancy one foetus right horn	5.1 (wt. of foetus)	45	Mature placenta. Placental haematoma
11	159.50	late pregnancy one foetus right horn	4.9 (wt. of foetus)	43	Mature placenta. Placental haematoma
12	170.00	late pregnancy two foetuses right horn	5.35;5.00 (wt.of foetuses)	50	Mature placenta. Placental haematoma
13	180.05	late pregnancy one foetus left horn	5.0 (wt. of foetus)	42	Mature placenta. Placental haematoma
14	168.90	mid-pregnancy right	4.84	39	Mature placenta

Table II (Cont'd)

15	157.00	late pregnancy one foetus left horn	5.5 (wt. of foetus)	42	Mature placenta. Placental haematoma
16	185.30	early pregnancy one foetus left horn	0.48 (wt. of loculi)	-	Showed establishment of chorioallantoic placenta
17	225.00	mid-pregnancy one foetus right horn	3.98 (wt. of foetus)	30	Definitive placenta
18	205.00	very early pregnancy both horns one foetus in each	-	-	Blastocyst stage

Table II (cont'd)

19	203.68	early pregnancy both horns one foetus in each	0.25;0.3 (wt. of loculi)	-	Showed establishment of chorioallantoic placenta
20	216.76	late pregnancy one foetus right horn	4.9 (wt. of foetus)	42	Mature placenta. Placental haematoma
21	207.35	late pregnancy one foetus left horn	5.3 (wt. of foetus)	44	Mature placenta. Placental haematoma
22	201.30	very early pregnancy one foetus left horn	-	-	Embryonic plate stage.

Table II (cont'd)

23	184.00	early pregnancy both horns one foetus in each	0.3;0.3 (wt. of loculi)	-	Showed establishment of chorioallantoic placenta.
24	209.05	mid-pregnancy one foetus right horn	4.5 (wt. of foetus)	36	Mature placenta.
25	213.00	early pregnancy both horns one in each	0.4;0.43 (wt. of loculi)	-	Showed establishment of chorioallantoic placenta
26	190.25	early pregnancy one foetus left horn	0.45 (wt. of loculus)	-	Showed establishment of chorioallantoic placenta

Table II (cont'd)

27	204.00	late pregnancy one foetus right horn	5.4 (wt. of foetus)	44	Mature placenta. Placental haematoma
28	194.00	not pregnant	-	-	Ovaries had large follicles
29	173.50	not pregnant	-	-	Small reproductive organs
30	177.00	not pregnant	-	-	Large mammary glands

## 2.1.1. Tissue fixation

Fixation of tissues was done either by immersion or perfusion. Perfusion was performed in order to obtain good fixation, especially for early conceptuses and placenta. The reproductive organs of root-rats numbers 1, 3, 6, 8, 10, 11, 12, 16, 19, 21, 23, 24, 25, 27 and 28 were fixed by perfusion and placental tissues from all the other animals were fixed by immersion.

### 2.1.1.1. Fixation of the organs by immersion

The abdominal cavity of each root-rat was opened along the ventral midline and the whole reproductive tract identified and carefully dissected out. In animals with very early, early or mid-term pregnancies the whole conceptus was immediately immersed in Bouin's fixative or 10% buffered formalin solution. Samples of placental tissue from animals with older pregnancies were cut with a sharp blade and immersed in fixative as described above. Material for electron microscopy was cut with a razor blade into small blocks of about  $1\text{ mm}^3$  and immersed in 2.5% glutaraldehyde in phosphate buffer (pH 7.5).

### 2.1.1.2. Fixation of the organs by perfusion

The abdominal cavity of each root-rat was opened by a ventral midline incision and the viscera were removed in order to expose

the abdominal aorta and caudal vena cava. The abdominal aorta was then ligated caudal to the renal arteries, and the caudal vena cava was opened to provide drainage. A cannula was then inserted into the aorta caudal to the ligature and connected by a plastic tube to a container suspended on a tripod 70 cm above the specimen. Physiological saline was poured into the container and infused by gravitational force into the aorta to clear blood from the tissues. The container was filled with fixative which was then infused slowly into the aorta for about 20 minutes, and due to the ligation of the aorta the fixative only perfused the lower half of the body.

#### **2.1.1.3. Tissue sampling and processing for morphological studies**

After perfusion the whole of the reproductive tract and placenta, when present, were dissected out and immediately cut into blocks for both light and electron microscopic examination. The cut blocks were further immersed into appropriate fixative for preservation before processing.

The tissues fixed by either Bouin's or formalin solutions were processed by routine histological methods and embedded in paraffin wax. Serial sections 7 $\mu$ m thick were cut from blocks containing the early and mid-term pregnancies and stained with either haematoxylin and eosin or Goldner stain and examined by light microscopy.

Tissue blocks for electron microscopy were rinsed in phosphate buffer and post-fixed in 1% osmium tetroxide, dehydrated through ascending concentrations of alcohol and propylene oxide

and embedded in epon-araldite. Semi-thin sections were cut with glass knives on a Sorvall "Porter-Blum" ultramicrotome and stained with toluidine blue for examination by light microscopy and orientation purposes. Thin sections were cut, mounted on 200 mesh copper grids and stained successively with uranyl acetate and lead nitrate (Venable & Coggeshall, 1965) and then examined with a Phillips CM12 electron microscope.

## 2.2. Quantitative materials and methods.

### 2.2.1. Structural basis of morphometry of the placenta.

In this study the placental parenchyma and non-parenchyma were distinguished as the main components of the root-rat placenta. The main components of the parenchyma include the maternal blood spaces, the interhaemal tissue barrier and the foetal capillaries. Non-parenchymal components include the large trophoblast cells and maternal blood channels lined by a thin endothelium-like cell layer. It was observed that sections of the placenta in all directions yielded similar pictures, and thus, the distribution of all the components of the placenta could be assumed to be homogenous. It was, nevertheless, necessary to express the volume proportions of the placental parenchymal components in the volume of the parenchyma alone in order to allow for comparisons of placental parameters between the root-rats. The placenta was therefore sampled in multiple stages and the stereological analyses was made at two levels (stages) of sampling. The main components of the

placenta were estimated at the first level of sampling and those of the placental parenchyma at the second level of sampling. Analysis at the first level of sampling was done on sections which were cut through the entire placenta.

### 2.2.2. Tissue sampling and processing for morphometry

Immersion fixed placentae from five adult female root-rats were analyzed for morphometric data. The root-rats were in the last half of the gestation period and had full-term placentae. The weight of the foetus in each root-rat was measured on an ordinary weighing scale and the results tabulated (Table IV). Placental volumes were determined using the water displacement method of Scherle (1970) in which the water displacement due to organ volume is recorded by weighing (fig. 2 and Table IV). In this method, a large container is filled to about two thirds with isotonic saline and placed on a weighing balance which is then adjusted to read zero. The organ is then totally submerged in the saline but not allowed to touch the vessel wall nor the bottom; the resulting weight ( $W$ ) is read off, and this represents the organ volume. Each placenta was then cut into small whole-diameter slices each 2 mm in width and serially numbered:

(1) each of the odd-numbered tissue slices was fixed by immersion in 10% buffered formalin and subsequently processed for paraffin sections by routine histological methods. Sectioning of each tissue block was done at 5-7 $\mu$ m thickness and used for the first level of stereological analysis (see below).

(2) each of the even numbered slices was further diced into many smaller blocks and a sample of four of these blocks were picked at random and processed for semi-thin sections (fig. 3). Each block was sectioned at 0.5 $\mu$ m thickness and four random sections were obtained (giving a total of sixteen) and stained with toluidine blue in 1% borax. From each of these sixteen sections, ten systematic random fields from each section were analyzed for morphometric data at the second level of sampling (see below).

### 2.2.3. Stereological analysis

#### 2.2.3.1. Analysis at the first level of sampling

This was made to estimate the volume proportions of the parenchyma and non-parenchyma. Each of the sections obtained for the first level of sampling was projected by a photomicroscope with a video camera attachment onto a 14" J.V.C television screen superimposed with a 414 point simple square lattice test system ( $\Lambda$ -100) of Weibel (1979). The section was then wholly analyzed field by field by point counting morphometry at a final magnification of X220. The volume density of each component was estimated on each section as the ratio of the total number of points falling on the component divided by the points falling on the whole field. Section sufficiency was tested by cumulative means and for non-parenchyma (NP) the cumulative mean lay within  $\pm 5\%$  of the mean after analyzing fifteen sections (Graph 1). The absolute volume of each component was estimated by multiplying the volume density of the component and the volume of the placenta as a whole (see Appendix 1)

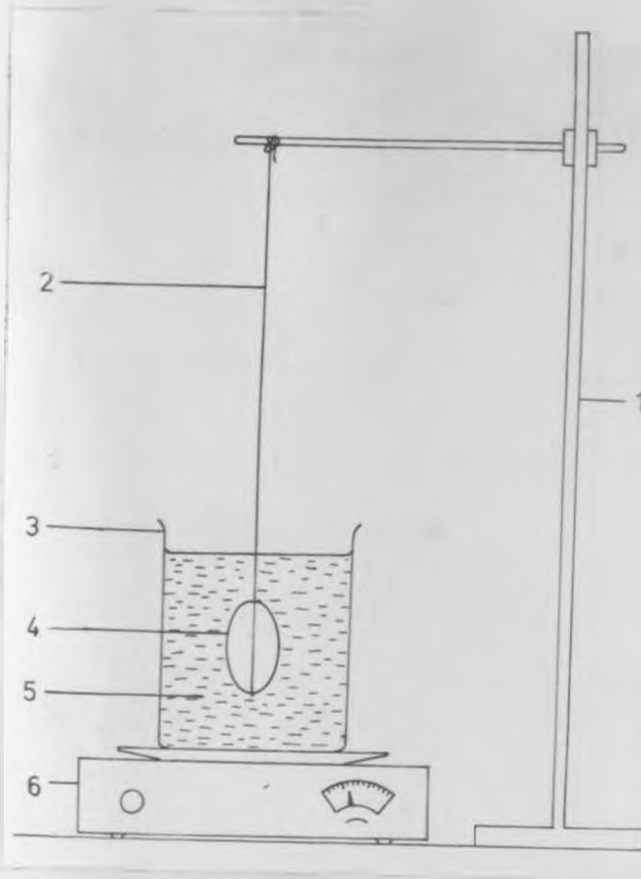


Figure 2. Apparatus illustrating Scherle's (1970) water displacement method for estimating placental volume.

1, tripod

2, thin string

3, beaker

4, organ

5, isotonic saline

6, weighing scale

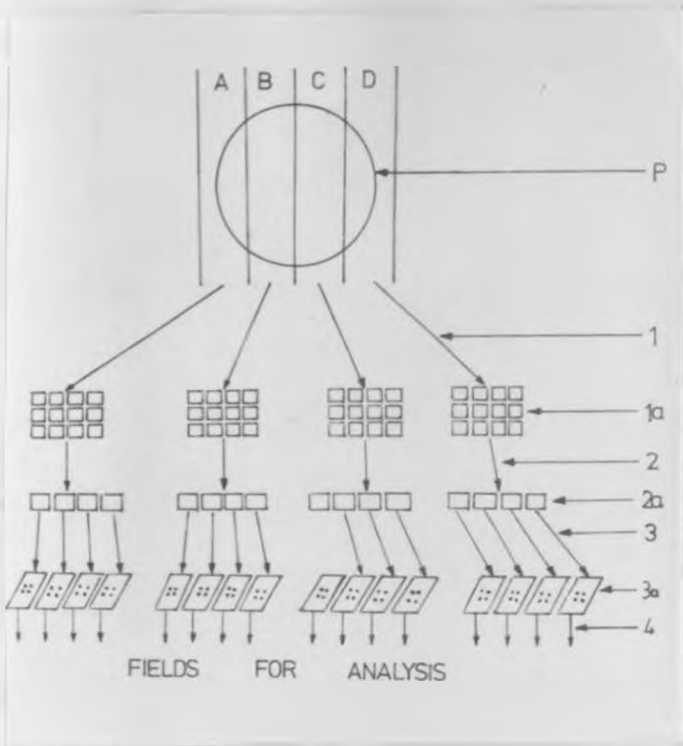


Figure 3. Tissue sampling for light microscopic analysis.

The placental disc was serially cut with a sharp blade resulting in several whole face blocks. The even numbered blocks were processed for semi-thin sections while the odd numbered blocks were processed for routine histology

A, B, C, D, represent whole face blocks of placenta; 1, 1a, dicing of placenta and resulting blocks; 2, 2a, selection and processing of tissue blocks; 3, 3a, cutting and staining of blocks; 4, light microscopic analysis.

Table III

Distribution on a monthly basis of the number of adult female root-rats which were pregnant and non-pregnant when captured (trapped)

Month and Year	Number of pregnant females	Number of non-pregnant females
November, 1990	2	6
December, 1990	4	4
January, 1991	6	9
February, 1991	4	2
March, 1991	2	8
April, 1991	2	5
May, 1991	1	5
June, 1991	0	10
July, 1991	3	5
August, 1991	0	7
September, 1991	0	11
October, 1991	2	6
November, 1991	1	5

### 2.2.3.2. Analysis at the second level of sampling

This was made to estimate the volume proportions, surface areas and harmonic thicknesses of the components of the parenchyma. Each of the sections obtained for the second level of sampling was projected by a photomicroscope onto a 14" J.V.C. television screen superimposed with a 414 point simple lattice test system (A-100). From the four blocks of resin embedded placenta a total of sixteen semi-thin sections were obtained and these provided systematic random fields (Weibel, 1979)) at a final magnification of X2200. All the placental parenchyma components and associated parameters were estimated on the same fields.

#### (a) The volume density

On each section ten fields were projected on the television screen and the counting done of the number of points falling on the maternal blood spaces, the interhaemal trophoblast (of the placental barrier), and the foetal capillary bed. The points obtained were used to estimate the volume densities of the parenchymal components (see Appendix 1).

From each placenta a total of 160 fields were analyzed and the sufficiency of fields sampled was tested by cumulative means. For the foetal capillary bed the cumulative mean lay within  $\pm 5\%$  of the mean after analyzing fifty fields. The absolute volume of each component was estimated by multiplying the volume density of the component and the volume of the parenchyma (see Appendix 1).

**(b) The surface density.**

The placental parenchyma components whose surface density were determined include the maternal erythrocytes, the maternal blood spaces, the foetal erythrocytes, and the interhaemal trophoblast (of the placental barrier). A square lattice grid with 18 horizontal lines, each 23 cm in length, was superimposed onto the T.V. screen field projections at a final magnification of X2200. The total length of the test lines was 414 cm. This value of 414 cm was divided by the final magnification to obtain the length of test lines in real units. The surface density of each component was estimated by multiplying the number of intersections by two and dividing the resulting value by the length of the test system in real units (see Appendix 1). The surface area of each component was then calculated by multiplying the surface density by the volume of the parenchyma.

A total of 160 fields were analyzed for each placenta and the sufficiency of fields sampled was tested by cumulative means. For the foetal erythrocytes the cumulative mean lay within  $\pm 5\%$  of the mean after analyzing eighty fields.

**(c) Harmonic mean thickness**

The same fields of analysis for estimating volume and surface densities were used to measure the harmonic thickness of the materno-foetal placental barrier. A square lattice grid similar to that used for surface density determination was superimposed on the

projected fields at a final magnification of X2200. Horizontal measurements were made on the length of line, in mm, between two intercepts of the materno-foetal placental barrier and their reciprocals determined. The harmonic mean thickness was then estimated by dividing the number of fields analyzed by the sum of the reciprocals and the final magnification.

#### **2.2.3.3. The placenta oxygen diffusing capacity $D_p$**

This was estimated by using the values obtained in earlier estimates, namely the surface area of the interhaemal trophoblast and the harmonic mean thickness of the placental membrane. A physicochemical quantity, the Krogh's diffusion coefficient was also used. Thus the placental diffusing capacity was estimated by multiplying the surface area of the interhaemal trophoblast and Krogh's diffusion coefficient divided by the harmonic mean thickness (see Appendix 1).

#### **2.2.4. Measurement of tissue shrinkage**

Tissue shrinkage is usually determined by measuring the area of tissue block before processing and dividing this value by the area of the same face of the block after processing. There is bound to occur some degree of shrinkage during tissue processing but the amount of shrinkage that may take place depends on the method used (Weibel, 1979). Paraffin processed sections tend to show the greatest percentage of shrinkage, but is much less important when using

epoxy plastic embedding (Weibel & Knight, 1964). It has been observed further that volume densities are generally not affected by isotropic uniform shrinkage, but other dimensions like surface densities are affected (Weibel, 1979). In this study therefore no attempt was made to correct for shrinkage as most parameters were determined on epoxy embedded sections and also because it is only the volume densities that were determined on paraffin-embedded sections.

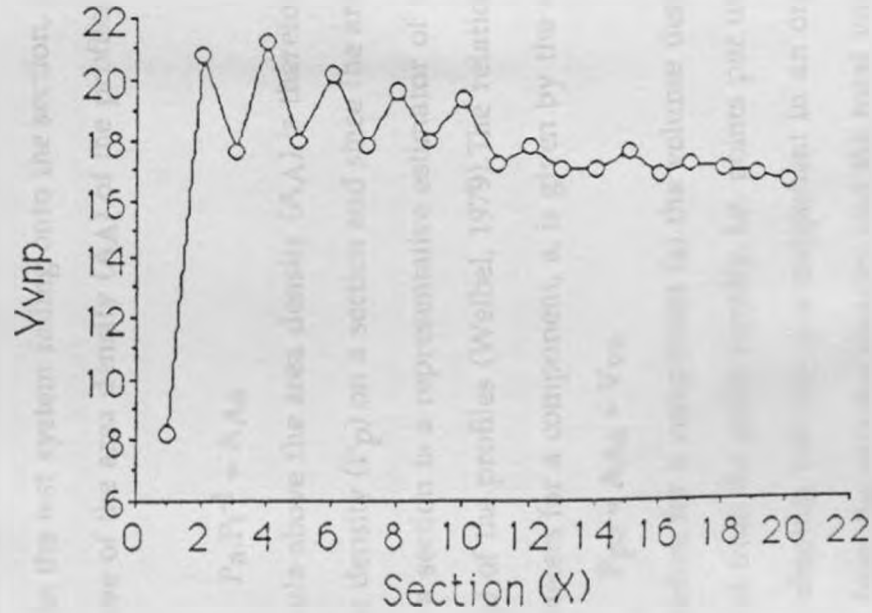
#### **2.2.5. Data handling**

In trying to establish the adequate number of sections and fields of analysis, a large number of sections from the first two specimens were analyzed for the relevant components, for example the volume density of the non-parenchyma. A cumulative mean graph of the values was then plotted (see Graph I). When there was no substantial change in the volume density ( $\pm 5\%$ ), the section number at which this occurred was taken as the sufficient number. A similar procedure was adopted in determining the sufficient number of fields to analyse for the components of the parenchyma. For all the specimens, values for each organ were employed to calculate component means and standard errors.

### **2.3. Stereological methods**

#### **2.3.1. Point counting morphometry as an estimator for volume density**

Graph 1. Cumulative mean graph of the weighted means of the non-parenchyma volume density (%) per section against the number of sections.



The point counting method, which was first described by Delesse' (1847), assumes that if random points are superimposed on a given section of tissue the number of points ( $p$ ) falling on profiles of a particular test component ( $a$ ) compared to the total number of points ( $P_t$ ) in the test system falling onto the section, is representative of the area density ( $A_A$ ) of the profiles of component ( $a$ ), i.e.,

$$P_a \cdot P_t^{-1} = A_{Aa} \quad (1)$$

In the formula above the area density ( $A_A$ ) is therefore represented by the point density ( $P_p$ ) on a section and since the area density of profiles on a section is a representative estimator of the volume density ( $V_v$ ) of the profiles (Weibel, 1979). The relationships between these parameters for a component,  $a$ , is given by the expression:

$$P_{pa} = A_{Aa} = V_{va} \quad (2)$$

Therefore for a component ( $a$ ) the volume density ( $V_{va}$ ) can be estimated from the point density, i.e. points per unit point set.

The absolute volume of a component in an organ is calculated from the volume density and the total volume of the organ ( $VP$ ). Thus for a component ( $a$ ) the absolute volume ( $V_a$ ) would be

$$V_a = V_{va} \cdot VP = \quad (3)$$

The stereological analyses to estimate the volume proportions of the placenta components on the histological sections was made using a square point lattice system (A-100) of Weibel (1979) 'see Appendix 1).

### 2.3.2 Intersection counting morphometry as an estimator for surface density and surface area

The surface density  $S_{Va}$  expresses the amount of surface area  $S(a)$  of a class of objects  $a$  that is contained in the unit containing volume  $V(c)$  (Weibel, 1979) such that:

$$S_{Va} = S(a)/V(c) \quad (4)$$

It has been stated further by Freere and Weibel (1967) and Weibel (1979) that if test lines are placed on an isotropic tissue section they will intersect the surfaces of the various components. In turn the number of intersection points  $I(a)$  can be related to the test line length in the tissue  $L(c)$  and thus the surface density can be determined by:

$$S_{Va} = 2.I(a)./L(c) \quad (5)$$

this formula was used to determine the surface densities of the placental parenchyma components mainly the maternal erythrocytes, maternal blood spaces, the foetal capillary endothelium. the foetal erythrocytes, and the interhaemal tissue barrier (see Appendix 1).

### 2.3.3. Intercept length as estimator for harmonic mean thickness

Harmonic mean has been defined as the sample number divided by the sum of the reciprocals (Weibel, 1979). Thus the harmonic mean thickness ( $\tau_h$ ) is calculated as

$$\tau_h = (n/\sum 1/L).M^{-1} \quad (6)$$

where  $n$  is the number of the quantities,  $\sum 1/L$  is the sum of the reciprocals of the quantities and  $M$  is the final magnification.

The harmonic mean thickness is the relevant measure of the effective average thickness offering resistance to oxygen diffusion through a barrier (Weibel & Knight, 1964). The reciprocals of the length intercepts are used in determining the harmonic mean thickness in order to attach greater significance to the thinner regions of the exchange barrier. The placenta interhaemal membrane has thin and thick regions and thus the above formula was used in estimating the harmonic mean thickness of the interhaemal membrane (see Appendix 1).

#### 2.3.4. Stereological estimation of the oxygen diffusing capacity of the placenta

The placental oxygen diffusing capacity ( $D_p$ ) defines the functional conductance of the placenta to oxygen (Mayhew *et al.*, 1984). The total placental barrier through which the oxygen passing from maternal to foetal erythrocytes must traverse comprises five main tissue compartments arranged in series. These include: the maternal erythrocytes ( $m_e$ ); maternal blood plasma ( $m_p$ ); placental membrane ( $p_m =$  trophoblast + foetal capillary endothelium); foetal blood plasma ( $f_p$ ) and foetal erythrocytes ( $f_e$ ). Each of these compartments behaves as a partial resistance to oxygen diffusion and therefore estimation of  $D_p$  can be achieved by evaluating the five partial conductances  $D_{m_e}$  through to  $D_{f_e}$  (Mayhew, *et al.*, 1984), and since resistance is the reciprocal of

conductance the overall resistance to diffusion in the placenta,  $R(p)$  is given by:

$$R(p) = 1/D_p = 1/D_{me} + 1/D_{mp} + 1/D_{pm} + 1/D_{fp} + 1/D_{fe} \quad (7)$$

It has been observed by Mayhew and Burton (1988) that the placental barrier is of uneven thickness and consequently gas conductance will vary from point to point on the exchange surface. At any one site therefore conductance will be inversely proportional to local thickness. To calculate the overall conductance the mean of the reciprocal local thickness will need to be estimated. This concept of harmonic mean thickness (Weibel & Knight, 1964) is commonly employed in diffusion studies in order to attach greater significance to the thinner regions of the exchange surface.

Oxygen diffusion proceeds across the trophoblast and then across the foetal capillary endothelium in the haemochorial placenta (Mayhew & Burton, 1988). This therefore means that a reliable estimate of the diffusing capacity can be obtained by estimating only two structural quantities namely the trophoblast surface area ( $S_{tr}$ ) and the harmonic mean thickness of the placental membrane ( $\tau_{hpm}$ ) (Mayhew & Burton, 1988). The gas conductance of the haemochorial placental membrane can then be rewritten as

$$D_{(pm)} = S_{tr} \cdot K / \tau_{hpm} \quad (8)$$

$K$  is Krogh's diffusion coefficient.

The application of this modified formula is preferred because technical limitations render it impossible to estimate accurately in the same organ all the variables necessary to calculate the overall  $D_{pm}$ . For example, perfusion fixation appears to be the only method which gives representative estimates of harmonic mean

thickness *in vivo* (Burton, *et al.*, 1987). However this method of fixation precludes the possibility of estimating harmonic thicknesses for the blood plasma compartments of the diffusion pathway.

### 2.3.5. Physicochemical quantity estimation

The physicochemical quantity used in this study was the Krogh's diffusion coefficient which, in a given tissue, is defined by the product of Bunsen's solubility coefficient of oxygen,  $\alpha$  (in  $\text{cm}^3 \cdot \text{cm}^{-3} \cdot \text{mmHg}^{-1}$ ) and the diffusivity of oxygen  $D$  ( $\text{cm}^2 \cdot \text{min}^{-1}$ ) (Mayhew, *et al.*, 1984). Since there are no experimental estimates of  $\alpha$  or  $D$  for the root-rat interhaemal membrane the value proposed for the human placenta of  $2.3 \times 10^{-8} \text{ cm}^2 \cdot \text{min}^{-1} \cdot \text{mmHg}^{-1}$  has been adopted for Krogh's diffusion coefficient (Mayhew, *et al.*, 1984) in this study.

## Chapter 3.

### 3.0. RESULTS

#### 3.1. General remarks

The root-rats examined in this study were adult females and their body weights ranged from 130 g to 225 g, with the mean body weight being 186 g. The body morphology of a typical female root-rat is shown in figure 4. Female root-rats resemble ordinary rats (*Rattus ratus*) and have small eyes and ear pinnae, short limbs and broad feet, a short tail and large prominent incisor teeth. Most of the rodents were dark-grey. Each female had four pairs of mammary glands extending from the caudal part of the pectoral region to the inguinal region. Each animal had two ovaries, two oviducts and a duplex uterus connected to the vagina via the cervical canals (Figs. 5 & 6).

Pregnant animals could be trapped in most months of the year (Table III) and they showed variations in the ages of the conceptuses (Table II) indicating that breeding occurs throughout the year in these rodents.

The ovaries of the non-pregnant animals were small, oval and flattened (Fig. 5). Each ovary was enclosed in an ovarian bursa. The ovaries were mostly smooth, but in some animals the tertiary follicles protruded slightly above the ovarian surface. These follicles were large and occupied a large part of the ovarian cortex.



Figure 4. Photograph of a female root ( *Tachyoryctes splendens* )  
Note the compact and hairy body and the medium-sized tail.

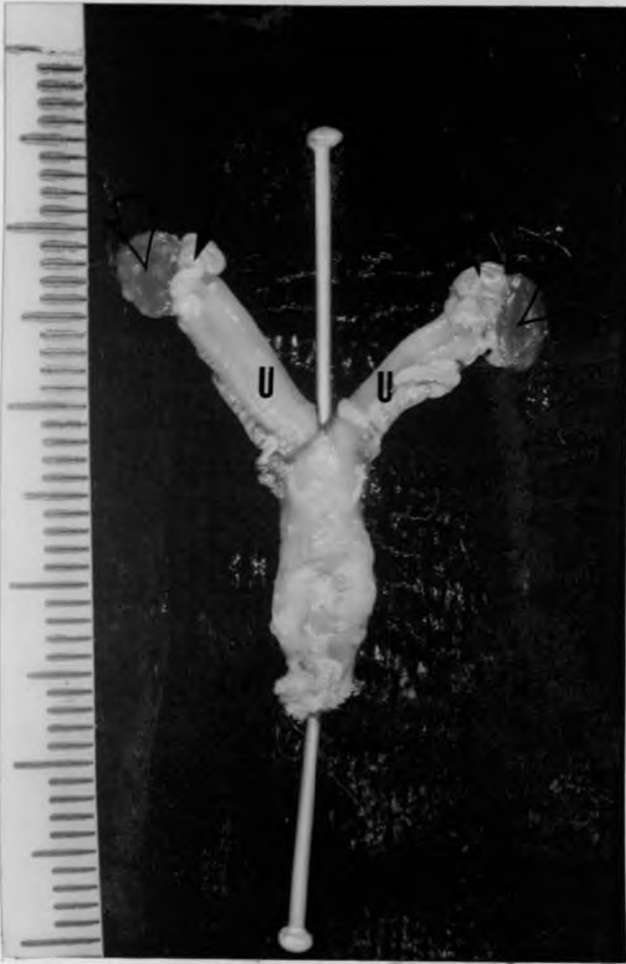


Figure 5. Photograph of the gross appearance of the gonadogenital organs of the root-rat. Note the flattened ovaries (arrowheads), coiled oviducts (small arrows) and the bicornuate uterus (U). X5.

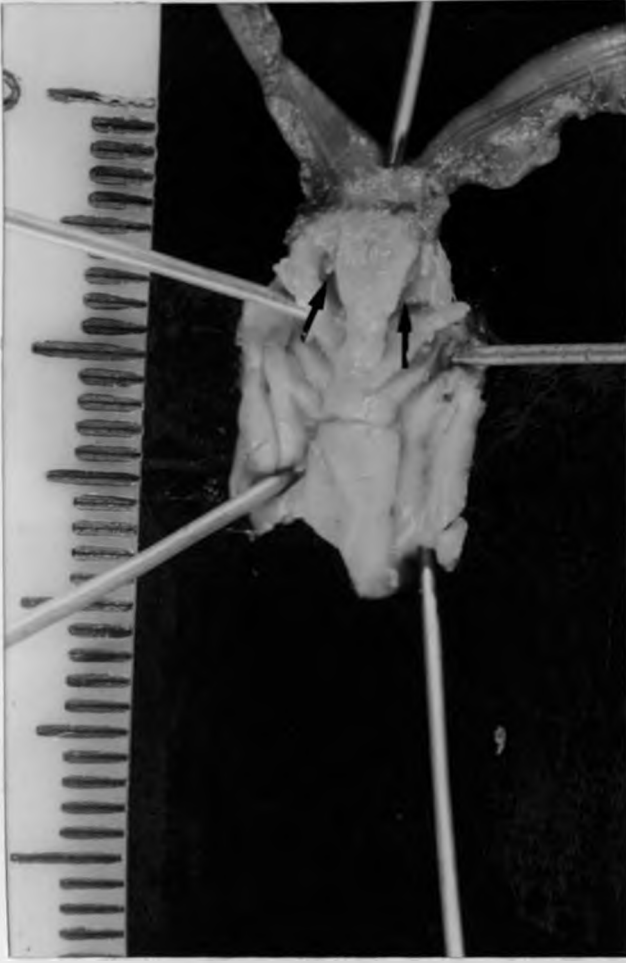


Figure 6. Photograph of the reproductive organs of the root-rat showing the gross appearance of the mucosa of the vagina and cervix (with ridges). Note the uterine tubes (arrows) joining externally at their cervical ends. X5.

Table IV. Maternal and foetal characteristics of the late-term pregnancy root-rats (*T. splendens*).

Specimen	Weight (g)	Nutritional status	Foetal crown-rump-length (mm)	Weight of foetus (g)	Volume of placenta (mm <sup>3</sup> )	Diameter of placenta (mm)
1	190.0	Fair	43.5	5.00	780	15.00
2	203.7	Good	44.0	5.13	970	13.52
3	215.7	Good	45.0	5.20	960	16.00
4	192.3	Fair	39.5	4.90	980	14.00
5	210.3	Good	40.3	6.03	960	15.54
Mean±S.D	202.4±10.0	-	42.5±2.2	5.25±0.40	910±73	14.81±0.93

## 3.2. Microscopic observations

### 3.2.1. Light microscopy of the ovary in the non-gravid root-rat.

The ovary of the non-pregnant root-rat had a single layer of low columnar cells forming the surface (germinal) epithelium (Fig. 7). Beneath the surface was a continuous layer of tunica albuginea. This layer was relatively thick and consisted of dense regular connective tissue fibres which stained distinctly with Goldner stain (Fig.8).

The two zones of the ovary were clearly distinguishable. The outer zone, the cortex, contained follicles, corpora lutea and other glandular structures. The follicles appeared to be in various stages of development and include primordial, primary, secondary, vesicular and atretic follicles. The primordial follicle had an oocyte surrounded by single layer of squamous cells, and a primary follicle had simple low cuboidal cells (Fig. 9). A secondary follicle had two or more layers of cuboidal cells. A vesicular follicle showed inner and outer granulosa cells, and a well developed zona pellucida. An antrum was present in most of the secondary and vesicular follicles. Atretic follicles were those in the process of degeneration. Secondary, vesicular and atretic follicles had distinct granulosa cells and thin thecal cell layers.

Interstitial glandular tissue was present in all the ovaries, and was divided into polygonal masses by the stromal connective tissue

(Fig. 10). The interstitial gland cells had a coarse vacuolar cytoplasm with round polychromatic nuclei.

The reticular fibres in the cortex were perpendicular to the ovarian surface, except where the follicles and corpora lutea occurred. The fibres relating to the follicles and corpora lutea formed semi-circular bundles along the borders of these structures. Just beneath the tunica albuginea most of the reticular fibres fanned out to run parallel to the surface of the ovary.

The inner zone, the medulla, consisted mainly of large blood and lymph vessels supported by loose connective tissue. The medulla also contained interstitial gland tissue and in some ovaries it had atretic follicles.

### 3.2.2. The ovary of pregnant root-rats.

The ovary of the pregnant root-rat was found to be non-lobulated and generally smooth, except where large follicles and corpora lutea projected prominently on the ovarian surface (Fig. 11). In most of the root-rats the ovary corresponding to the pregnant uterine horn contained one large corpus luteum and two or more accessory corpora lutea irrespective of the number of foetuses. The ovary on the non-gravid side had varying numbers of corpora lutea which appeared relatively smaller in size. The corpora lutea of pregnancy occupied a relatively large part of the ovarian stroma (Fig. 11).

A fully developed corpus luteum in early pregnancy consisted of a solid mass of large round luteal cells with round nuclei and

prominent nucleoli (Fig 12). These cells, which formed the *theca interna* layer, were well supplied with sinusoidal blood. Along the periphery of the corpus luteum and the vascular stromal connective tissue were smaller cells which had oval nuclei and formed the *theca externa*. As pregnancy progressed the corpus luteum became more vascularized and was filled with more connective tissue elements. In late pregnancy the corpus luteum showed marked shrinkage and degeneration. The luteal cells had intracytoplasmic vacuoles, deeply basophilic pyknotic nuclei, and lightly staining cytoplasm.

### 3.2.3. The pregnant uterus.

The pregnant uterine horns were identified by the locular swellings (Fig.13) or the presence of developing foetuses. Root-rat number twelve had two embryos in the right horn and none on the left horn. Placental scars were a common feature in most of the uteri examined.

Histologically the pregnant uterus was characterized by a well developed endometrium which had well developed blood vessels. The uterine wall had relatively abundant stromal connective tissue and relatively little glandular tissue (Fig. 14). At the implantation sites most of the uterine glands had been displaced by the decidual cells especially on the mesometrial side.

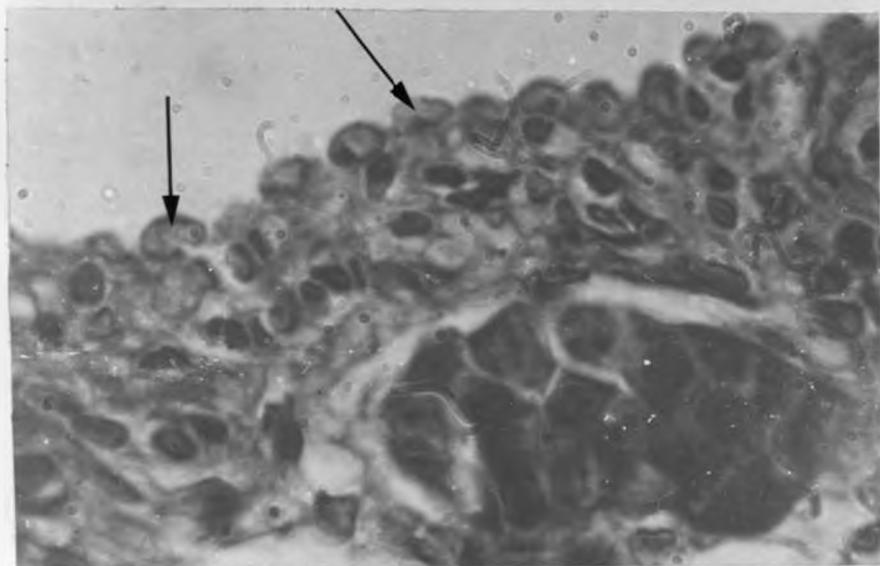


Figure 7. This is part of a histological section of the outer zone (cortex) of the ovary showing the single layer of low columnar cells of the surface epithelium (arrows). H.E. X250.

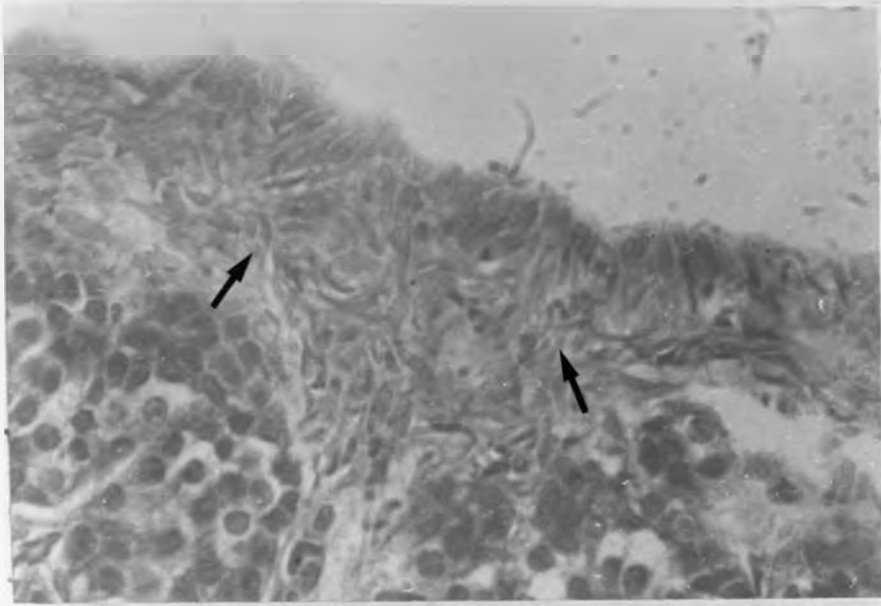


Figure 8. Section of the superficial layer of the cortex showing part of the continuous tunica albuginea (arrows) below the surface epithelium. Goldner X160.

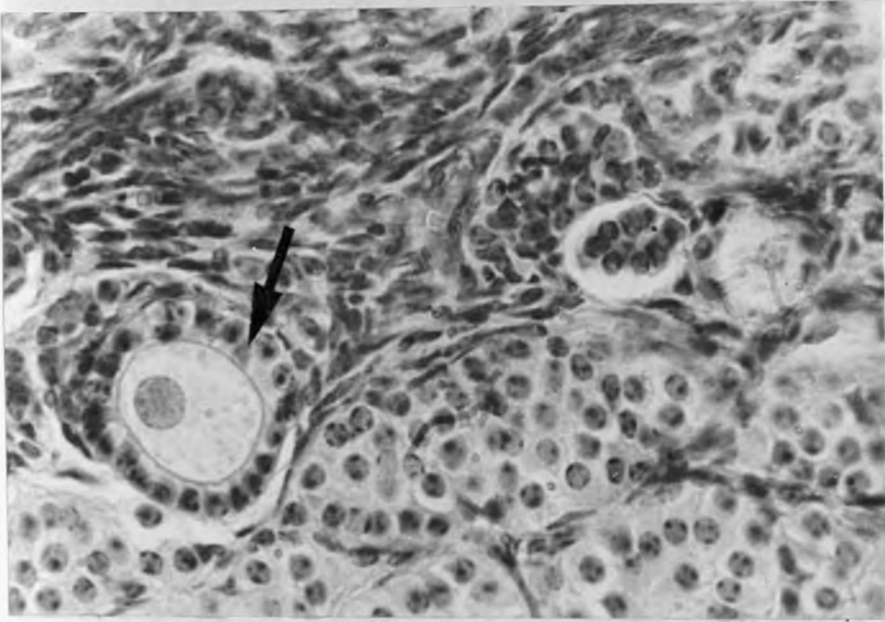


Figure 9. Photomicrograph to show one of the primary follicles (arrow) in the cortical region of the ovary. H.E. X100.

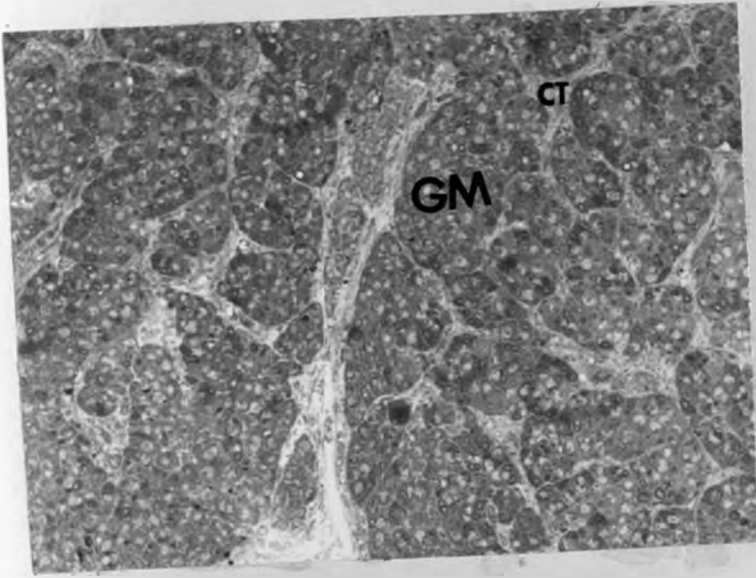


Figure 10. Photomicrograph of the interstitial gland tissue with stromal connective tissue (CT) dividing the gland into masses (GM). H.E X100.

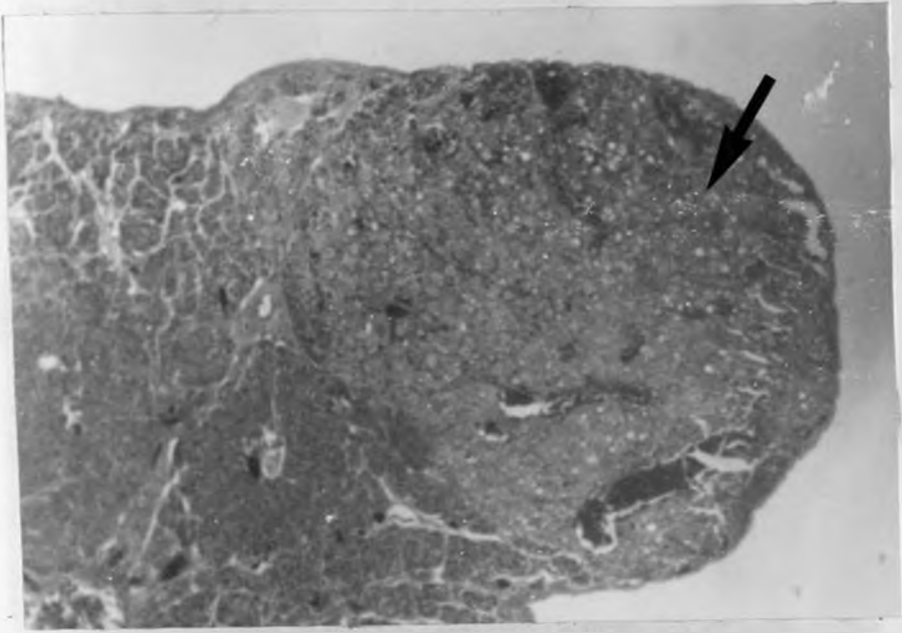


Figure 11. Photomicrograph of a corpus luteum (arrow) of early pregnancy protruding on the ovarian surface. H.E. X60.

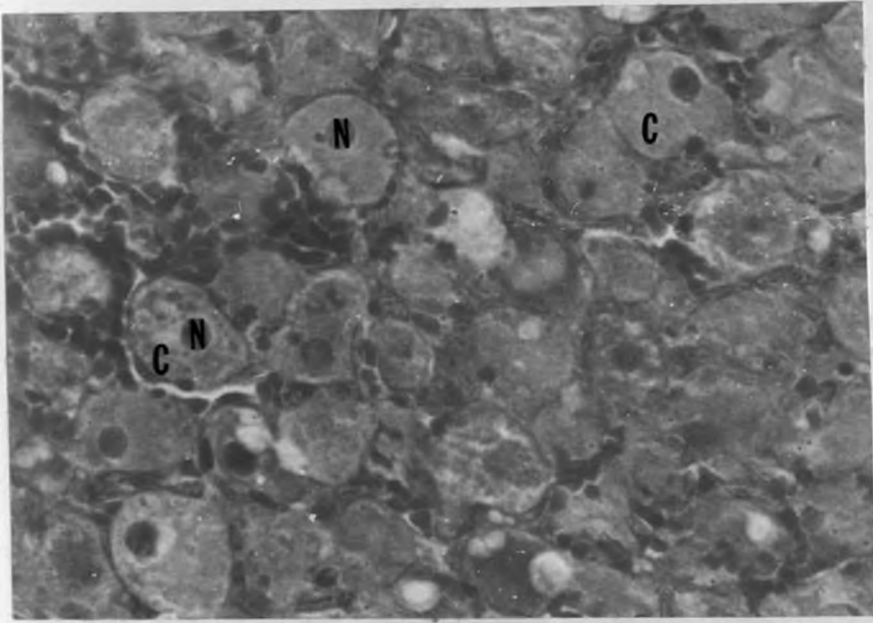


Figure 12. A higher magnification of the cells of the corpus luteum shown in figure 11. Note the uniform distribution of the luteal gland cells (C) and their prominent nuclei (N). H.E. X400.

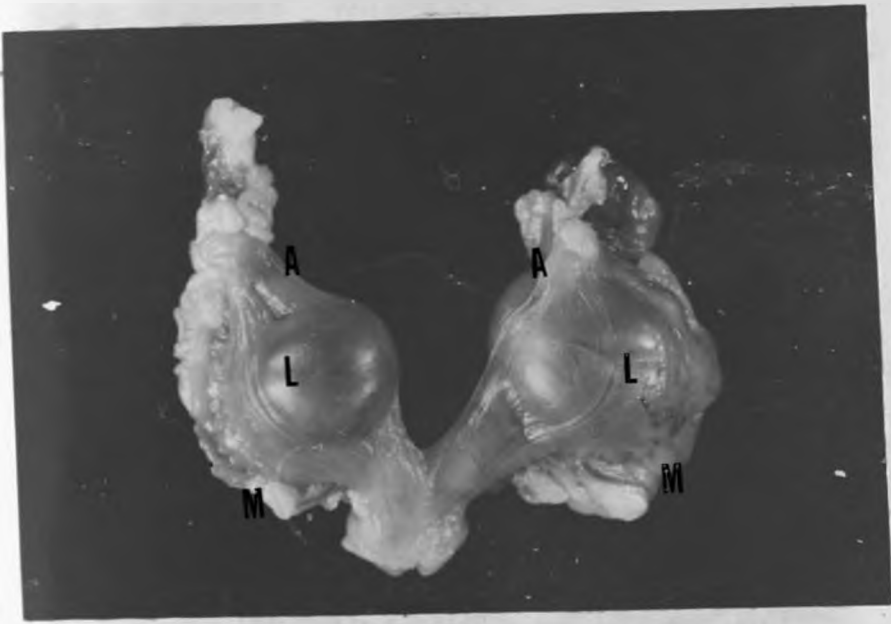


Figure 13. Picture of pregnant uteri to show the locular swellings (L) indicating the site of the developing foetus. A = antimesometrial side; M = mesometrial side.

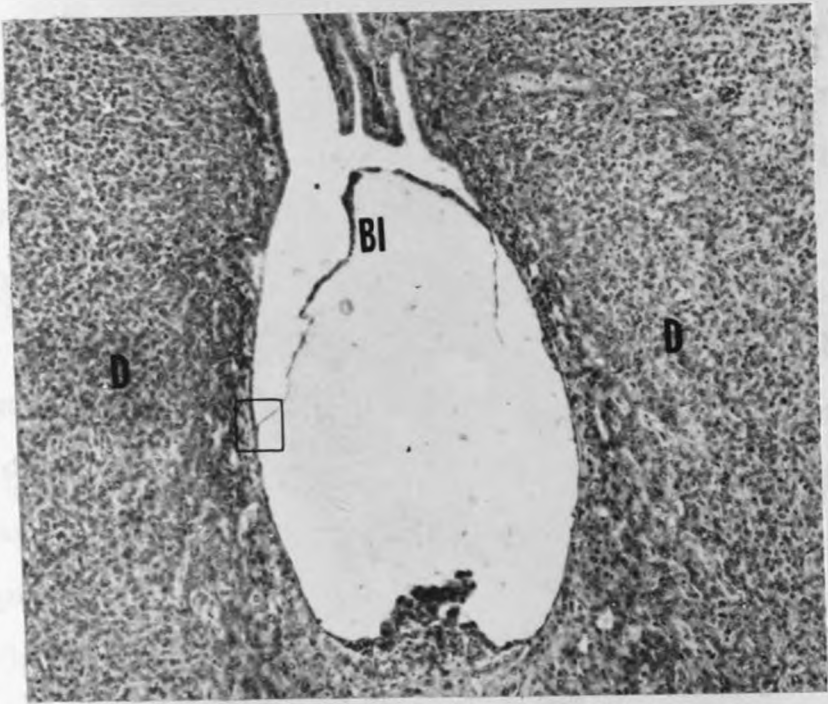


Figure 14. A section through the gestation sac of the root-rat to show the antimesometrial attachment of the blastocyst (BI). Note the advanced decidual reaction (D). H.E. X40

### 3.2.4. Implantation.

The earliest stage of development recognized was in the blastocyst stage (Fig. 14) (root-rats numbers 3 and 8.) The blastocyst initially occupied a shallow diverticulum of the uterine lumen on the antimesometrial side. The inner cell mass was oriented mesometrially and consisted of two layers of cells, an outer ectoderm and inner endoderm. The mesometrial mucosa opposite the implantation chamber was thrown into longitudinal folds each composed of tall columnar epithelium (Fig. 14).

In the blastocyst stage shown in figure 14 the trophoblast cells lining the abembryonic pole appeared to be larger than those at the sides and near the inner cell mass (Fig. 15). In the region where the trophoblast had come into contact with the uterine wall the epithelial lining had undergone degeneration and lost its outline (Fig. 16) such that the blastocyst was now partly encapsulated by stromal cells. Thus the initial implantation pattern in all the root-rats was eccentric; however in the older stages of pregnancy, there was complete breakdown of the epithelial lining of the implantation chamber and the blastocyst lay within the tissue of the uterine wall (Fig. 17). Therefore the root-rat showed an eccentric and secondarily interstitial implantation. The antimesometrial region of the implantation chamber had highly dilated blood vessels. There was a subsequent increased vascular permeability followed rapidly by the development of oedema in the stroma underlying the blastocyst (Figs. 17 & 18).

At the blastocyst stage the maternal decidual reaction was already quite advanced, with marked swelling of the endometrium surrounding the implantation chamber. Most of the decidual cells were large and their nuclei were spherical. Large areas of their cytoplasm appeared clear and vacuolated and the blood vessels were highly distended (Fig. 18).

### 3.2.5. Expansion stage.

This stage of development was observed in root-rat numbers 6 and 9. During the egg-cylinder stage there is rapid proliferation of the endoderm which eventually lines the entire blastocoele and leads to formation of the yolk sac cavity observed in the expansion stage (Fig. 17). The implantation chamber enlarges considerably and the conceptus becomes spherical. This enlargement of the implantation chamber may be due to the elongation of the embryo along mesometrial-antimesometrial axis. The visceral endoderm covers the developing embryo whereas the parietal endoderm cells lie against the Reichert's membrane as sparsely scattered squamous or round cells (Figs. 17 & 19).

Formation of the amnionic and chorionic membranes was not observed but in the expansion stage these membranes were distinct and separate, leaving a large cavity, the exocoelom (Fig. 17). The chorion formed a diaphragm across the exocoelom and as a result three cavities were created, namely a large epamnionic cavity which was temporarily open to the uterine cavity; a large exocoelomic cavity whose roof was formed by the amnion and the

lateral walls by the visceral or proximal endodermal cells while its floor was formed by the chorion (see fig. 17). The third cavity, the amniotic cavity, was enclosed by the amnion which stretched across the dorsal surface of the cup-shaped embryonic disc. The yolk sac wall was lined by a layer of endoderm cells except at the embryonic disc area. At the abembryonic pole the visceral yolk sac wall was reflected back as the parietal yolk sac wall. There was degeneration of the yolk sac ectoderm such that the parietal yolk sac wall was represented by isolated endoderm cells lying against the Reichert's membrane (Fig. 19). There was therefore late inversion of the yolk sac. The epamniotic cavity was only transitory because the growing chorion sagged on to the surface of the ectoplacental cone and fused with it.

Growth of the relatively large allantois into the exocoelomic cavity occurred from the caudal end of the embryo in the angle between the amnion and the visceral yolk sac endoderm. The allantois contained a cavity surrounded by endodermal cells (Figs. 17 & 20). This allantoic vesicle or diverticulum was observed up to the limb bud stage. The allantois was richly supplied by foetal blood which eventually vascularized the chorion to form the chorioallantoic membrane.

### 3.2.6. Development of the chorioallantoic placenta.

At the time of the limb bud stage the allantoic mesenchyme had made contact with the central portion of the chorionic trophoblast, and thus forms the chorioallantoic membrane. This

was followed soon by penetration of villi of vascular chorioallantoic mesoderm into the trager trophoblast (figs. 21 & 22). As these villi penetrated they were accompanied by trophoblast cells of the trager plate. Subsequently the villi irregularly branched and trapped the maternal blood channels between them (figs. 22 & 23). There was now circulation of embryonic blood and the labyrinth zone became established in the early placenta.

As the allantois made contact with the chorion and the trager trophoblast there was inflection of the margins of the developing placenta (see fig. 21). At this stage both the capsular and parietal deciduas had become reduced in size, while the basal decidua was still relatively large. As growth of the placenta continued, the inflected rim finally became acutely bent such that only a thin band of vascular allantoic mesoderm now separated the inflected rim from the placental base, and thus gave the early placenta a pileate shape (fig. 24).

### 3.2.7. The definitive placenta.

The placenta of the root-rat developed its definitive form and structure but not its full size at the foetal crown-rump length of 30 mm (fig. 24). This stage of placental growth was represented in root-rats nos. 4, 5, and 17. The definitive placenta of the root-rat was disc-shaped. The relative thickness of the labyrinth had increased it occupied a greater portion of the placental disc. This thickness was due to the increased growth of the allantoic mesenchyme. Microscopically, the labyrinth was made up of numerous

trophoblastic tubules enclosing maternal blood spaces (Fig. 25). Adjacent to the trophoblastic tubules were the foetal allantoic mesenchyme. The foeto-maternal placental barrier varied in thickness but the closest proximity between the foetal and maternal circulations consisted of a thin layer of trophoblast and the foetal capillary endothelium- thus a haemochorial type of placenta existed (Figs. 25 & 26). The definitive placenta also showed clearly defined endoderm-lined sinuses or placental pits (Fig. 27). These sinuses separated the chorioallantoic mesenchyme from the trophoblast of the placental surface and were mostly located towards the foetal side of the placental disc.

As the placenta matured (36 mm C.R.L.) the labyrinth progressively increased in size and it constituted 75% or more of the placental disc; however the basic structure of the labyrinth remained as described above. An annular zone of trophoblastic giant cells, some of which were binucleate, covered the foetal surface of the placental disc. The outermost layer of these giant cells was bathed in maternal blood and contained large dark staining granules (Fig. 28).

The trophospongium of the mature placenta was relatively thin (see fig 24) and contained a network of venous channels containing maternal blood. These venous channels were lined by an endothelial layer. There were a few giant cells scattered within the stroma of the trophospongium.

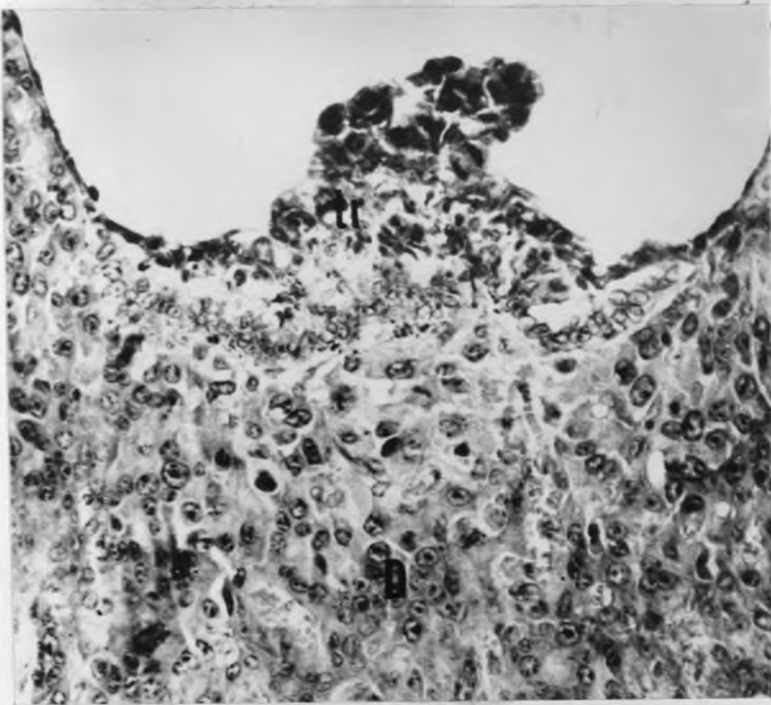


Figure 15. A closer view of the abembryonic pole of the implantation chamber and uterine stroma showing the trophoblast giant cells (tr) and the decidual reaction (D). H.E. X160.

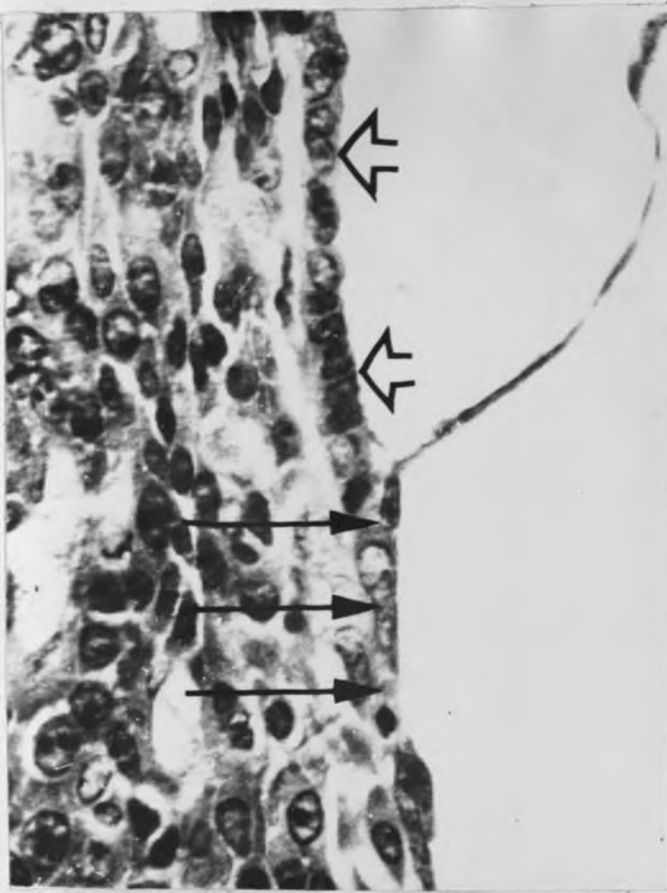


Figure 16. Higher magnification of the squared area in figure 14 showing an area of contact between the uterine wall and blastocyst wall. Note the loss of outline of uterine epithelium (arrows) compared to the area (arrowheads) where no contact has occurred. H.E. X320.

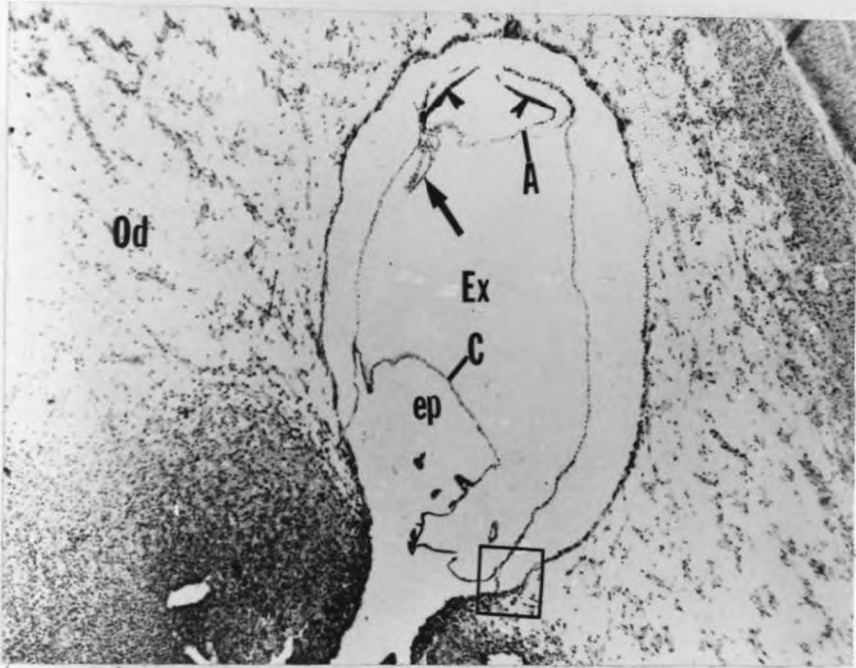


Figure 17. Photomicrograph showing the conceptus in the expansion stage. The trilaminar embryonic disc (arrowheads) attaches to the amnion (A) which is now separated from the chorion (C) by the exocoelom (Ex). The allantois (arrow) protrudes into the exocoelom. Note the oedematous stroma (od). ep = epamniotic cavity. H.E. X40.

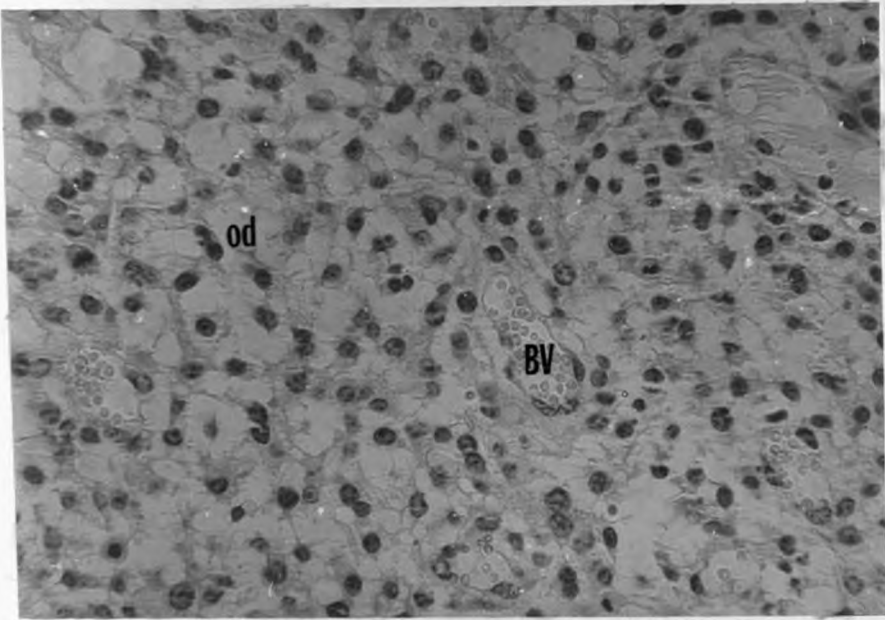


Figure 18. Higher magnification of the decidua during the expansion stage. Note the oedema (od) and the distended blood vessels (BV).  
H.E. X320.

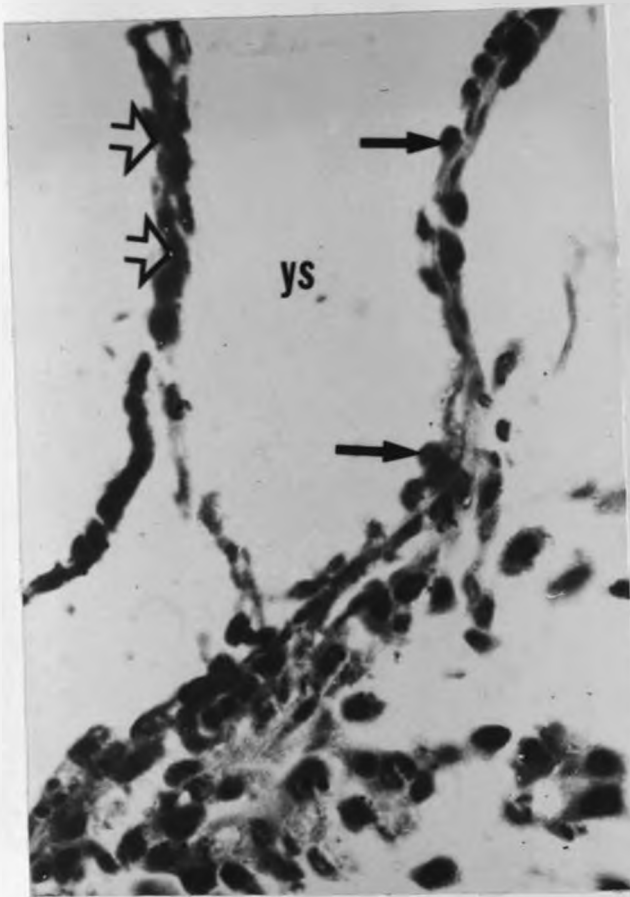


Figure 19. An enlarged view of the square area in figure 17 to show the backward reflection of the parietal yolk sac that continues as the isolated cells of the distal endoderm (arrows) resting on the Reichert's membrane. Arrowheads = visceral endoderm; ys = yolk sac.

H.E. X400.

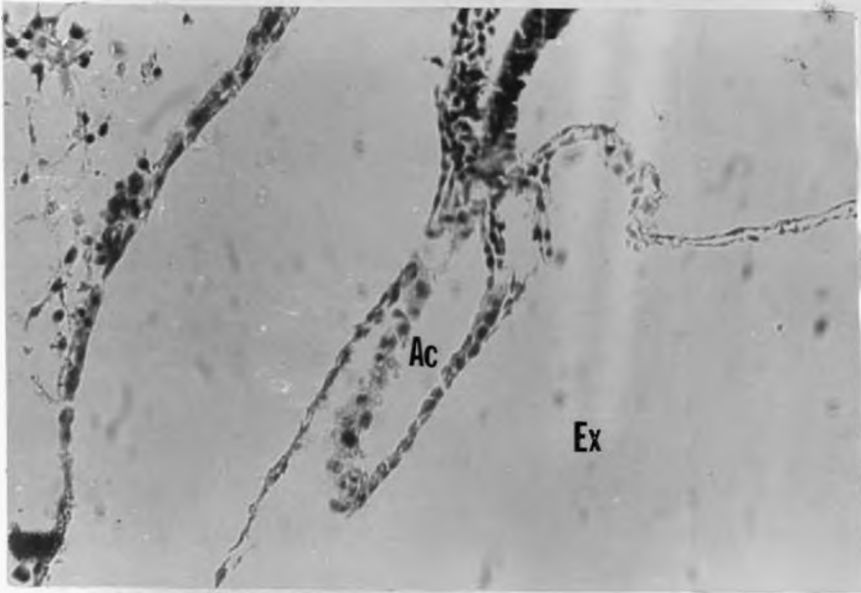


Figure 20. A higher magnification of the allantois. Note the presence of an allantoic cavity (Ac). Ex = exocoelom. H.E. X320.

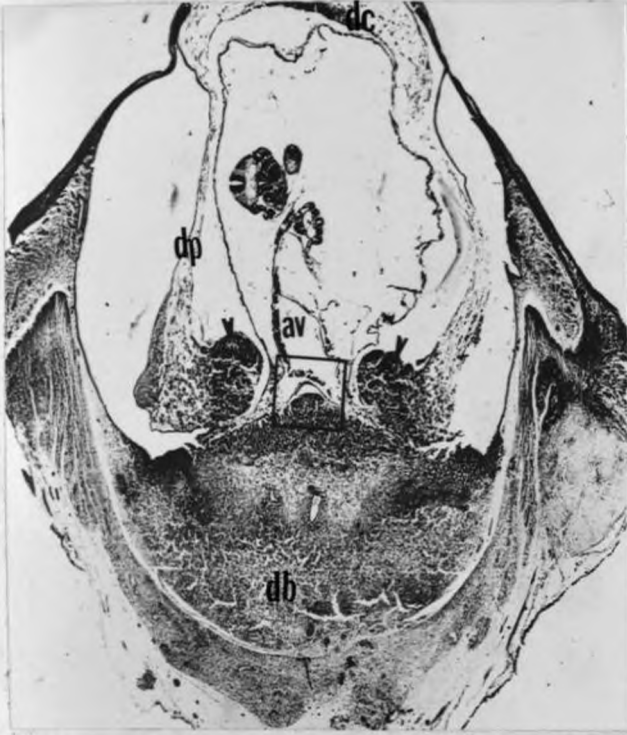


Figure 21. Section through the gestation sac of an early limb bud stage embryo showing the allantoic vesicle (av) and the inflection of the margins (arrowheads) of the early placenta of the root-rat giving it a pileate shape. Note the thinned out decidua capsularis (dc) and decidua.parietalis (dp). db = decidua basalis. H.E. X25.

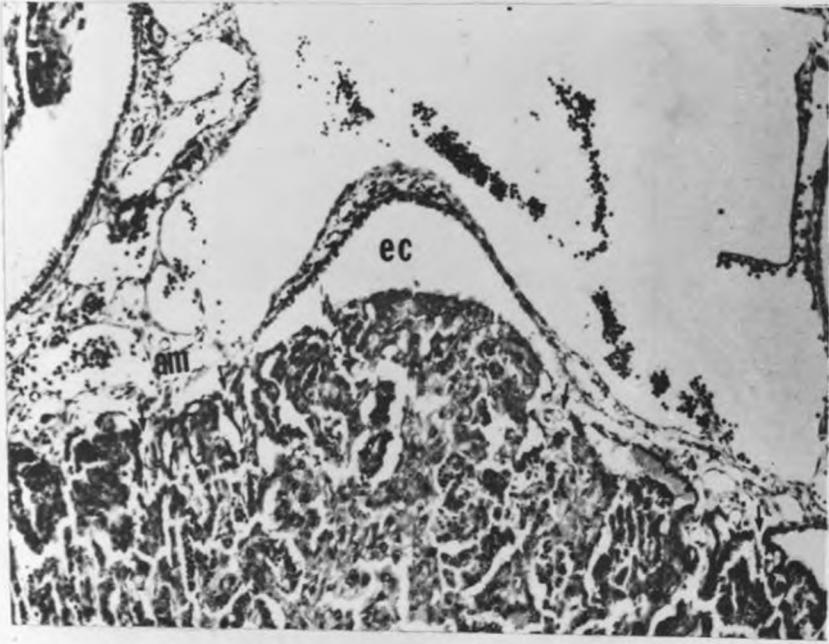


Figure 22. Higher magnification view of the square area in figure 21 showing the invasion of the vascularised allantoic mesenchyme (am) into the chorionic-trager plate. Allantoic mesodermal villi (small arrows) penetrate the plate at irregular intervals. Note the small epamniotic cavity (ec). H.E. X320.

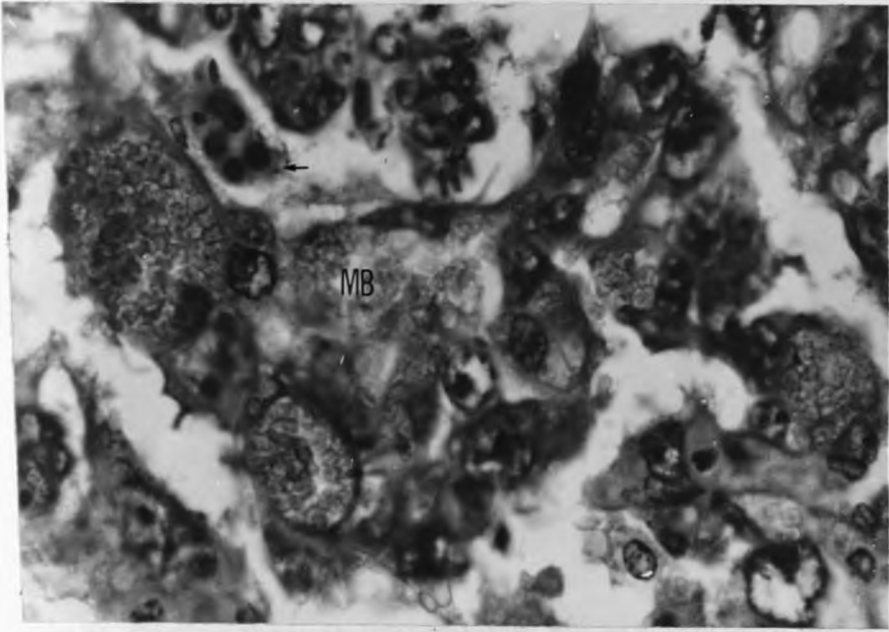


Figure 23. Photomicrograph to show the presence of maternal blood channels (MB) between the irregularly branching villi (small arrows) carrying foetal blood. H.E. X400.

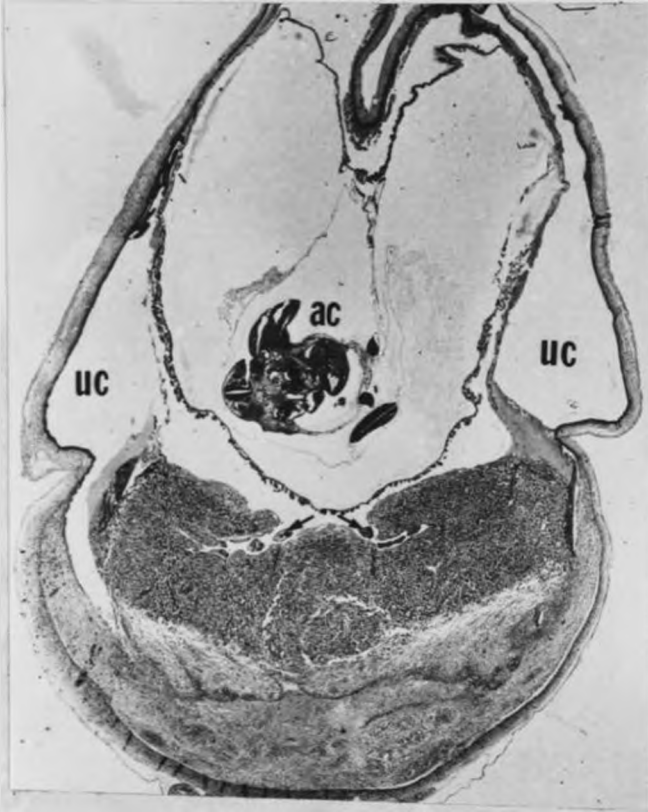


Figure 24. Section through the gestation sac of a late limb bud stage embryo with a well established placenta having a relatively thick labyrinth and a thinner trophospongial zone (dark area). Note the thin band of vascular allantoic mesoderm (small arrows) lying in between the inflected rim and base of the placenta. ac = amniotic cavity; uc = uterine cavity. H.E. X25.

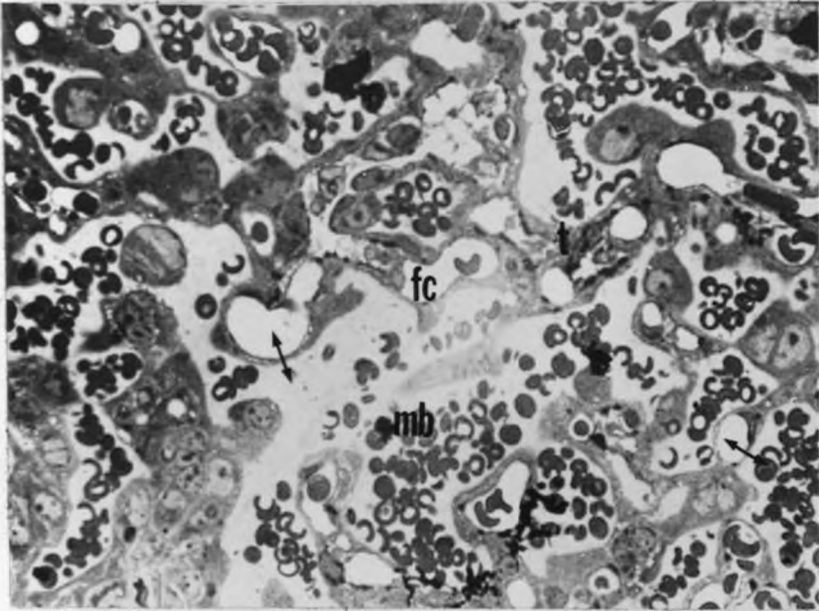


Figure 25. Light micrograph of the placental labyrinth to show the proximity of the foetal and maternal circulations. Note the thinness of the interhaemal membrane (see double-ended arrows). *fc* =foetal capillary; *mb* =maternal blood space; *t* =trophoblast. Toluidine blue. X720.

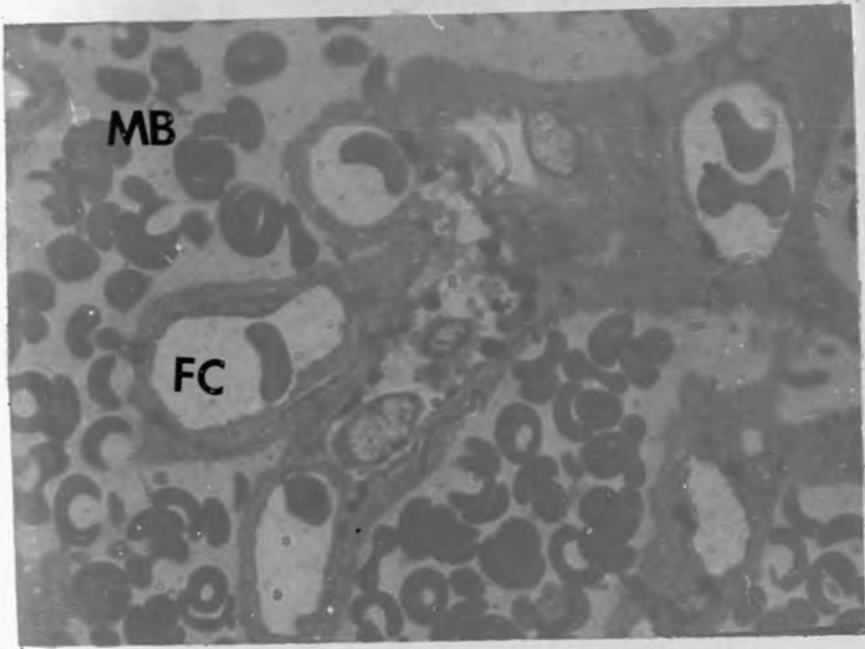


Figure 26. Higher magnification of part of the placental labyrinth to show the marginalization of the foetal capillaries (FC).  
MB=maternal blood spaces. Toluidine blue. X1000.

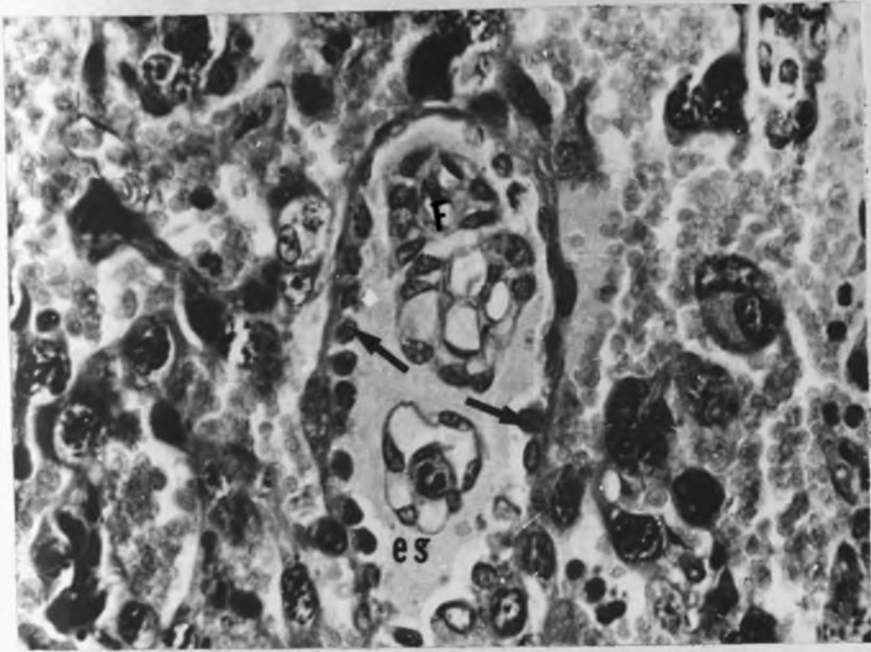


Figure 27. Part of the labyrinth near the surface of the placenta showing an endodermal sinus (ES) lined by endodermal cells (arrows). Note the centrally placed mesenchyme accompanied by foetal capillaries (F).

H.E. X400.

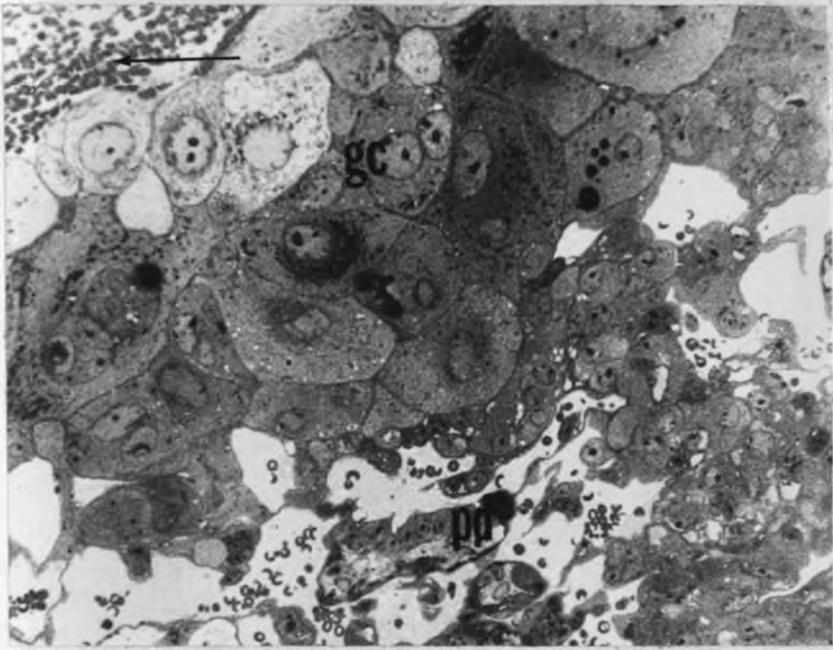


Figure 28. Section through the definitive placenta of the root-rat to show part of the annular zone of giant cells (gc) lining the foetal side of the placental disc (pd). Note the pool of maternal blood (arrow). Toluidine blue. X720.

### 3.2.7.1 Ultrastructural observations on the chorioallantoic placenta.

Ultrastructurally the definitive placenta of the root-rat was found to be labyrinthine and haemotrichorial (Fig. 29). The interhaemal membrane (placental barrier) consisted of three layers of trophoblast and the foetal capillary endothelium. The outer layer of trophoblast facing the maternal blood spaces was cellular and the cell boundaries more distinct (Fig. 29). In the areas where the interhaemal membrane appeared to be thin, the outer trophoblastic layer was relatively much thicker. The cells of the outer trophoblastic layer were thick in the perinuclear area, but attenuated in most other parts. The cells had irregular projections and occasional pinocytotic vesicles on the free surface. The outer layer of trophoblast had very few cellular organelles. The granular endoplasmic reticulum (gER) and mitochondria were the two organelles that were easily identified (Fig. 30). These cytoplasmic organelles were frequently identified in the thicker areas of the cell as compared to the attenuated parts. The shapes and sizes of the mitochondria varied greatly the commonest forms being large round, slender, and elongated. Branching of the mitochondria was commonly observed (Fig. 31). The matrix of the mitochondria was quite dense with numerous tightly packed cristae which were oriented at right angles to the long axis of the trophoblastic cells. The gER was slightly dilated and its cisternal lumina sometimes contained moderately electron dense substances particularly in those cells where there was minimal dilation of the endoplasmic reticulum (Fig. 32). The cisternae had a high number of ribosomes

closely associated with their surfaces. Clusters of free ribosomes were often observed in the outer layer of trophoblast but these were apparently fewer than those associated with the cisternal membranes. The Golgi complex was rarely observed in most cells.

Desmosomes, which appeared to be spaced at regular intervals, were present between the outer layer of trophoblast and the middle layer (Figs. 29 & 32). In between the desmosomes were clear intercellular spaces and it is in these areas that the outer layer of trophoblast was loosely apposed to the middle layer. The middle layer was apparently syncytial as no cell boundaries were present (Fig. 29). This layer showed variations in thickness, being thickest in the region of the nucleus (Fig. 33). This middle layer was relatively thinner than the outer layer and approximately equal in size to the inner layer of trophoblast. The middle layer was relatively more closely apposed to the inner layer than to the outer layer of trophoblast (see fig. 29). The plasma membranes of the cells of the middle and inner layers were therefore closely apposed in most areas where the two layers were in contact. Occasional desmosomes were observed between the plasmalemmae of these two layers of trophoblast (see fig. 33). The cell organelles in the middle layer were less abundant than in the outer layer.

The innermost layer of trophoblast had a continuous layer of cytoplasm and apparently no distinct cell boundaries, and therefore, like the middle layer, it was syncytial. The cytoplasm of this trophoblastic layer contained a few cisternae of gER, few mitochondria and large lipid droplets (Figs. 30, 32 & 33).

Separating the innermost trophoblastic layer from the foetal capillary endothelial cells was a basal lamina. This basal lamina was well developed and appeared as a single relatively dense layer. Distinct cell boundaries, with desmosomes, were present between the capillary endothelial cells. Caveolae could be seen in some parts of the endothelial cells (Fig. 34). In some areas the endothelial cells appeared disjointed suggesting the presence of pores in the endothelial wall. There were occasional irregular folds that projected from the endothelial cell wall into the capillary lumen (see figs. 29 & 33). These were observed mainly at the junctions between endothelial cells.

### 3.2.8. The decidua.

The area of the first decidual reaction was immediately around the implanting blastocyst on the antimesometrial side of the uterus (Fig. 14). The decidual reaction was accompanied by hypertrophy of the uterine tissue in the vicinity of the blastocyst. This resulted in the formation of an "implantation chamber" that bulged antimesometrially from the uterine lumen (see Fig. 14). This implantation chamber had a diameter slightly greater than that of the blastocyst and appeared relatively broad and shallow. The decidual cells were large and had large nuclei with a prominent nucleoli. At the blastocyst stage, most of the decidual cells contained a single nucleus (Fig. 15).

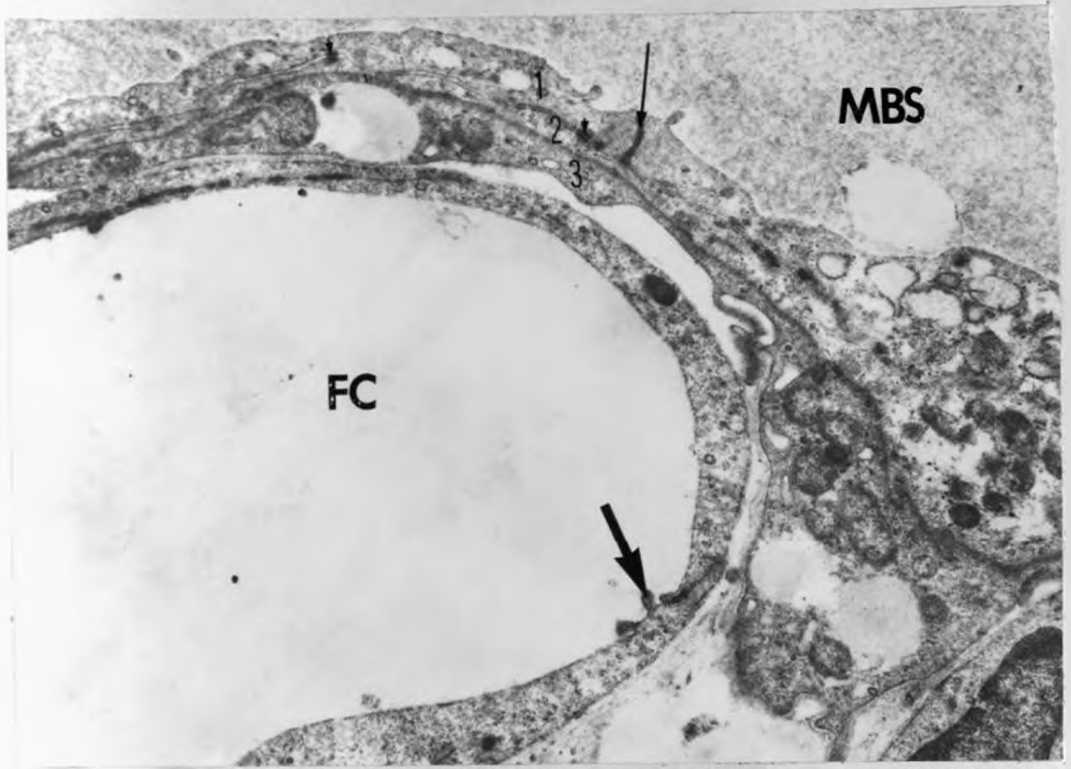


Figure 29. Electron micrograph of the labyrinth of the placenta of the root-rat to show the interhaemal membrane. Note the distinct three layered pattern of the trophoblast (1,2,3). At the lower left is a foetal capillary (FC) while the maternal blood space (MBS) is at the upper right corner. A cell boundary (thin arrow) can be seen in the outer layer of trophoblast. Desmosomes (arrowheads) are exhibited between the outer and middle layers. An irregular fold (thick arrow) projects from the endothelial wall (E). X5000.

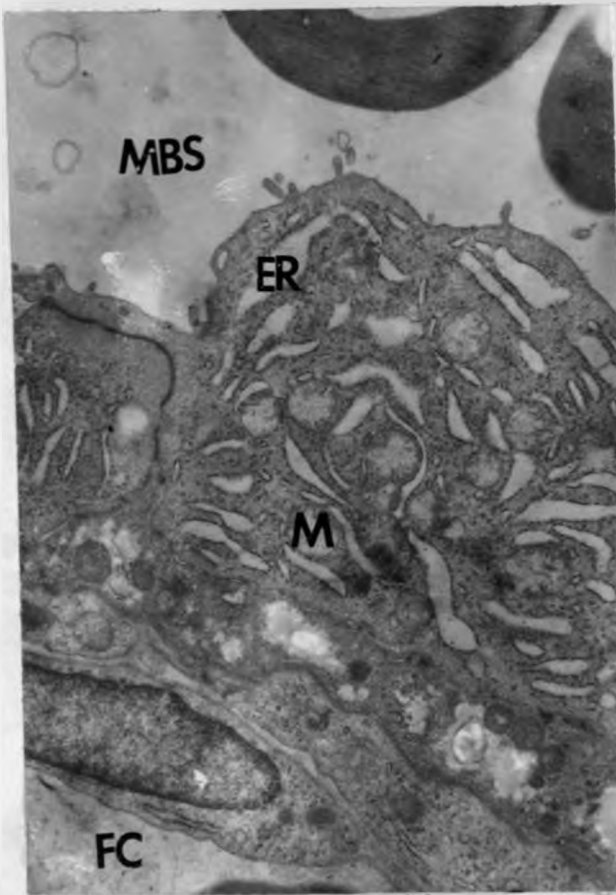


Figure 30. A section of the root-rat interhaemal membrane showing the predominant granular endoplasmic reticulum (ER) and mitochondria (M) in the outer layer of trophoblast. MBS = maternal blood spaces; FC = foetal capillary. X7500.

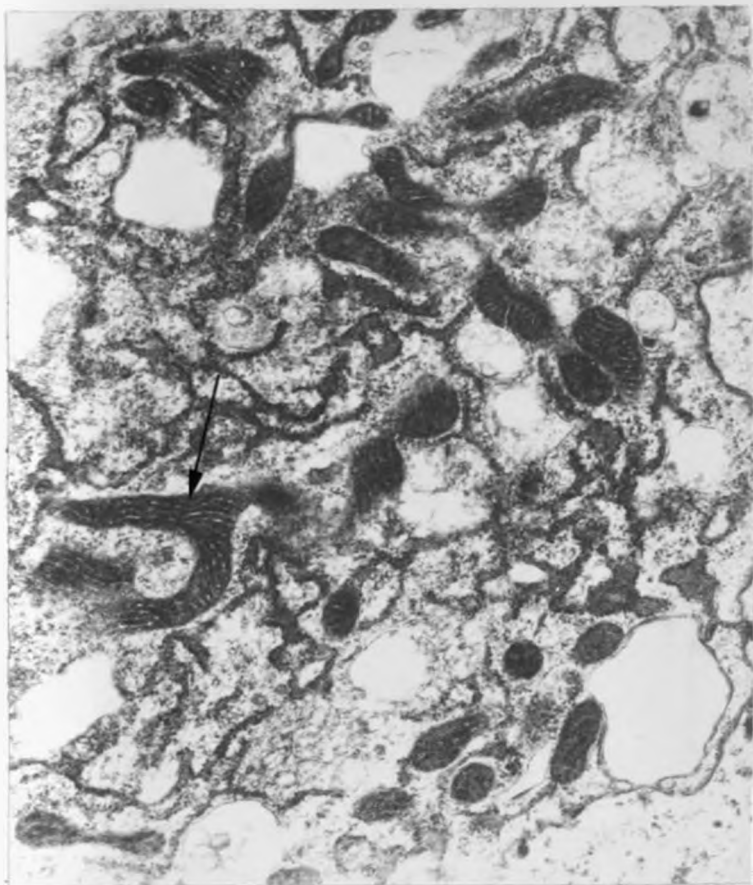


Figure 31. Electronmicrograph of the outer layer of trophoblast showing mitochondrial branching (arrow). X11000.

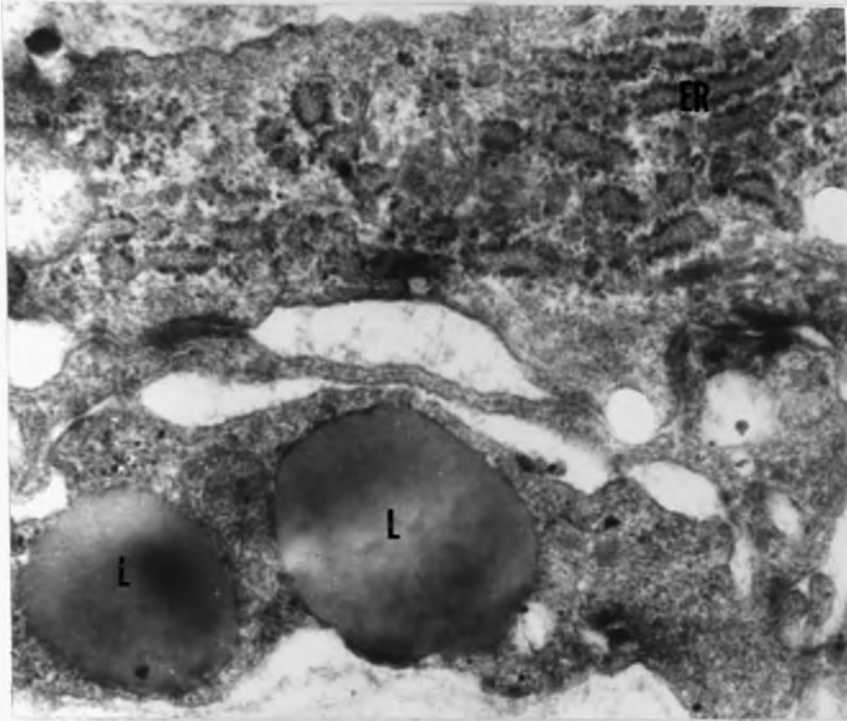


Figure 32. Section through the three layers of trophoblast. Note the dense substance within the lacuna of the granular endoplasmic reticulum (ER) in the outer layer. L = lipid droplets in the inner layer. X8000.

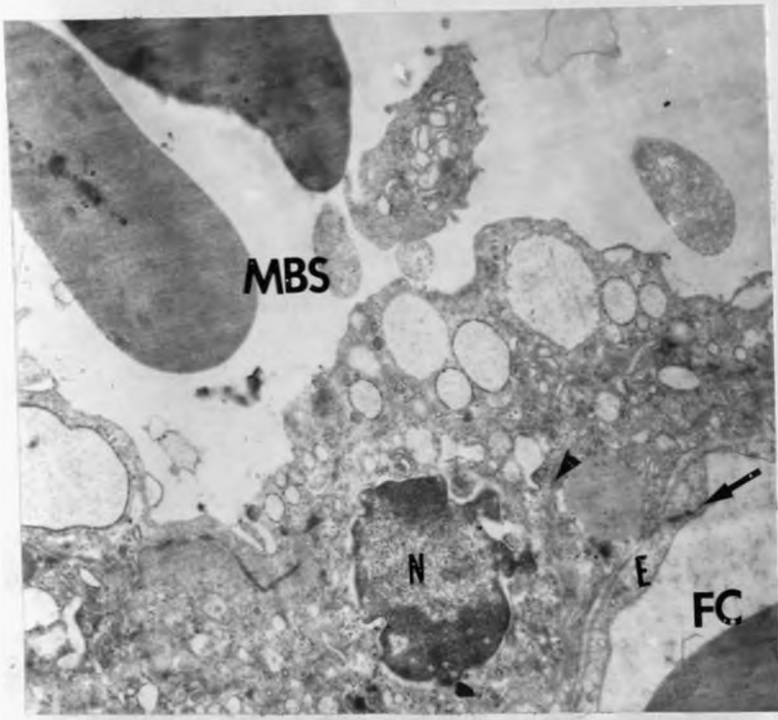


Figure 33. Section showing a thick middle layer at the region of the nucleus (N). Note cell boundary (arrow) of the capillary endothelium (E) and desmosome between middle and inner layers of trophoblast (arrowhead). MBS = maternal blood spaces; FC = foetal capillary. X5000.

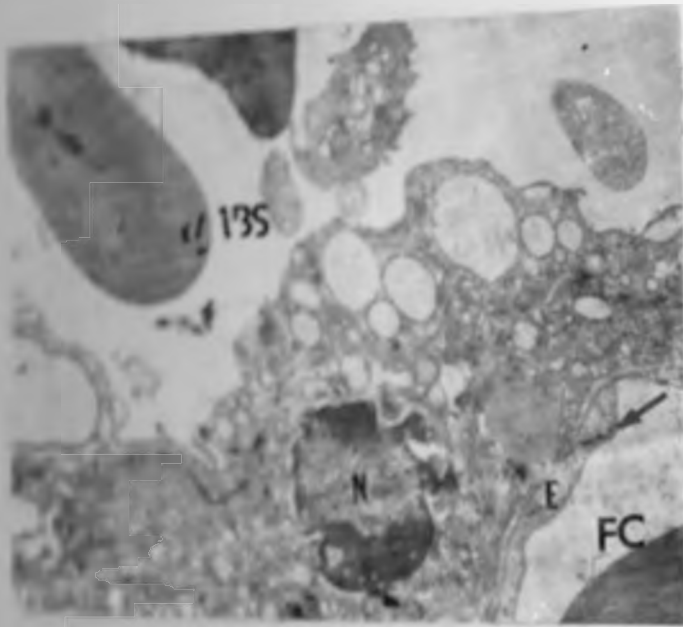


Figure 11 Section showing a thick middle layer at the region of the nucleus (N). Note cell boundary (arrow) of the capillary endothelium (E). MBS = maternal blood spaces; FC = foetal capillary.

135

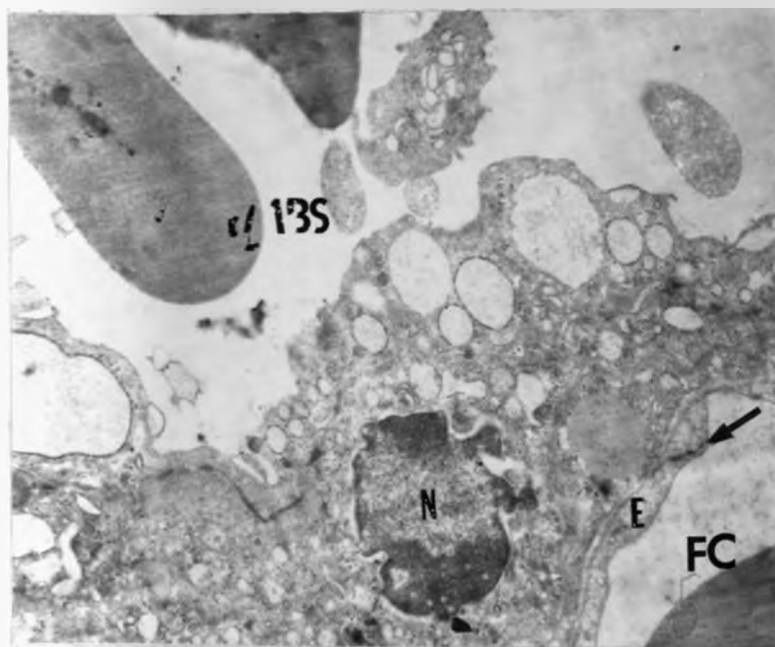


Figure 33. Section showing a thick middle layer at the region of the nucleus (N). Note cell boundary (arrow) of the capillary endothelium (E). MBS = maternal blood spaces; FC = foetal capillary. X5000.

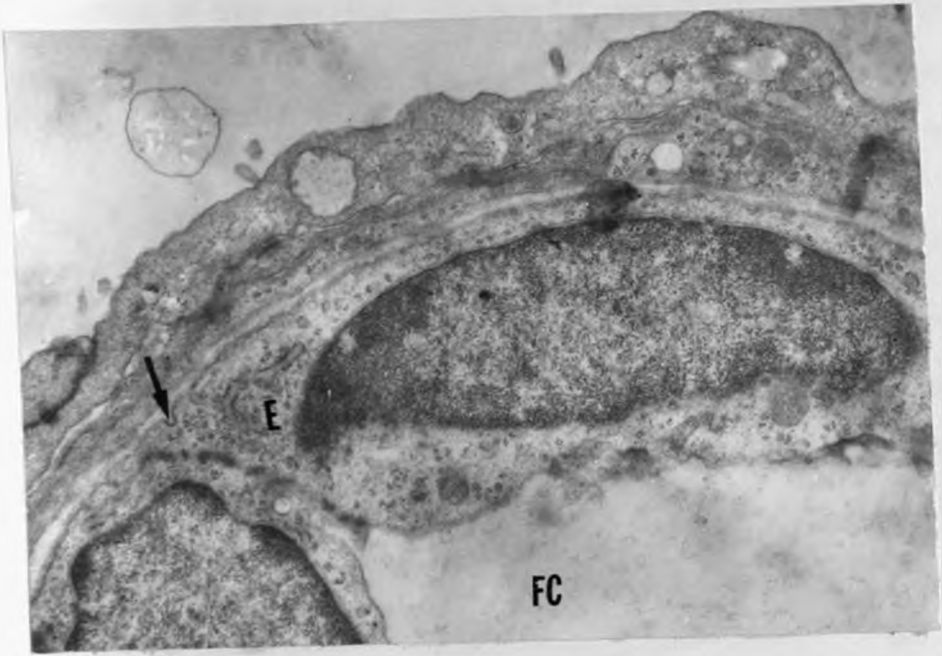


Figure 34. Electron micrograph of the interhaemal membrane showing caveolae (arrow) in the endothelial cells (E) of the foetal capillary (FC). N = nucleus. X7500.

Due to the rapid expansion of the conceptus, both the decidua capsularis and decidua parietalis became stretched and subsequently thinned out. The decidua capsularis was closely bordered by giant cells which may have played a role in the destruction of this decidua. There was very little healthy decidua remaining at this stage. The decidua basalis remained thick unlike the decidua parietalis and decidua capsularis. There were eosinophilic granular cells observed in the decidua basalis.

As pregnancy advanced, there was a marked thinning and degeneration of the decidua capsularis and parietalis (Fig. 21) and in some instances no trace of these decidua remained. Likewise large venous channels draining the placenta passed through the decidua basalis giving it a spongy appearance (Fig.21). Necrotic areas were observed in some regions of the decidua basalis adjacent to the trophospongial zone.

### 3.2.9. The foeto-maternal circulation within the labyrinth.

Maternal blood circulates in the trophoblastic tubules which border the foetal capillaries (see fig. 25). In some areas within the labyrinth the placental membrane or barrier was thin, and thus facilitated the close approximation of the maternal tubules and foetal capillaries (Figs. 25 & 26). This arrangement indicated that the placenta of the root-rat may have a foeto-maternal counterflow arrangement.

The maternal arterial blood, which originates from the uterine artery, is carried through the decidua basalis towards the

foetal surface of the placenta. From the foetal surface the artery divides into smaller branches which then enter the labyrinthine zone. The maternal blood then drains into the base of the placenta where it is collected in large thin-walled veins.

### 3.3. The Yolk sac, the Amnion and the Allantois

At the expansion stage (see fig. 17) two regions of the yolk sac wall could be identified, that is the parietal and visceral walls. The ectodermal cells of the parietal yolk sac wall had disappeared resulting in the Reichert's' membrane lying directly in contact with the uterine tissues (Fig. 17 & 19). The endodermal cells appeared as a single layer placed at regular intervals. The visceral or vascular portion of the yolk-sac lay relatively close to the endoderm of the bilaminar omphalopleure. These developmental events give rise to the late inversion of the yolk sac. Eventually, the Reichert's membrane and endodermal cell layer of the bilaminar omphalopleure disintegrated, and thus the visceral yolk sac came into contact, through its endoderm, with the uterine stroma. This resulted in complete inversion of the yolk sac thus forming the foetal component of the inverted yolk-sac placenta which persists till term (Fig. 35). The yolk sac wall subsequently becomes well vascularized and the mesometrial portion close to the placental disc shows considerable folding which gives the yolk sac a villous appearances (Figs.35 & 36).

Figure 17 shows the amnion stretching across the dorsal surface of the cup-shaped embryonic disc. The amnion was formed

by an inner layer of flattened ectodermal cells and an outer layer of mesoderm.

As mentioned earlier the allantois developed at the caudal end of the embryo (Fig. 17) and contained an allantoic cavity lined by endodermal cells. Eventual growth and contact of the allantois with the chorion resulted in the formation of the chorioallantoic membrane. An allantoic vesicle was present up to the limb-bud stage. The allantoic mesoderm was well vascularized with allantoic blood vessels.

#### **3.4. The haemophagous-like organ.**

The complete breakdown of the decidua parietalis and capsularis and the rupture of the Reichert's membrane, results in the accumulation of a massive pool of maternal blood and tissue debris between the inverted vascular yolk sac and the margins of the placental disc (Fig. 35 & 36). The inverted yolk sac was now bathed in the pool of blood which gave the marginal borders of the placenta a greenish colour. Dense granules were observed in the cytoplasm of the cytotrophoblastic giant cell layer on the foetal side of the placenta bordering the haemophagous-like organ (Fig. 36). Similar granules were also observed in the cells of the visceral yolk sac wall bordering the haematoma.

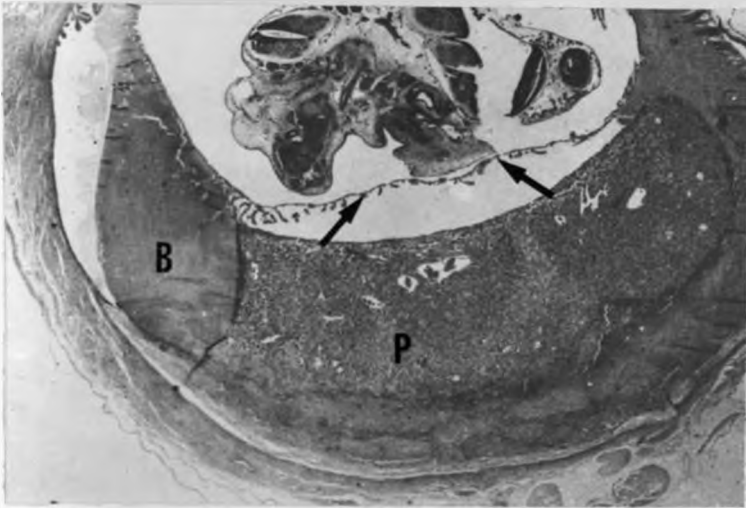


Figure 35. Photomicrograph through a gestation sac of a late term pregnancy root-rat. Note the inverted portion of the yolk sac placenta (arrows) which persists till term. P = placenta. B = accumulated pool of maternal blood. H.E. X20.

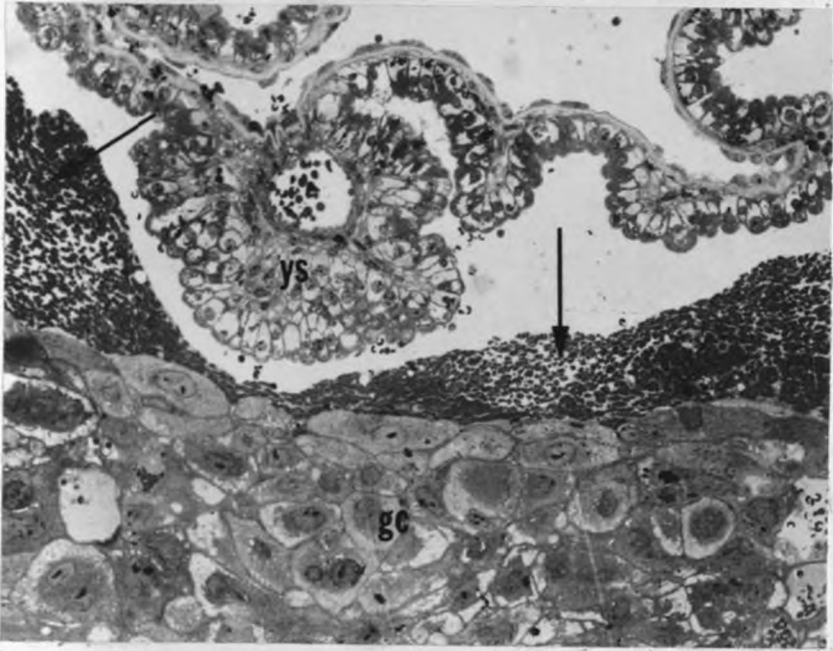


Figure 36. Section showing part of the pool of maternal blood and tissue debris (arrows) lying at the placental margins in between the giant cells of the placental disc (gc) and the vascular yolk sac (ys ). Toluidine blue. X720.

### 3.5. Quantitative observations

#### 3.5.1. The maternal and foetal body weights and the volume of the placenta.

Table IV shows the body weights of the root-rats and their foetuses, the placental diameters, and the placental volume of the five animals used for the morphometric studies. The body weights of the root-rats ranged from 190 g to 215.65 g and the mean ( $\pm$ S.D.) value was  $202.4 \pm 5.9$  g. The weights of the foetuses ranged from 4.90 g to 6.03 g and the mean ( $\pm$ S.D.) value was  $5.25 \pm 0.23$  g. The diameter of the placental discs ranged from 13.52 mm to 16 mm the mean ( $\pm$ S.D.) being  $14.81 \pm 0.52$  mm. The range of the placental volume fell between  $780 \text{ mm}^3$  to  $970 \text{ mm}^3$  and the mean ( $\pm$ S.D.) volume was  $910 \pm 40 \text{ mm}^3$ .

#### 3.5.2. The stereological parameters of the root-rat placenta.

Figure 37 shows the application of the A-100 lattice test grid on the placental sections in order to sample points and intersections and to measure the harmonic mean distance. Point sampling was used to estimate the volume density of the placenta components namely the parenchyma and non-parenchyma, the maternal blood spaces, the interhaemal tissue barrier, and the foetal capillary bed. Intersection sampling was used to estimate the surface density of the maternal erythrocytes, the maternal blood spaces, the interhaemal trophoblast, the foetal capillary endothelium, and the foetal erythrocytes. Intercept length measurements were used to

estimate the harmonic mean thickness of the foeto-maternal placental barrier. The values estimated for the trophoblastic surface area and the harmonic mean thickness were used to calculate the placenta oxygen diffusing capacity. The results are shown in tables V, VI, VII, and VIII.

The volume density of the placental parenchyma ranged from 84.43 to 91.57% and the mean value was 89%, whereas that of the non-parenchyma ranged from 8.4 to 13.4 the mean value being 11.3% (Table V). The placental parenchyma comprised about 50% maternal blood spaces ( $401 \pm 9 \text{ mm}^3$ ), 41% interhaemal tissue ( $330 \pm 19 \text{ mm}^3$ ), and 9% foetal capillary bed ( $76.3 \pm 3.6 \text{ mm}^3$ ). Thus the maternal blood spaces were approximately 4-6 times more voluminous than the foetal capillary bed (Table VI).

Table VII shows the values for the surface densities of the maternal erythrocytes, maternal blood spaces, the foetal capillary endothelium, foetal erythrocytes and the interhaemal trophoblast of the placental barrier. The highest mean ( $\pm$ S.D.) value for membrane surface area was that of the maternal red blood cells ( $1200 \pm 76 \text{ cm}^2$ ) and the lowest was that for foetal erythrocytes ( $168 \pm 10 \text{ cm}^2$ ). The mean ( $\pm$ S.D.) value for the surface area of the maternal blood spaces was  $591 \pm 32 \text{ cm}^2$ , that for the foetal capillary endothelium was  $455 \pm 24 \text{ cm}^2$  and that for the trophoblast of the interhaemal barrier was  $259 \pm 16 \text{ cm}^2$  (see Table VIII).

The value for the harmonic mean thickness ranged from 1.95  $\mu\text{m}$  to 2.49  $\mu\text{m}$  and the mean ( $\pm$ S.D.) value in all the five animals was  $2.32 \pm 0.11 \mu\text{m}$  (Table VIII).

The overall (total) diffusing capacity of the placenta ranged from 0.0217 to 0.0290  $\text{cm}^3 \cdot \text{min}^{-1} \cdot \text{mmHg}^{-1}$ , and the mean ( $\pm$ S.D.) value was  $0.0248 \pm 0.0028 \text{ cm}^3 \cdot \text{min}^{-1} \cdot \text{mmHg}^{-1}$ . The specific diffusing capacity ranged from 4.23 to 5.21  $\text{cm}^3 \cdot \text{min}^{-1} \cdot \text{mmHg}^{-1} \cdot \text{Kg}^{-1}$ , and the mean ( $\pm$ S.D.) value in all the animals was  $4.73 \pm 0.33 \text{ cm}^3 \cdot \text{min}^{-1} \cdot \text{mmHg}^{-1} \cdot \text{Kg}^{-1}$ . (Table VIII).

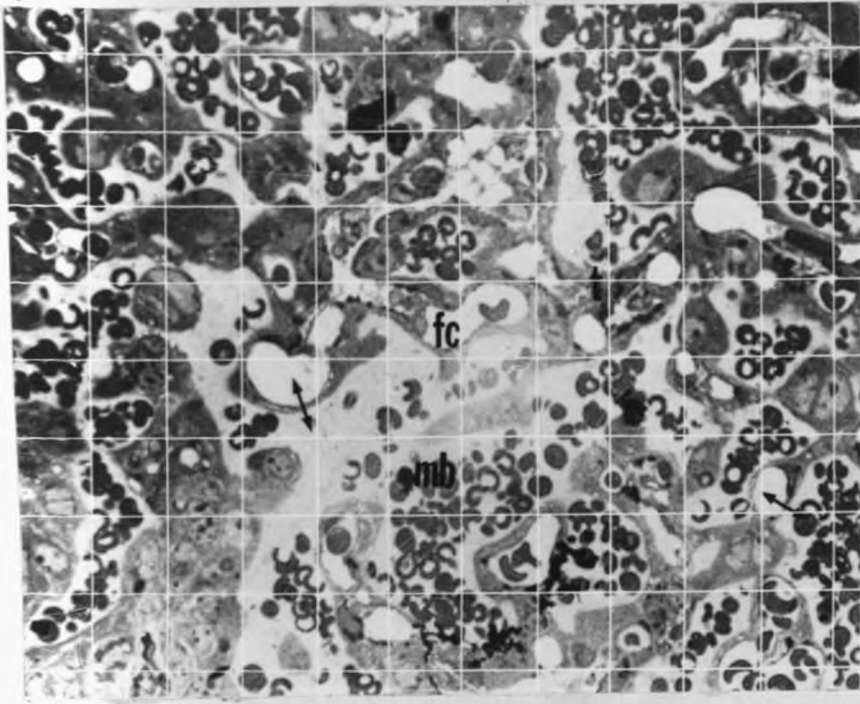


Figure 37. Photomicrograph of placental labyrinth shown in figure 25 with a superimposed lattice test system illustrating its use in estimating the parameters of various parenchyma components using point and intersection counts and measuring barrier thickness. Length of test lines = 10 mm

Toluidine blue, x 720

Table V. The volume densities (%) and absolute volumes ( $\text{mm}^3$ ) of the main components of the late-term placenta, namely the parenchyma (p) and non-parenchyma (np), of the root-rat.

Specimen	parenchyma (p)		non-parenchyma (np)	
	(%)	( $\text{mm}^3$ )	(%)	( $\text{mm}^3$ )
1	86.58	675	13.4	105
2	84.43	819	15.5	151
3	89.41	858	10.6	102
4	91.57	806	8.4	74
5	91.18	875	8.6	85
Mean $\pm$ S.D	88.63 $\pm$ 2.74	807 $\pm$ 70	11.3 $\pm$ 2.8	103 $\pm$ 26

Table VI. Volume densities (%) and absolute volumes (mm<sup>3</sup>) of the components of the parenchyma of five root-rats.

Specimen	Maternal blood spaces		Interhaemal barrier		Foetal capillary bed	
	(%)	(mm <sup>3</sup> )	(%)	(mm <sup>3</sup> )	(%)	(mm <sup>3</sup> )
1	49.87	337	40.35	272	9.79	66.1
2	49.82	408	40.06	328	10.23	83.0
3	49.07	421	42.46	364	8.47	72.7
4	49.60	400	40.09	323	10.31	83.1
5	50.01	438	41.21	361	8.76	76.7
Mean±S.D.	49.67±0.33	401±34	40.83±0.91	330±33	9.47±0.74	76.3±6.5

Table VII. Surface densities of maternal erythrocytes ( $S_{vme}$ ), maternal blood spaces ( $S_{vms}$ ), the foetal capillary endothelium ( $S_{vc}$ ), foetal erythrocytes ( $S_{vfe}$ ) and the interhaemal (trophoblast) barrier ( $S_{vt}$ ) in the root-rat.

Specimen	$S_{vme}$ ( $\text{cm}^2 \cdot \text{cm}^{-3}$ )	$S_{vms}$ ( $\text{cm}^2 \cdot \text{cm}^{-3}$ )	$S_{vc}$ ( $\text{cm}^2 \cdot \text{cm}^{-3}$ )	$S_{vfe}$ ( $\text{cm}^2 \cdot \text{cm}^{-3}$ )	$S_{vt}$ ( $\text{cm}^2 \cdot \text{cm}^{-3}$ )
1	1396	723	564	201.2	351
2	1452	745	585	202.1	277
3	1380	702	574	212.8	330
4	1489	734	535	209.0	306
5	1468	755	560	213.8	346
Mean	1437	732	564	207.8	322
S.D	42	18	17	5.3	27

Table VIII. Surface areas of the maternal erythrocytes ( $S_{me}$ ), maternal blood spaces ( $S_{ms}$ ), the foetal capillary endothelium ( $S_c$ ), foetal erythrocytes ( $S_{fe}$ ) and the trophoblast of the interhaemal barrier ( $S_t$ ) in the root-rat. Values for harmonic mean thickness ( $\tau_h$ ) and overall and specific placental oxygen diffusing capacity ( $D_p$ ) are included.

Specimen	$S_{me}$ ( $cm^2$ )	$S_{ms}$ ( $cm^2$ )	$S_c$ ( $cm^2$ )	$S_{fe}$ ( $cm^2$ )	$S_t$ ( $cm^2$ )	$\tau_h$ ( $\mu$ )	Overall $D_p$ ( $cm^3 \cdot min^{-1} \cdot$ $mmHg^{-1}$ )	Specific $D_p$ ( $cm^3 \cdot min^{-1} \cdot$ $mmHg^{-1} \cdot$ $kg^{-1}$ )
1	940	488	381	136	237	2.40	0.0227	4.54
2	1200	610	479	166	227	2.34	0.0217	4.23
3	1200	602	493	183	283	2.41	0.0271	5.21
4	1200	592	431	168	247	1.95	0.0237	4.84
5	1300	661	490	187	303	2.49	0.0290	4.81
Mean $\pm$ S.D	1200 $\pm$ 120	591 $\pm$ 57	455 $\pm$ 43	168 $\pm$ 18	259 $\pm$ 29	2.32 $\pm$ 0.19	0.0248 $\pm$ 0.0028	4.73 $\pm$ 0.33

## Chapter 4.

### 4.0. DISCUSSION AND PHYLOGENETIC CLASSIFICATION

#### 4.1. The ovary

The ovary of the root-rat, like those of other rodents (Mossman, 1966; Mossman & Duke, 1973), is enclosed in an ovarian capsule and is invested by a thick tunica albuginea. Two or more follicles ripen during estrum to give rise to multiple corpora lutea during pregnancy. Accessory corpora lutea are commonly observed in the ovaries of the root-rat. These findings are similar to those made on the root-rat by Jarvis (1969a,b) and Jarvis and Sale (1971). The presence of numerous accessory corpora lutea has been demonstrated in a number of animals, for example in the Hystricomorphs (Mossman & Judas, 1949; Mossman, 1966; Weir, 1966, 1971a; Oduor-Okelo, 1978), elephant shrew (Horst & Gillman, 1911) and some antelopes (Kayanja, 1972). These corpora lutea have been found to arise from atretic follicles (Mossman & Duke, 1973). The occurrence of large numbers of accessory corpora lutea in the root-rat is unique among the myomorph rodents. It has been shown, for example, that in the laboratory white rat the presence of true accessory corpora lutea is a rare occurrence (Hall, 1952).

During pregnancy the thecal gland tissue appeared to be well developed. This phenomenon has been observed in the ovaries of the jumping mice ( *Zapus & Napaezapus* ), whose theca interna was several layers thick, and also in the pocket gophers ( *Geomys & Thomomys* ) (Mossman, 1966; Mossman & Duke, 1973).

Most members of the hystricomorphs show poorly developed thecal gland tissue only a few cells thick; in addition this tissue is often absent in some areas of the follicle (Mossman & Duke, 1973). However it has been observed that in the cane rat (*Thryonomys swinderianus*) the theca interna cells are several layers thick during pregnancy (Oduor-Okelo, 1978). Initial investigations on the function of the thecal gland indicated that it may be a source of estrogens (Corner, 1938). More recent histochemical and electron microscopic studies have shown that these glands are steroid secretors (Belt & Pease, 1956; Falk, 1959; Tam, 1971, 1972). It is likely that the thecal gland in the root-rat ovary may perform a similar function.

The amount of interstitial gland tissue in the root-rat ovary was relatively abundant. Large amounts of interstitial gland tissue have been observed in a few rodents, notably the naked mole rat (Kayanja & Jarvis, 1971), springhare (Mossman, 1966; Olianga-Owiti, 1983), agouti (Weir & Rowlands, 1971) and the cane rat (Oduor-Okelo, 1978). The presence of large amounts of well developed interstitial gland tissue in the root-rat ovary, and the presence of numerous accessory corpora lutea, may contribute to the continual production of progesterone that is necessary for maintenance of the relatively long gestation period in this rodent. Similar observations have been made in the cane rat where in addition to the luteinization of the interstitial gland tissue atretic follicles are converted into luteal tissue and thus contribute to the continual production of progesterone necessary for maintenance of the pregnancy (Oduor-Okelo, 1978).

#### 4.2. Ovulation and breeding pattern.

In this study pregnant root-rats were obtained in most months of the year even though the numbers varied from month to month. There were also variations in the gestation age and in some instances two or more different stages could be obtained in the same month. These findings indicated that the root-rat may breed throughout the year. This is in agreement with previous observations on the breeding pattern of these rodents (Jarvis, 1969 a & b). Jarvis (1969 a & b) further suggested that these animals are polyoestrous and breed throughout the year.

The number of conceptuses in the pregnant uterine horns were one to two. However, the most common occurrence was a single foetus. These observations are similar to those made by Jarvis and Sale (1971). The presence of placental scars in both the pregnant and non-pregnant animals was an indication of either early embryonic death or site of previous pregnancies. In the pregnant animals where one horn had a foetus, the placental scars in the non-pregnant horn indicated probable early embryonic deaths with subsequent resorption. As pointed out by Jarvis (1969a) foetal resorption with resultant scar formation is a common occurrence in the root-rat. In this study one animal was found to have two foetuses in one horn while the non-pregnant horn had placental scars, further confirming the foetal resorption phenomenon in these

rodents. Amoroso (1952) points out that the distribution of the foetuses is always equal in both horns in mammals bearing two or more offspring. The phenomenon of early embryonic deaths, particularly in rodents, could be due to defects in the implantation mechanism or inadequate supply of (or incorrect synergistic balance between) the different hormones necessary for the maintenance of pregnancy, particularly progesterone and oestrogens (Boyd & Hamilton, 1952). These hormones may affect the blastocyst directly or may act on the decidua and thus alter the developmental environment of the foetus. No studies have been made on the causes of embryonic deaths in the root-rats but it may be suggested that it could be due to one or a combination of the above factors.

In most rodents, ovulation occurs simultaneously from both ovaries resulting in two or more eggs. An exception to this is the mountain viscacha *Lagidium peruanum* which is a monovulator; ovulation occurs only from the right ovary and only one young is delivered at term (Pierson, 1949; Wimsatt, 1975). This is in sharp contrast to its counterpart the South American plains viscacha (*Lagostomus maximus*) in which ovulation results in the production of many eggs most of which are resorbed and only two young are delivered at term (Weir, 1971a,b, 1974). Restriction of ovulation to only one ovary has also been reported in some antelopes (Kayanja, 1972) In the root-rat ovulation occurs simultaneously from both ovaries and one or two young are delivered at term.

The gestation length of the root-rat was not estimated in this study, but a gestation period of 45-50 days has been reported by

Rahm (1969). In the major families of myomorpha (Muridae & Cricetidae) the average gestation period ranges from 19-21 days (Newton, 1952). The only other myomorph rodent with a long gestation period of 46 days is the Australian rat *Mesembryomys gouldii* (Crichton, 1969). In rodents, long gestation periods are mainly associated with the suborder Hystricognaths. It has been suggested that these prolonged gestation periods may be due to a delay in fertilization, a delay in implantation or slow growth of the foetus (Weir, 1974). It has also been observed that suckling a large litter produced just previously to a second gestation causes prolonged periods of gestation in some rodents (Pinard, 1905). In the root-rat, the prolonged gestation period may be attributed to one or a combination of the above factors.

### 4.3. Implantation

Observations made in this study showed that the blastocyst first attachment was antimesometrial with the germ disc oriented mesometrially. Similar observations have been made in most members of the major families of the suborders Sciuromorpha, Myomorpha and Hystricomorpha (Mossman, 1937, 1987; Boyd & Hamilton, 1952; Mossman & Strauss, 1963; Wimsatt, 1975). The relatively large blastocyst of the root-rat gradually becomes encapsulated by the stromal cells of the decidual reaction. The uterine epithelium at this stage has degenerated and so the blastocyst is in direct contact with the uterine stroma. The type of implantation occurring in the root-rat is therefore eccentric and

secondarily interstitial. It has been observed by Finn (1982) that in this kind of implantation the blastocyst lies to one side of the uterus and the uterine epithelial cells surrounding it die and are removed, partly at least by the trophoblast giant cells, so that the blastocyst comes to be surrounded by the stromal cells. The implantation process seen in the root-rat is similar to that of the pocket gopher, a condition that has been described by Mossman and Strauss (1963) as being intermediate between the primitive method of membrane development in rabbits and squirrels and the more specialized conditions of the guinea pigs and porcupines. The root-rat differs though from the pocket gopher in that in the latter the implanting blastocyst is in the morula stage with about 128 cells but no blastocyst cavity exists.

The first area of blastocyst attachment in the order Rodentia may either be on the mesometrial side or antimesometrial side of the uterine lumen. However, most members of this order that have been investigated so far show that first attachment is antimesometrial (Fischer & Floyd, 1972; Fischer & Mossman, 1969; King & Mossman, 1974; Luckett, 1971, 1980; Mossman, 1937, 1987). The only rodent in which mesometrial attachment has been documented is in the mountain viscacha, which is a hystricomorph, (Wimsatt, 1975). In the *Ctenodactylus (gundi)* implantation occurs eccentrically but tends to be in an antimesometrial position (Luckett, 1980). Implantation in the root-rat is antimesometrial and is therefore similar to that in the major families of myomorpha.

The type of implantation in any rodent suborder can be correlated with the phenomenon of inversion of the germ layers

(Mossman, 1937; Boyd & Hamilton, 1952; Roberts & Perry, 1974). In rodents with superficial implantation like the sewellels, squirrels, and beavers, inversion of the germ layers is incomplete and occurs late in pregnancy (Harvey, 1959; Mossman, 1937; Fischer, 1971). In rodents with partial or secondary interstitial implantation like the pocket gophers, the jumping mouse, and *Dipodomys*, inversion of the germ layers begins soon after implantation and continues to mid-pregnancy (Mossman & Hisaw, 1940; King & Mossman, 1974). Where complete interstitial and secondary interstitial implantations occur like in most hystricomorph and myomorph rodents, the inversion of the germ layers is complete and occurs early in post-implantation as a result of the disintegration of the parietal trophoblast (Roberts & Perry, 1974; Mossman, 1937; Fischer & Floyd, 1972a; Luckett & Mossman, 1981; Oduor-Okelo & Gombe, 1991; Otianga-Owiti, *et. al.*, 1992).

Inversion of the germ layers was observed to occur in the root-rat. Complete inversion of these germ layers followed the disintegration of the decidua capsularis and the rupture of Reichert's membrane and therefore like in *Zapus* and *Jaculus* (King & Mossman, 1974) it is a slow or tardy inversion. This late inversion of the germ layers in the root-rat is unique among the major families of myomorpha in which inversion occurs very early. The root-rat is therefore in an intermediate position between the primitive condition seen in the sciuriforms (incomplete inversion) and the more specialized condition in the myomorphs and hystricomorphs (early and complete inversion).

#### 4.4. The Amnion

Among the animals examined in this study there was no developmental stage to clearly show the process of amnion formation. It has been suggested by various authors that there is a direct correlation between the mode of implantation and the type of amnion formation, especially in the order Rodentia (Mossman, 1937, 1987; Boyd & Hamilton, 1952). In the species where implantation is superficial amniogenesis is by folding, this is true for example in the squirrels (Mossman & Weisfeldt, 1939) sewellels (Harvey, 1959), gundis (Luckett, 1980), beavers (Fischer, 1971), pocket gophers (Mossman & Strauss, 1963) and jerboas and jumping mice (King & Mossman, 1974). In the cricetids and murids, which show eccentric and secondarily interstitial implantation, amniogenesis is by cavitation (Snell, 1941; Bridgman, 1948a,b; Ward, 1948; Adams & Hilleman, 1950; Mossman, 1987). In the species showing complete interstitial implantation, amniogenesis is also by cavitation, for example in the North American porcupine (Perrotta, 1959), the guinea pig (Maclaren & Bryce, 1933; Mossman, 1937), plains viscacha (Roberts & Weir, 1973) and *Bathyergus* (Luckett & Mossman, 1981). Implantation in the root-rat was observed to be eccentric and secondarily interstitial. Therefore amniogenesis is likely to occur by cavitation as in the major families of myomorpha.

#### 4.5. The Allantois

The allantois in most rodents develops at the posterior end of the embryo as a club-shaped structure without an endodermal cavity and the distal part is vesicular in character (Amoroso, 1952). The presence of an allantoic vesicle or sac varies from being small and permanent for example as in sewellels (Harvey, 1959) and the thirteen-striped ground squirrel (Mossman & Weisfeldt, 1939) to being rudimentary or completely absent as in the murids and cricetids (Snell, 1941; Adams & Hilleman, 1950).

The observations made in this study show the allantois appearing as an endodermal bud at the end of the primitive streak, in the angle between the amnion and the yolk sac wall. Similar observations have been reported in the rat and mouse (Ellington, 1985; Amoroso, 1952) and the Mongolian gerbil (Fischer & Floyd, 1972b). However, the root-rat allantois has an endoderm-lined cavity, a condition similar to that seen in most sciuriforms (Mossman, 1937; 1987) in which it appears small and persists to term. In the present investigation, the allantoic sac was only observed up to the limb-bud stage and therefore can be said to be transient. These observations again place the root-rat in an intermediate position in foetal membrane development within the rodentia.

#### 4.6. The yolk sac and Reichert's membrane.

In most members of the order Rodentia, the endoderm of the yolk sac wall differentiates quite early; this layer together with

## UNIVERSITY OF NAIROBI LIBRARY

the trophoblast forms the bilaminar omphalopleure. The distal endoderm cells of the yolk sac wall form a somewhat uniform continuous layer over the inner surface of the parietal ectoderm (Amoroso, 1952). As observed by Snell (1941) a non-cellular homogeneous membrane, the Reichert's membrane, appears between the extraembryonic endoderm and the parietal trophoblastic ectoderm. Similar observations were made in this study during the expansion stage of the embryo. The Reichert's membrane was present between the distal endoderm and the decidua capsularis, a clear indication that the parietal ectoderm had already degenerated. The Reichert's membrane is thought to be a derivative of the endoderm (Fawcett, *et al*, 1947; Fawcett, 1950; Pierce, *et al*; 1964) or the ectoderm (Wislocki & Padykula, 1953). Jollie (1968) made further investigations and came to the conclusion that the Reichert's membrane may be a product of both ectoderm and endoderm. Functionally the permeability of this "membrane" may help to regulate materno-foetal exchange (Jollie, 1968).

The parietal part of the yolk sac wall disappears relatively early in most rodents showing complete inversion of the germ layers. The inverted splanchnopleuric yolk sac in most of these rodents tends to be large and villous, a condition commonly seen in the pocket gophers (Mossman & Strauss, 1963), kangaroo rats (Nielson, 1940), jumping mouse and jerboa (King & Mossman, 1974), and in cricetids and murids (Ward, 1948; Bridgman, 1948a). Similar findings were made in this study and the inverted splanchnopleuric yolk sac was highly vascularized with the mesometrial portion showing considerable folding giving it a

villous appearance. The yolk sac wall was in direct contact with the uterine tissues and this may represent an important pathway that could facilitate the transfer of substances from the maternal side to the foetus. Moreover, it has been shown that the parietal and visceral yolk sac walls play a role in facilitating the movement of substances from the maternal side, across the yolk sac cavity, to the foetus (Mossman, 1937; Jollie, 1968; Brambell, 1970).

#### 4.7. The chorioallantoic placenta morphology

The early placenta of the root-rat showed an inflection along the margins giving it a pileate-shaped form or the appearance of a mushroom cap. Although the developmental sequence leading to this formation was not obtained during this study, it is likely that the process of inflection may be similar to that described in the pocket gophers (Mossman & Strauss, 1963). In these pocket gophers there is a rapid bulbous enlargement of the distal allantoic mesoderm which becomes surrounded by a mass of cellular trophoblast resulting in a prominent hillock. This placental hillock then initiates the formation of the pileate shape of the placenta of the pocket gopher. The functional significance of this inflection of the placenta is to economize on space and on the distance foetal blood must flow to reach the labyrinth margins (Mossman & Strauss, 1963). In the rodents which give birth to large mature foetuses the economy of space is achieved by placental lobulation, as in the guinea pig (Davidoff, 1973), porcupine (Perrotta, 1959); Chinchilla (Tibbits & Hillemann, 1959; Roberts & Weir, 1973), the

jumping hare (Mossman & Fischer, 1969) and nutria (Hillemann & Gaynor, 1961). As observed by Mossman and Strauss (1963), lobulation is the most efficient in terms of economy of space. The inflection of the margins of the placenta in the root-rat like in the pocket gophers, again places it in an intermediate position between the more primitive rodents and more specialized rodents in foetal membrane development.

The labyrinthine definitive placenta of the root-rat could be divided into two distinct zones: (a) the zona intima composed of trophoblastic tubules enclosing maternal blood separated from the foetal capillary endothelium by a basal lamia; (b) the trophospongium, which contains large trophoblast cells and maternal blood channels lined by a thin endothelium-like cell layer. On this basis, the root-rat placenta can be classed as haemochorial in the zona intima. In the rat (Jollie, 1964) and pocket gophers (Mossman & Strauss, 1963) the endothelium-like layer of the trophospongium is separated from the surrounding trophoblast cells by a PAS positive membrane and a similar situation may be present in the root-rat.

With the advent of the electron microscope it is now possible to fully define the organization of the placental barrier. Using these fine structural studies of the interhaemal membrane, Enders (1965) introduced a classification scheme for the haemochorial placentae. This was based on the number of layers of trophoblast between the maternal blood space and foetal vessels. Thus a placenta with one layer of trophoblast was designated

haemomonochorial, those with two layers of trophoblast-haemodichorial and those with three layers haemotrichorial.

A haemomonochorial type of placenta is found in chinchilla (King & Tibbits, 1976); guinea pig (Davidoff, 1973) jumping mice and jerboas (King & Mossman, 1974) scally-tailed squirrel (Luckett, 1971), the thirteen-striped ground squirrel (Mossman & Weisfeldt, 1939; Mossman, 1987) and in the cane rat (Oduor-Okelo, 1984). Haemodichorial placentation has been described in the rabbit (Enders, 1965) and the gundis (Luckett, 1980). The haemotrichorial condition is found in the zona intima of the cricetid and murid rodents (Wislocki & Dempsey, 1955; Enders, 1965; Jollie, 1976; Metz *et al* , 1976; King & Hastings, 1977). In the present study it has been demonstrated that the root-rat possesses a haemotrichorial type of placenta. The outer layer of trophoblast enclosing the maternal blood spaces was cellular and in most instances appeared to be the thickest of the three layers. The latter finding was to some extent different from the characteristics of the placenta in the rat, mouse and hamster in which the outer layer was apparently the thinnest of the three layers of trophoblast (Jollie, 1964; Enders, 1965; Carpenter, 1972, 1975; King & Hastings, 1977). The origin of the three layered pattern has been investigated by Carpenter (1975) in the golden hamster. The middle and outer layers of trophoblast differentiate from trophoblastic cells of the trager, whereas the inner layer is derived from the chorionic ectoderm. The origin of the three layered pattern was not ascertained in this study; nevertheless, this pattern in the root-rat

placenta could probably arise in the same manner as in the golden hamster.

Ultrastructural observations on the trophoblastic layers showed a highly developed granular endoplasmic reticulum, (gER) especially in the outer layer enclosing maternal blood spaces, free ribosomes, mitochondria, Golgi complex and lipid droplets. The presence of these cellular organelles and inclusions, particularly in the outer cellular layer, indicates an ongoing process of synthesis and secretion of some substance. Any products resulting from such synthetic activity would get to the maternal blood more easily than into the foetal blood because of the close proximity of the outer trophoblast layer to the maternal blood spaces. Rhodin (1974) has shown that the presence of gER and Golgi complexes in the trophoblast indicates the production of placental hormones. It has been demonstrated in the human and non human primate placentae that the syncytial trophoblast is the source of gonadotrophic hormones (Midgley & Pierce, 1962; De Ikonoff & Cedard, 1973).

It has been shown that desmosomes are a common feature between the outer and middle layers of trophoblast in haemotrichorial placentas (Enders, 1965; King & Hastings, 1977). In many of the rodents studied there are apparently no desmosomes between the middle and inner layers of trophoblast. In the present study distinct desmosomes are found both between the outer and middle layers and the middle and inner layers of trophoblast. The rat interhaemal membrane trophoblast is characterized by the presence of caveolae (Enders, 1965). However, the presence of these

structures was not demonstrated in the trophoblast of the interhaemal membrane of the root-rat placenta.

#### 4.8. The decidua.

The decidua can be defined as a maternal tissue that has differentiated from the endometrial stroma by hypertrophy and functional modification of the connective tissue cells (Mossman, 1987). The origin of the precursors of decidual cells has not been fully established. Kearns and Lala (1982) have proposed that these precursors are derived from the bone marrow. Experimental work has recently shown that this is not so (Fowlis & Ansell, 1984). The decidual reaction occurs either in pregnancy, pseudopregnancy, or in artificially or pathologically stimulated deciduomata. Three regions have been designated for the decidua on the basis of its relation to the chorion, namely decidua basalis, decidua capsularis and decidua parietalis (Amoroso, 1952). The positions of the three regions of the decidua in rodents has clearly been presented by Mossman (1987). The basal decidua in the root-rat, like in other mammals, occurs mesometrially. The parietal decidua in rodents is a U-shaped band, continuous with the basal decidua extending around the lateral and antimesometrial surfaces of the conceptus from one side of the basal decidua to another. The capsular decidua develops at either end of each nidation chamber. The decidua is complete and persists longest in species with interstitial implantation although it develops to some extent in all rodents (Mossman, 1937; Finn, 1982). In the root-

rat, the capsular and parietal deciduas disintegrated relatively late in pregnancy and the decidua basalis persisted to term.

The cellular characteristics and amount of decidua show certain peculiarities in rodents. The types of decidual cells may range from binucleate to polyploid like those found in the mice and rats (Ansell, *et al.*, 1974; Vladimirsky *et al.*, 1977). The binucleate and much enlarged decidual giant cells have been described in the South African mole rat (Luckett & Mossman, 1981) and in the cane rat (Oduor-Okelo & Gombe, 1982). In the cane rat, the decidua basalis hypertrophies rapidly and the polyploid giant cells have a vacuolated cytoplasm containing fibrous structures.

The function of the decidua is not fully understood. It has been demonstrated experimentally that cultured and *in situ* rat decidua produces significant amounts of prostaglandin E (Vladimirsky, *et al.*, 1977). The decidual cells have been shown to be directly involved in protein synthesis in pseudopregnant rat decidua (O'Shea, *et al.*, 1983). Further evidence on the secretory functions of the decidual cells has been provided by ultrastructural studies (Herr, *et al.*, 1978; Basuray & Gibori, 1980).

The decidual reaction in the root-rat initially involves the stromal cells of the uterine connective tissue within the endometrium. There is also involvement of the endometrial blood vessels which become more permeable and this leads to oedema in the stroma. This decidual reaction in the root-rat is more intense than that observed in the rat (Finn, 1982). The decidua in the root-rat is complete, and thus is composed of the decidua basalis, decidua capsularis and the decidua parietalis. The decidual reaction is more

intense in the parietal and capsular deciduas during the initial phases of pregnancy. The giant cells associated with the decidual reaction in the root-rat are large, multinucleated and have a vacuolated cytoplasm.

#### 4.9. The placental haemophagous organ.

Mossman (1987) describes the placental haemophagous organ as an absorptive area specialized for phagocytosis of extravasated maternal blood. Placental haematomes, a term used commonly when referring to the carnivore haemophagous organ, are a characteristic feature of the carnivore placentation (Amoroso, 1952; Biggers & Creed, 1962; Leiser & Enders, 1980). However, these haemophagous organs or areas have also been described in the shrew, an insectivore, (King, *et al.*, 1978) and tenrec (Strauss, 1914), some chiroptera, namely emballonurid bats (Wimsatt & Gopalakrishna, 1958), sheep (Myagkaya & Vreeling-Sindelarova, 1976), elephants (Amoroso & Perry, 1964) and manatees (Wislocki, 1935). In most of the cases reported so far, the haemophagous areas are associated with the epitheliochorial type of placentation as in sheep (Myagkaya & Vreeling-Sindelarova, 1976) or with the endotheliochorial type of placentation as in carnivores (Anderson, 1969; Bjorkman, 1973), some members of chiroptera (Wimsatt, 1958; Karim, *et al.*, 1979) and shrews (Verma, 1965; Lockett, 1968).

In the present investigation a haemophagous area is associated with the definitive haemochorial placenta of the root-rat. As has already been pointed out the decidual reaction is initially

intense, especially in the parietal and capsular deciduas. With an increase in the gestation age, there is a complete breakdown of the decidua resulting in a massive accumulation of maternal blood and tissue debris and this situation is similar to the marginal haematoma or the haemophagous organ (Biggers & Creed, 1962). Judging from the literature the presence of a haemophagous area in the root-rat is unique among rodents and indeed among mammals that possess the haemochorial type of placentation except in some carnivores like the hyena (Morton, 1957; Wynn & Amoroso, 1964). Moreover, with the exception of the shrew, the foetal component of the haemophagous organ involves the chorioallantoic membrane and in particular the cytotrophoblast. In the shrew (King, *et al.*, 1978), the foetal component is a specialized region of the invasive trophoblast, the trophoblast curtain, which participates in the formation of the haematoma. In the root-rat the massive accumulation of maternal blood and tissue debris bathes both the cytotrophoblast and the visceral yolk sac, i.e. the haemophagous area lies in the utero-yolk sac cavity.

In those animals in which the haemophagous organ has been described, the cytotrophoblast of the placental part has been shown to be involved in erythrophagocytosis (Gulamhussein & Beck, 1975; King, *et al.*, 1978). This could represent an important route for the transfer of iron to the foetus. King, *et al.*, (1978) observed that in the placenta of the shrew the endodermal cells of the visceral yolk sac wall had electron-dense granules in their cytoplasm by mid-gestation and that these granules increased in size and became a vivid green colour easily seen with the naked eye. In

the root-rat the green coloration was clearly visible at the margins of the discoid placenta. Dense granules were observed in the cytoplasm of the cytotrophoblastic giant cell layer on the placenta bordering the haemophagous area. Similar granules were apparent in the cytoplasm of the endodermal cells of the visceral yolk sac bordering the haematoma. The granules may represent phagocytosed erythrocytes and hence these may be important routes of iron transfer to the foetus.

#### 4.10. Morphometry of the late-term placenta

Stereological measurements are based on the assumption that the sample on which these measurements are made is representative of the whole organ (Weibel, 1979). The stereological data is greatly influenced by the preservation of cell and tissue dimensions, and thus correct osmolarity of all solutions used for tissue preparation was necessary. The fixation, dehydration and embedding methods used in this study have been shown (Weibel & Knight, 1964) to introduce minimal dimensional changes in tissues.

There is limited information on the morphometry of the placenta of small mammals and particularly in rodents. The gross and microscopic morphology of the haemochorial placenta of the root-rat is essentially similar to that of the major families of myomorpha (Mossman, 1937, 1987). The mean volume of the root-rat placenta was  $4.5 \text{ cm}^3 \cdot \text{kg}^{-1}$  body weight, and this value is slightly lower than that of the laboratory white rat ( $5.5 \text{ cm}^3 \cdot \text{kg}^{-1}$  Body weight) reported by Baur (1977), but much lower than that for the

guinea pig ( $8.0 \text{ cm}^3 \text{ kg}^{-1}$  Body weight) (Baur, 1977; Kaufman & Davidoff, 1977). The mean surface area of the trophoblast of the interhaemal (tissue) barrier of the root-rat per unit body weight was  $1.26 \text{ cm}^2 \text{ g}^{-1}$ , a value relatively close to that of the laboratory white rat ( $1.62 \text{ cm}^2 \text{ g}^{-1}$ ) (Baur, 1977). The mean harmonic mean thickness of the interhaemal (tissue) barrier of the root-rat ( $2.32 \mu\text{m}$ ) was lower than that in the guinea pig ( $3.2 \mu\text{m}$ ) (Kaufman & Davidoff, 1977) and man ( $4.08 \mu\text{m}$ ) (Mayhew, *et al.*, 1984). The mean value of  $1.58 \mu\text{m}$  obtained by van der Heijaen (1981) on the guinea pig placenta differed from the value of  $3.2 \mu\text{m}$  reported by Kaufman and Davidoff (1977). This could be due to differences in the methods for measuring the harmonic mean thickness. The method used by Kaufman and Davidoff (1977) took into consideration the unevenness of the placental barrier and therefore may be more acceptable. The mean weight specific diffusing capacity of the root-rat placenta ( $4.73 \text{ cm}^3 \cdot \text{min}^{-1} \cdot \text{mmHg}^{-1} \cdot \text{kg}^{-1}$ ) was higher than that for man ( $1.86 \text{ cm}^3 \cdot \text{min}^{-1} \cdot \text{mmHg}^{-1}$ ) reported by Mayhew, *et al.*, (1984). The values for the placenta oxygen diffusing capacities in the rat and guinea pig have apparently not yet been reported.

In the haemochorial placenta of the root-rat, the foetal capillaries were closely associated with the overlying trophoblast resulting in the marginalization of these capillaries. This may have contributed to the thinning of the placental barrier in the root-rat placenta. This feature was similar to the placental adaptational mechanism reported in the placenta of man inhabiting a high altitude area (Jackson, *et al.*, 1988). As a consequence of the high altitude life the villous core is more irregular in outline.

Bacon, *et al.*, (1984) pointed out that there was a thinning of the diffusion barrier in the guinea-pig placenta during maternal hypoxia. The root-rat lives in hypoxic hypercarbic conditions (Chapman & Bennett, 1975) and this could also contribute to the thinning of the placental diffusion barrier in this animal. Teasdale (1978) observed that if some regions of the human placenta are exposed to hypoxic conditions they show a high incidence of vasculosyncytial membranes and dilated foetal capillaries. Interlobular differences in barrier thicknesses in human placentae have also been described (Burton & Crichley, 1986) but these could not be attributed to foetal capillary distension. Variations in thickness of the placental barrier were found in the root-rat placenta; however these variations could not be conclusively related to foetal capillary distension. On the other hand, it is likely that this thinning of the barrier could be attributed to peripheralization of the foetal vessels within the villi. Another possible explanation could be the reduction in growth of the placental villi resulting in relatively smaller total volume, surface area and length of the placental exchange area compared to the higher values in the laboratory white rat and guinea pig (Baur, 1977; Kaufman & Davidoff, 1977). Such a loss of exchange area is compensated for by the reduction in the placental barrier (Jackson, *et al.*, 1988). The overall effect is an increase in the oxygen diffusing capacity of the placenta ( $D_p$ ) of the root-rat.

In conclusion, the compensatory thinning seems to be sufficient to maintain the membrane oxygen diffusing capacity such that it is able to allow enough oxygen into the foetal capillary bed for

onward transfer to the growing foetus. Thus the compensatory thinning apparently increases the functional diffusing capacity of the placenta.

#### 4.11. Phylogenetic classification.

It has been suggested and demonstrated that foetal membrane morphogenetic characters are of much value as phylogenetic indicators among the major groups of mammals (Mossman, 1953; 1987). This value is attributed to their conservativeness as compared to the development and morphological characters of the body itself. In any mammalian order, certain foetal membrane developmental characteristics are fairly constant, for example the orientation of the embryonic disc to the uterus at the time of implantation, the nature of the yolk sac splanchnopleure and the allantoic vesicle and the nature and detailed structure of the definitive placenta.

The foetal membrane characteristics have been used to classify the major suborders of the order Rodentia, ranging from the primitive types found in sciuridae to the specialized forms seen in hystricomorpha (Mossman, 1937, 1987). In the suborder Sciuiomorpha, the primitive nature of their foetal membranes may be attributed to the following characteristics: (1) large blastocysts and a superficial implantation; (2) the decidua capsularis is incomplete and short-lived; (3) amniogenesis is by folding; (4) yolk sac inversion is late and incomplete; (5) a well developed , temporary choriovitelline placenta; (6) presence of a small allantoic sac; (7)

villus-like trabecular arrangement in the labyrinthine zone; (8) occurrence of a prominent area of giant cells in the junctional zone; (9) a haemomonochorial interhaemal membrane (Mossman & Weisfeldt, 1939; Mossman, 1987).

The common characteristics of the foetal membrane development of the suborder Myomorpha include: (1) a small blastocyst with a secondary interstitial implantation; (2) early complete inversion of the yolk sac; (3) amniogenesis by cavitation; (4) absence of choriovitelline placenta; (5) no allantoic sac; (6) a persistent periplacental bilaminar omphalopleure; (7) deep placental pits ("endodermal sinuses") on the foetal side of the placental disc; (8) a large inverted splanchnopleuric yolk sac with numerous and often complexly branched villi on its mesometrial hemisphere; (9) a haemotrichorial placenta (Mossman, 1937; Amoroso, 1952; Fischer & Floyd, 1972a,b; Adams & Hilleman, 1950; King & Hastings, 1977).

Among the Rodentia the third suborder, the Hystricomorpha, is regarded as the most specialized group and some of their foetal membrane characteristics include: (1) complete interstitial implantation; (2) amniogenesis by cavitation; (3) very early and complete inversion of the germ layers; (4) a small preplacenta; (5) absence of a choriovitelline placenta; (6) large, villous inverted yolk sac; (7) a prominently lobulated, labyrinthine haemochorial placenta with a conspicuous subplacenta; (8) no allantoic sac; (9) prominent and persistent decidua (Luckett & Mossman, 1981; Rowlands, 1974; Roberts & Perry, 1974; Oduor-Okelo, 1984; Oduor-Okelo & Gombe, 1982).

In the present investigation the root-rat ( *Tachyoryctes splendens* ) foetal membranes have been shown to possess the following characteristics: (1) secondary interstitial implantation; (2) amniogenesis is probably by cavitation; (3) presence of a temporary allantoic sac; (4) late complete inversion of the yolk sac; (5) deep placental pits ("endodermal sinuses") on the foetal side of the placental disc; (6) a large inverted splanchnopleuric yolk sac with numerous villi on its mesometrial hemisphere; (7) a haemotrichorial placenta. These findings indicate that some of the developmental patterns of the foetal membranes and placenta of the root-rat are a combination of intermediate rodent traits, like those of the pocket gopher (Mossman & Strauss, 1963) and those that exist in several other groups particularly the myomorphs. Because of these variations *Tachyoryctes* should not be placed in the families *Spalacidae* or *Muridae* as suggested by Simpson, (1945).

From this study it is evident that the development of the foetal membranes of the root-rat shares some features with both the *Geomys* and *Muridae* (Table IX). The development of the foetal membranes in the root-rat indicates that the membranes of *Tachyoryctes* are intermediate in type between those of sciuriforms and the major families of myomorpha. In conclusion it is suggested that the root-rat should be placed in a sub-family, *Tachyoryctoidea*, on its own and until the foetal membranes of the bamboo rat have been described it should not be classed together with the bamboo rat in the family Rhizomyidae. However, the subfamily *Tachyoryctoidea* should be retained in the suborder Myomorpha because the major foetal developmental characteristics

(Table IX) are closer to those found in the common rats, mice and the Mongolian gerbil.

Table IX. Comparison of foetal membrane morphology and placental characters of the root-rat and other rodents.

		Name
		APLODONTIDAE
		Sewellel
Uterus		duplex, long
Yolk sac orientation		antimesometrial
First attachment		antimesometrial
Nidation dept		superficial
Amniogenesis		folding
Bilaminar	juxtaterine	permanent
omphalopleure	periplacental	none
Choriovitelline placenta		temporary
Splanchnopleuric yolk sac		incomplete inversion, always present, small and nonvillous.
Chorion		permanent, large
Preplacenta		broad, thin
Chorioallantoic placentation:		
	shape	discoid
	location	mesometrial
	cord attachment	mesometrial
	pattern	labyrinthine
	lobulation	indistinct
	placental sinuses	none
	interhemal membrane	hemochorial

Table IX (continued)

trophospongium	thin, mainly giant cells
haematomes	none
Invasive trophoblastic giant cells	present
Decidual cell tissue	present
Allantoic sac	permanent, small
Source(s) of information	Harvey,1959;Mossman,1937,1987

Table IX (cont'd)

Name	
GEOMYIDAE	
Pocket gophers	
Uterus	duplex, long
Yolk sac	antimesometrial
First attachment	antimesometrial
Nidation dept	partly interstitial
Amniogenesis	folding epamniotic "cup" only
Bilaminar           juxtaterine	temporary
omphalopleure    periplacental	on outer surface of cup, permanent
Choriovitelline placenta	none
Splanchnopleuric yolk sac	complete inversion, permanent, large, villous mesometrially
Chorion	temporary, small (roof of open epamniotic cavity)
Preplacenta	thin
Chorioallantoic placentation:	
shape	cupulate (like an acorn cup)
location	mesometrial
cord attachment	mesometrial
pattern	labyrinthine
lobulation	indistinct
placental sinuses	none
interhernal membrane	hemochorial
trophospongium	thick, giant cells present
haematomes	none

Table IX (cont'd)

Invasive trophoblastic giant cells	present
Decidual cell tissue	present
Allantoic sac	none
Source(s) of information	Mossman & Strauss, 1963; Mossman, 1937, 1987..

Table IX (cont'd)

Name	
CTENODACTYLIDAE	
Gundis	
Uterus	bicornuate, long
Yolk sac orientation	antimesometrial
First attachment	antimesometrial
Nidation dept	superficial
Amniogenesis	folding
Bilaminar      juxtauterine	permanent
omphalopleure    periplacental	permanent
Choriovitelline placenta	temporary?
Splanchnopleuric yolk sac	incomplete inversion, mesometrial, half villous
Chorion	absent
Preplacenta	thin
Chorioallantoic placenta:	
shape	discoid
location	mesometrial
cord attachment	mesometrial
pattern	labyrinthine
lobulation	indistinct
placental sinuses	none
interhemal membrane	haemodichorial
trophospongium	present
haematomes	none
Invasive trophoblastic giant cells	present

Table IX (continued)

Decidual cell tissue	present
Allantoic sac	permanent, small
Source(s) of information	Luckett, 1980; Mossman, 1937, 1987.

Table IX (cont'd)

		Name _____	
		PEDETIDAE	DIPODIDAE
		Springhaas	Jerboa
Uterus		duplex, long	bicornuate, long
Yolk sac orientation		antimesometrial	antimesometrial
First attachment		antimesometrial	antimesometrial
Nidation depth		superficial	partly interstitial
Amniogenesis		folding	folding (open epamniotic cavity)
Bilaminar	juxtauterine	permanent	temporary
omphalopleure	periplacental	free surface from disc margin to base	permanent
Choriovitelline placenta		temporary	absent
Splanchnopleuric yolk sac		incomplete	complete
		inversion, entirely villous	inversion permanent, large, villous mesometrially
Chorion		temporary, small	temporary, small
Preplacenta		unusually massive	chiefly giant cells
Chorioallantoic placentation:			
	shape	discoid	discoid
	location	mesometrial	mesometrial
	cord attachment	mesometrial	mesometrial
	pattern	labyrinthine	labyrinthine, entirely giant cells
	lobulation	many, distinct	indistinct

Table IX (cont'd)

placental sinuses	none	none
interhemal membrane	haemodichorial	haemomonochorial
trophospongium	present	giant cells only
haematomes	none	none
Invasive trophoblastic giant cells	medium size cells, lateral and antimesometrial only	present
Decidual cell tissue	present	present
Allantoic sac	permanent, small	none
Source(s) of information	Fischer & Mossman, 1969  Mossman & Fischer, 1969	King & Mossman, 1974  Mossman, 1937, 1987

Table IX (cont'd)

		Name	
		HYSTRICIDAE	CAVIIDAE
		African porcupine	Guinea pig
Uterus		bicornuate	duplex, V-cervix, long
Yolk sac orientation		antimesometrial	antimesometrial
First attachment			antimesometrial
Nidation depth			interstitial
Amniogenesis			cavitation, epamnion
Bilaminar	juxtauterine	temporary	disappears in early blastocyst
omphalopleure	periplacental	permanent	permanent
Choriovitelline	placenta		none
Splanchnopleuric	yolk sac	complete inversion, permanent, large, villous	complete inversion, permanent, large, villous
		capillary ring	capillary ring
Chorion		none	none
Preplacenta		-	present
chorioallantoic	placentation:		
	shape	discoid	discoid
	location	mesometrial	mesometrial
	cord attachment	mesometrial	mesometrial
	pattern	labyrinthine	labyrinthine

Table IX (cont'd)

lobulation	many, distinct (subplacenta)	many, distinct (subplacenta)
placental sinuses	none	none
interhemal membrane	hemochorial	haemomonochorial
trophospongium	present	present
haematomes	none	none
Invasive trophoblastic giant cells		present
Decidual cell tissue	present	present
Allantoic sac	late	none
Source(s) of information	Luckett & Mossman, 1981; Mossman, 1987	Davidoff, 1973; Mossman, 1937, 1987 Blandua, 1949.

Table IX (cont'd)

Name		
	CRICETIDAE	MURIDAE
	<i>Meriones</i>	Rats
Uterus	duplex, long	duplex, long
Yolk sac orientation	antimesometrial	antimesometrial
First attachment	antimesometrial	antimesometrial
Nidation depth	interstitial	interstitial
Amniogenesis	cavitation, epamnion	cavitation; epamnion
Bilaminar      juxtauterine	temporary	temporary
omphalopleure      periplacental	permanent, forms endodermal sinuses on placental surface	permanent, forms endodermal sinuses on placental surface
Choriovitelline placenta	none complete inversion	none complete inversion
Splanchnopleuric yolk sac	permanent, large mesometrial half villous	permanent, large, mesometrial half villous
Chorion	none	none
Preplacenta	present (Trager)	present (Trager)

Table IX (cont'd)

**Chorioallantoic Placentation:**

shape	discoid	discoid
location	mesometrial	mesometrial
cord attachment	mesometrial	mesometrial
pattern	labyrinthine	labyrinthine
lobulation	indistinct	indistinct
placental sinuses	present	present
interhaemal membrane	haemotrichorial	haemotrichorial
trophospongium	thin	thin
haematomes	none	none
Invasive trophoblastic giant cells	present	present
Decidual cell tissue	present	present
Allantoic sac	none	none
Sources of information	Fischer & Floyd, 1972a,b	Mossman, 1937, 1987
	Salzmann, 1963	Amoroso,1952; Ellington,1987

Table IX (cont'd)

Name	
RHYZOMYIDAE	
<i>Tachyoryctes splendens</i>	
Uterus	duplex, long
Yolk sac orientation	antimesometrial
First attachment	antimesometrial
Nidation depth	interstitial
Amniogenesis	cavitation
Bilaminar      juxtaterine	temporary
Omphalopleure   periplacental	permanent, forms endodermal sinuses on placental surface
Choriovitelline placenta	none
Splanchnopleuric yolk sac	complete inversion, permanent, large, mesometrial mostly villous
Chorion	none
Preplacenta	present
Chorioallantoic placentation	
shape	discoid
location	antimesometrial
cord attachment	mesometrial
pattern	labyrinthine
lobulation	indistinct

Table IX (cont'd)

placental sinuses	present
interhaemal membrane	haemotrichorial
trophospongium	thin
haematomes	present
Invasive trophoblastic giant cells	present
Decidual cell tissue	present
Allantoic sac	small, temporary
Source(s) of information	Own observations.

## Appendix 1

Examples of calculations for the light microscopic stereological analysis of the late term root-rat placenta using the data obtained for root-rat number one.

### A: Analysis at the first level of sampling

At this level of sampling the volume densities of the parenchyma (p) and non-parenchyma (np) were estimated by point counting on sixty fields in fifteen sections of the placenta. The volume density of the parenchyma ( $V_{vp}$ ) is given by the expression:

$$V_{vp} = P_p / P_T$$

where  $P_p$  is points sampled on parenchyma and  $P_T$  is total points on placental tissue.

$$P_p / P_T = 21320 / 24624$$

$$\text{therefore } V_{vp} = 0.8658$$

The  $V_v$  of np is given by the expression:

$$V_{vnp} = P_{np} / P_T$$

$$= 3304 / 24624$$

$$= 0.1342$$

Thus the percentage volume density of the parenchyma is 86.58% and that of non-parenchyma is 13.42%.

The absolute volume in  $\text{mm}^3$  is obtained by multiplying the the volume density of a component with the volume of the organ as a whole. Therefore the absolute volume of the parenchyma (p) in the placenta which had a volume of  $780 \text{ mm}^3$ :

$$= 0.8658 \times 780 = 675 \text{ mm}^3$$

that of the non-parenchyma (np) =  $0.1342 \times 780 = 105 \text{ mm}^3$

## **B: Analysis at the second level of sampling.**

### **(a) volume density of parenchymal components**

The volume densities (%) and absolute volumes ( $\text{mm}^3$ ) of the following components of the parenchyma were estimated: the maternal blood spaces, the placental interhaemal barrier, and the foetal capillary bed. All these components were estimated by point counting on 160 fields in 16 sections of the placenta.

The volume density of the maternal blood spaces ( $V_{vm}$ ) is given by the expression:

$$V_{vm} = P_m / P_a$$

where  $P_m$  is points sampled on maternal blood spaces and  $P_a$  is total points on parenchymal tissue.

$$P_m / P_a = 9290 / 18630$$

$$\text{therefore } V_{vm} = 0.4987$$

Thus the percentage volume density of the maternal blood spaces is 49.87%. The absolute volume in  $\text{mm}^3$  is obtained by multiplying the volume density of the component by the volume of the parenchyma. Therefore the absolute volume of the maternal blood spaces in the parenchyma which had a volume of  $675 \text{ mm}^3$ :

$$= 0.4987 \times 675 = 336.62 \text{ mm}^3$$

Similar steps were followed as above in calculating the volume densities and absolute volumes of the other parenchymal components (see Table VI).

### (b) surface density of parenchymal components

The surface densities of the following components were estimated: the maternal erythrocytes, maternal blood spaces, trophoblast of the interthaemal barrier, the foetal capillary endothelium, and the foetal erythrocytes. All these components were estimated by intersection counting on 160 fields in 16 sections of the placenta .

The surface density of the maternal erythrocytes ( $S_{vme}$ ) is given by:

$$S_{vme} = 2I_m/Lt$$

where  $I_m$  is the number of intercepts on the maternal erythrocytes,  $Lt$  is the total length of the test system.

$$\text{therefore } S_{vme} = 2 \times 131.2/0.188 \text{ cm} = 1395.94 \text{ cm}^{-1}$$

The surface area of the maternal erythrocytes ( $S_{me}$ ) was estimated by multiplying the surface density of the maternal erythrocytes and the volume of the placenta parenchyma which was  $0.675 \text{ cm}^3$ .

$$\text{therefore } S_{me} = 2395.74 \text{ cm}^{-1} \times 0.6675 \text{ cm}^3 = 942.12 \text{ cm}^2$$

The surface densities and surface areas of the other parenchymal components were estimated using the steps outlined above (see Tables VII & VIII).

### (c) the harmonic mean thickness of the placental barrier

The harmonic mean thickness ( $\tau_h$ ) was estimated by measuring the placental barrier intercept lengths and determining

their reciprocals. The number of fields analysed (n) was then divided by the sum of the reciprocals ( $\Sigma 1/L$ ) and the value obtained was divided by the final magnification (M):

$$\begin{aligned}\tau_h &= (957/181.336\text{mm})/2200 \\ &= 2.4 \times 10^{-3} \text{ mm} \\ &= 2.4\mu\text{m}\end{aligned}$$

(d) the oxygen diffusing capacity of the materno-foetal placental barrier ( $D_{pm}$ ):

Overall  $D_{pm}$  calculation:

$$\begin{aligned}D_{pm} &= S_t \cdot K \cdot \tau_h^{-1} \\ &= 237\text{cm}^2 \times 2.3 \times 10^{-8} \text{cm}^2 \cdot \text{min}^{-1} \text{mmHg}^{-1} / 2.4 \times 10^{-4} \text{ cm} \\ &= 0.02271 \text{cm}^3 \cdot \text{min}^{-1} \cdot \text{mmHg}^{-1}.\end{aligned}$$

The mean overall gas diffusing capacity of the placenta for the five specimens was  $0.0248 \pm 0.0015 \text{cm}^3 \cdot \text{min}^{-1} \cdot \text{mmHg}^{-1}$ .

The specific diffusing capacity was arrived at as follows:

$$\text{Weight of foetus} = 5 \times 10^{-3} \text{ kg}$$

$$\text{Overall diffusing capacity} = 0.02271 \text{cm}^3 \cdot \text{min}^{-1} \cdot \text{mmHg}^{-1}.$$

Therefore per kg Bwt will be:

$$= 0.02271/0.005$$

$$= 4.54 \text{cm}^3 \cdot \text{min}^{-1} \cdot \text{mmHg}^{-1} \cdot \text{kg}^{-1}.$$

The mean specific diffusing capacity for the five specimens was  $4.73 \pm 0.18 \text{cm}^3 \cdot \text{min}^{-1} \cdot \text{mmHg}^{-1} \cdot \text{kg}^{-1}$ .

## BIBLIOGRAPHY

- Adams, F. W., and H. H. Hillemann. (1950). Morphogenesis of the vitelline and allantoic placenta of the golden hamster ( *Cricetus auratus* ). *Anat. Rec.* 108, 368-384.
- Amoroso, E.C. (1952). Placentation In: *Marshall's Physiology of Reproduction*, II: 127-311 (ed. A.S.Parkes). Longman and Green.Lond.
- Amoroso, E.C., and J.S. Perry. (1964). Foetal membranes and placenta of the African elephant ( *Loxodonta africana* ). *Trans. Zool. Soc. Lond.* 248, 1-34.
- Anderson, J.W. (1969). Ultrastructure of the placenta and fetal membranes of the dog. I. Placental labyrinth. *Anat. Rec.* 165,15-36.
- Ansell, J.D., P.W. Barlow, and A. Maclaren. (1974). Binucleate and polyploid cells in the decidua of the mouse *J. Embryol. Exp. Morph.* 31, 223-227.
- (As cited by Jarvis, 1969).
- Bacon, B.J., R.D. Gilbert, P. Kaufman, A.D. Smith, F.T. Trevino, and L.D. Longo. (1984). Placental anatomy and diffusing capacity in guinea pigs following long-term maternal hypoxia. *Placenta*, 5, 475-488.
- Basuray, R., and G. Gibori. (1980). Luteotropic action of decidual tissue in the pregnant rat. *Biol. Reprod.* 23, 507-512.
- Baur, R. (1977). Morphometry of the placental exchange area. *Adv. Anat. Embryol. Cell. Biol.* 53, 1-65.
- Belt, W.D., and D.C. Pease. (1956). Mitochondrial structure in sites of Steroid secretion. *J. Biophys. Biochem. Cytol.* II (Suppl.), 369-374.

- Biggers, J.D., and R.F.S. Creed. (1962). Two morphological types of placentae in the racoon. *Nature* (Lond.) 194, 103-104.
- Bjorkman, N.H. (1973). Fine structure of the fetal-maternal area of exchange in the epitheliochorial and endotheliochorial type of placentation. *Act. Anat.* 86, Suppl. 61, 1-22.
- Blandua, R.J. (1949). Observations on implantation of the guinea pig ovum. *Anat. Rec.* 104, 331-359.
- Boyd, J.D. and W.J. Hamilton. (1952). Cleavage, early development and implantation of the egg. In: *Marshall's Physiology of Reproduction* II, 1-26 (ed. A.S. Parkes). Longman and Green Lond.
- Brambell, F.W.R. (1970). The transmission of passive immunity from mother to young. North Holland Pub-Co., Amsterdam, pp.1-385.
- Bridgman, J. (1948a). A morphological study of the development of the placenta of the rat. I. An outline of the development of the placenta of the white rat. *J. Morph.* 83, 61-85.
- Bridgman, J. (1948b). A morphological study of the placenta of the rat. II. A histological and cytological study of the development of the chorioallantoic placenta of the white rate. *J. Morph.* 83, 195-223.
- Burton, G.J. and G. Critchley. (1986). Intralobular variations in villous membrane thickness. *Placenta* , 7, 461-462,
- Burton, G.J. Ingram, S.C. & Palmer, M.E. (1987). The influence of mode of fixation on morphometrical data derived from terminal villi in the human placenta at term: a comparison of immersion and perfusion fixation. *Placenta*, 8, 221-234.
- Carpenter, S.J. (1972). Light and electron microscopic observations on the morphogenesis of the chorioallantoic placenta of the golden

- hamster (*Cricetus auratus* ). Days seven through nine of gestation. *Am. J. Anat.* 135, 445-476.
- Carpenter, S.J. (1975). Ultrastructural observations on the maturation of the placenta labyrinth of the golden hamster. Days 10 to 16 of gestation. *Am. J. Anat.* 143, 315-348.
- Chapman, C.R. and F.A. Bennett. (1975). Physiological correlates of burrowing in rodents. *Comp. Physiol.* 514A, 599-603.
- Corner, G.W. (1938). The sites of formation of estrogenic substances in the animal body. *Physiol.Rev.* 13, 117-146.
- Crichton, E.G. (1969). Reproduction in the pseudomyine rodent, *Mesembriomys gouldii* (Gray). *Muridae. Aust. J. Zool.* 17, 785-797.
- Davidoff, M. (1973). Guinea pig placenta: Fine structure and development. *Acta Anat.* , 86 (Suppl. 61), 23-46.
- De Ikonoff, L,K., and L. Cedard. (1973). Localization of human chorionic gonadotrophic and somatotrophic hormone by the peroxidase immunohistoenzymic method in villi and amniotic epithelium of human placenta (from six weeks to term). *Am.J.Obstet. Gynec.* 116, 1124-1132.
- Delesse, M A. (1847) Procédé mécanique pour déterminer la composition des roches. *C. R. Acad. Sci. (Paris)* 25, 544.  
(As cited by Weibel, 1979).
- Ellerman, J. R. (1940). The families & genera of living rodents. I. *Brit. Mus. Nat. Hist.* 689p.
- Ellerman, J. R. (1941). The families & genera of living rodents II. *Brit. Mus. Nat. Hist.* 689p.
- Ellington, S.K. (1985). A morphological study of the development of the allantois of rat embryos *in vitro*. *J. Anat.* 142, 1-11.

- Enders, A.C. (1965). A comparative study of the fine structure of the trophoblast in several hemochorial placentas. *Am. J. Anat.* 116, 29-68.
- Falk, B. (1959). Site of production of oestrogen in rat ovary as studied in microtransplants. *Acta. Physiol. Scand.*, 47, suppl. 163, 1-101.
- Fawcett, D.W. (1950). Development of mouse ova under the capsule of the kidney. *Anat. Rec.*, 108., 71-91.
- Fawcett, D.W., G.B. Wislocki, and C.M. Waldo. (1947). The development of the mouse ova in the anterior chamber of the eye and in the abdominal cavity. *Am. J. Anat.*, 81, 413-444.
- Finn, C.A. (1982). Cellular changes in the uterus during pregnancy in rodents. *J. Reprod. Fert. Suppl.* 31, 105-111.
- Fischer, T.V. (1971). Placentation in the American beaver (*Castor canadensis*). *Am. J. Anat.* 131, 159-184.
- Fischer, T.V. and A.D. Floyd. (1972a). Placental development in Mongolian Gerbil (*Meriones unguiculatus*). I. Early development of the time of chorioallantoic contact. *Am. J. Anat.* 134, 309-320.
- Fischer, T.V. and A.D. Floyd. (1972b). Placental development in the Mongolian Gerbil (*Meriones unguiculatus*). II. From the establishment of the labyrinth to term. *Am. J. Anat.* 134, 321-336.
- Fischer, T.V. and H.W. Mossman. (1969). The fetal membranes of *Pedetes capensis*, and their taxonomic significance. *Am. J. Anat.* 124, 89-116.
- Fowles, D.J. and J.D. Ansell. (1984). Decidual cells are not derived from bone marrow. *J. Embryol. Exp. Morph.*, Suppl.1, 63(abst).
- Freere, R.H. and E.R. Weibel. (1967). Stereologic techniques in microscopy. *J. Ro Micr Soc.*, 87, 25-34.

- Gulamhusein, A.P. and F. Beck. (1975). Development and structure of the extraembryonic membranes of the ferret. A light microscopic and ultrastructural study. *J. Anat.* 120, 349-365.
- Hall, O. (1952). Accessory corpora lutea in the wild Norway rat. *Tex. Rep. Biol. Med.* 10, 32-38.
- Harvey, E.B. (1959). Placentation in Aplodontidae. *Am. J. Anat.* 105, 63-89.
- Herr, A.T., P.M. Heidger, J.R. Scott, J.W. Anderson, L.B. Curet, and H.W. Mossman. (1978). Decidual cells in the human ovary at term. I. incidence, gross anatomy and ultrastructural features of merocrine secretion. *Am. J. Anat.* 152, 7-28.
- Hilleman, H.H. and A.I. Gaynor. (1961). The definitive architecture of the placenta of nutria *Myocaster coypus* (Molina). *Am. J. Anat.* 109, 299-318.
- Horst, C.J. van der & J. Gillman. (1941). The number of eggs and surviving embryos in *Elephantulus*. *Anat. Rec.* 80, 443-452
- Jackson, M.R., T.M. Mayhew, and J.D. Haas. (1988). On the factors which contribute to thinning in the villous membrane in human placentae at high altitude. II. An increase in the degree of peripheralization of fetal capillaries. *Placenta*, 9, 9-18.
- Jarvis, J.U.M. (1969a). The breeding season and litter size of African mole rats. *J. Reprod. Fert. Suppl.* 6, 237-248.
- Jarvis, J.U.M. (1969b). Some aspects of the Biology of the East African mole-rats. PhD Thesis University of East Africa, Nairobi.
- Jarvis, J.U.M. and J.B. Sale. (1971). Burrowing and burrowing patterns of East African mole rats, *Tachyoryctes*, *Heliophobius* and *Heterocephalus*. *J. Zool. (Lond.)* 163, 451-479.

- Jollie, W.P. (1964). Fine structural changes in the placental labyrinth of the rat with increasing gestational age. *J. Ultrastruc. Res.* 10, 27-47.
- Jollie, W.P. (1968). Changes in the fine structure of the parietal yolk sac of the rat placenta with increasing gestational age. *Am. J. Anat.* 122, 513-532.
- Jollie, W. P. (1976). The fine structure of the interhemal membrane of the rat chorioallantoic placenta during prolonged pregnancy. *Anat. Rec.* 184, 73-90.
- Karim, K.B., W.A. Wimsatt, A.C. Enders, and A. Gopalakrishna. (1979). Electron microscopic observations on the yolk-sac of the Indian fruit bat, *Rousettus leschenaulti* (Pteropidae). *Anat. Rec.* 195, 493-510.
- Kaufmann, P. and M. Davidoff. (1977). The guinea pig placenta. *Adv. Anat. Embryol., Cell Biol.* Springer, Berlin.
- Kayanja, F.I.B. (1972). Reproduction in antelopes; Reproduction in the female impala. Nairobi, East African Monographs in Biology. I. 12-54.
- Kayanja, F.I.B. and J. U. M. Jarvis. (1971). Histological observations on the ovary, oviduct and uterus of the naked mole rat. *Z. Saugertiere*, 36, 114-121.
- Kearns, M. and P. Lala. (1982). Bone marrow origin of decidual cell precursors in the pseudopregnant mouse uterus. *J. Exp. Med.* 155, 1537-1554.
- King B.F. and R.A. Hastings, II. (1977). The comparative fine structure of the interhemal membrane of chorioallantoic placentas from six genera of myomorph rodents. *Am. J. Anat.* 149, 165-179.

- King, B. F., A.C. Enders, and W.A. Wimsatt.** (1978). Annular haematoma of the shrew yolk-sac placenta. *Am. J. Anat* 152, 45-58.
- King, B.F. and F.D. Tibbits.** (1976). The fine structure of the chinchilla placenta. *Am. J. Anat.* 145, 33-56.
- King, B.F. and H.W. Mossman.** (1974). Fetal membranes and unusual giant cell placenta of the jerboa ( *Jaculus* ) and jumping mouse (*Zapus* ). *Am. J. Anat.* 140, 405-432.
- Kingdon, J.** (1974). East African mammals: An atlas of Evolution in Africa. Vol. II. Part B(Hares and Rodents) pp.495-500 Acad. Press Lond.
- Leaky, M.D., R.L. Hay, B.H. Curtis, R.E. Drake, M.K. Jackes and T.D. White.** (1976). Fossils hominids from the Laetolil beds. *Nature (Lond.)*, 262, 460-466.
- Leiser, R., ands A.C. Enders.** (1980). Light and electron microscopic study of the near term paraplacenta of the domestic cat. II. Paraplacental haematoma. *Acta Anat.* 162, 266-285.
- Luckett, W.P.** (1968). Morphogenesis of the placenta and fetal membranes of the tree shrews (family Tupaiidae). *Am. J. Anat.* 123, 385-428.
- Luckett, W.P.** (1971). The development of the chorioallantoic placenta of the African scally-tailed squirrels (family Anomaluridae). *Am. J. Anat.* 130:, 159-178.
- Luckett, W.P.** (1980). Fetal membranes and placental development in the African hystricomorphous rodent *Ctenodactylus*. *Anat. Rec.* 196, 116A.
- Luckett, W.P. and H.W. Mossman**(1981). Development and phylogenetic significance of the fetal membranes and placenta of the African

- hystricognathous rodents, *Bathyergus* and *hystrix*. *Am. J. Anat.* 162, 266-285.
- MacLaren, N.H.W and T.H.Bryce. (1933). The early stages in the development of *Cavia*. *Tans. Roy. Soc. Edin.* 57, 647-664.  
(As cited by Mossman, 1987).
- Mayhew, T.M. & G.J. Burton. (1988). Methodological problems in placental morphometry: Apologia for the use of stereology based on sound sampling practice. *Placenta*, 9, 565-581.
- Mayhew, T.M., C.F.Joy and J.D. Haas. (1984). Structure function correlation in the human placenta: the morphometric diffusing capacity for oxygen at full term. *J. Anat.*, 139, 691-708.
- Metcalf, J., H. Bartels, W. Moll(1967) Gas exchange in the pregnant uterus. *Physiol. Rev.*, 47, 782-838.
- Metz, J., D. Heinrich, and W.G. Forssmann. (1976). Ultrastructure of the labyrinth in the rat full-term placenta. *Anat. Embryol.* 149, 123-148.
- Midgley, A.R. and G.B. Pierce (1962). Immuno-histochemical localization of human chorionic gonadotrophin. *J. Exp. Med.* 155, 289-294.
- Missone, X. (1968). Rodentia: Main text. Smithsonian Institution. Preliminary identification Manual for African Mammals. 19, 55.
- Morton, W.R.M. (1957). Placentation in the spotted hyena (*Crocuta crocuta* Eclenben ). *J. Anat*, 91, 374-382.
- Mossman, H.W. (1937). Comparative morphogenesis of the fetal membranes and accessory uterine structures. *Carnegie Inst. Contrib. Embryol.* 26, 129-246.
- Mossman, H.W. (1953). The genital system and the fetal membranes as criteria for mammalian phylogeny and taxonomy. *J. Mammal.* 34, 289-298.

- Mossman, H.W. (1966). The rodent ovary. In: Comparative Biology of Reproduction in mammals. *Symp. Zool. Soc. London*, (ed. J.W. Rowlands). Acad Press Lond. and New York. 15pp 455-470.
- Mossman, H.W. (1987) Vertebrate fetal membranes: Comparative Ontogeny and Morphology: Evolution, Phylogenetic significance; Basic Functions; Research Opportunities, Rutgers University Press, New Brunswick, New Jersey.
- Mossman, H.W., and F.L Hisaw (1940). The fetal membranes of the pocket gopher illustrating an intermediate type of rodent membrane formation. 1. From the unfertilized tubal egg to the beginning of allantois. *Am J. Anat.* 66, 367-391.  
(As cited by Mossman & Strauss, 1963)
- Mossman, H.W. and F. Strauss(1963). The fetal membranes of the pocket gopher illustrating an intermediate type of rodent membrane formation. II. From the beginning of the allantois to term. *Am. J. Anat.* 113, 447-477.
- Mossman, H.W. and I. Judas (1949). Accessory corpora lutea, lutea cell origin, and the ovarian cycle in the Canadian Porcupine. *Am. J. Anat.* 85, 1-39.
- Mossman, H.W. and K. L. Duke (1973). Comparative morphology of the mammalian ovary. The University of Wisconsin Press, Madison.
- Mossman, H.W. and L.A. Weisfeldt(1939). The fetal membranes of a primitive rodent, the thirteen striped ground squirrel. *Am. J. Anat.*, 64, 59-109.
- Mossman, H.W. and T.V. Fischer, (1969). The preplacenta of *Pedetes*, the trager, and the maternal circulation patter in rodent placentae. *J. Reprod. Fert.*, Suppl.6, 175-184.

Myagkaya, G. and H. Vreeling-Sindelarova. (1976). Erythrophagocytosis by cells of the trophoblastic epithelium in the sheep placenta in different stages of gestation. *Acta. Anat.*, 95, 234-238.

Nielson, P.E. (1940). The fetal membranes of the Kangaroo rat, *Dipodomys*, with a consideration of the Phylogeny of the Geomyoidea. *Anat. Rec.*, 77, 103-127.

Newton, W. H. (1952). Changes in the maternal organism during pregnancy. In: *Marshall's Physiology of Reproduction II*, 442-489 (ed. A.S. Parkes). Longman and Green Lond.

Oduor-Okelo, D. (1978). A histological study on the ovary of the African cane rat (*Thryonomys swinderianus*). *E. Afr. Wildl. J.*, 16, 257-164.

Oduor-Okelo, D. (1984). An electron microscopic study of the Chorioallantoic placenta and the subplacenta of the cane rat (*Thryonomys swinderianus* Temminck). *Placenta* 5, 433-442.

Oduor-Okelo, D. and S. Gombe. (1982). Placentation in the cane rat (*Thryonomys swinderianus*). *Af. J. Ecol.* 29, 35-59. P.20

Oduor-Okelo, D. and S. Gombe. (1991). Development of the foetal membranes in the cane rat (*Thryonomys swinderianus*): a re-interpretation. *Afr. J. Ecol.* 29, 157-167.

O'Gara, B. W. (1969). Unique aspects of reproduction in the female pronghorn (*Antilocapra americana* Ord). *Am. J. Anat.* 125, 217-232.

O'Shea, G.L., R.G. Kleinfield, and H. A. Morrow (1983). Ultrastructure of decidualization in the pseudopregnant rat. *Am. J. Anat.* 166, 127-298.

Otianga-Owiti, G.E. (1983). The histology and fine structure of the reproductive organs, fetal membranes and placenta of the East

- African springhare ( *Pedetes capensis larvalis* Hollister). M.Sc. Thesis University of Nairobi.
- Otianga-Owiti, G.E., D. Oduor-Okelo, and S. Gombe. (1992). Foetal membranes and placenta of the springhare (*Pedetes capensis larvalis* Hollister). *Afr. J. Ecol.*, 30, 74-86.
- Pierson, O.P. (1949). Reproduction in a South American rodent, the mountain viscacha. *Am. J. Anat.*, 84, 143-173.
- Perrotta, C.A. (1959). Fetal membranes of the Canadian Porcupine, *Erethizion dorsatum*. *Am. J. Anat.*, 104, 35-59.
- Pierce, G.B.J. T. F., Beals, J.S. Ram, and A.C. Midgley (1964). Basement membrane. Epithelial origin and immunologic cross-actions. *Am. J. Path.*, 45, 929-961.
- Pinard, A. (1905). Gestation. *Richets Dictionnaire de physiologie*, 7. Paris (As cited by Marshall & Moss in Marshall's physiology of Reproduction II (1952)).
- Rahm, U. (1969). Zur Fortpflanzungsbiologie von *Tachyoryctes ruandae* (Rodentia, Rhizomyidae). *Rev. Suisse Zool.*, 76(3).
- Rhodin, J. A. G. (1974). Histology. A Text and Atlas. Oxford University Press, Oxford.
- Roberts, C. M. and B.J, Weir (1973). Implantation in the plains viscacha, *Lagostomus maximus*. *J. Reprod. Fert.* 33, 299-307.
- Roberts, F.M. and J.S. Perry (1974). Hystricomorph Embryology. *Symp. Zool. Lond.*, 34, 333-340.
- Rowlands., I.W. (1974). The Biology of Hystricomorph Rodents. *Symp. Zool. Soc. London*, No. 34. Academic Press, New York.

- Salzman, R.C. (1963). Beitrage Zur Fortphanzungs - biologie von Meriones Shawi (Mammalia: Rodentia). *Rev Suisse Zool.* 70, 343-452.
- Scherle, W. (1970). A simple method for volumetry of organs in quantitative stereology. *Mikroskopie*, 26, 57
- Simpson, G.G. (1945). *The Principles of Classification and a classification of mammals*. Bull. Am. Mus. Natural Hist., Vol. 85, 196-213.
- Snell, G.D. (1941). The early embryology of the mouse. In: *Biology of the laboratory mouse*, ed. G.D.Snell: 1-54. Blaskiston, Philadelphia.
- Strauss, F. (1944). Die Bedeutung des placentaren. Blutbeutels in vergleichender Betrachtung. *Rev. Suisse Zool.*, 51, 360-368.  
(As cited by Mossman, 1987).
- Tam, W.H. (1971). The production of hormonal steroids by ovarian tissue of chinchilla (*Chinchilla laniger*). *J. Endocr.*, 50, 267-279.
- Tam, W.H. (1972). Steroid metabolic pathways in the ovary of the chinchilla (*Chinchilla laniger*). *J. Endocr.*, 52, 37-50.
- Teasdale, F. (1978). Functional significance of the zonal morphologic differences in the normal human placenta: a morphometric study. *Am. J. Obstet. Gynec.* 130, 773-781.
- Thomas, O. (1896). On the genera of rodent; an attempt to bring up to date the current arrangement of the order. *Proc. Zool. Soc. Lond.* 1012-1028
- Tibbits, F.D. and H.H. Hillemann. (1959). The development and histology of the chinchilla placentae. *J. Morph.* 105, 317-366.
- Tulberg, T. (1899). Uber das system der Nagethiere. *Nova Acta R. Soc. Scient, Upsal.* 18 Ser 3, 1-514.

- van der Haijdaen, F.L. (1981). Compensation mechanisms for experimental reduction of the functional capacity in the guinea pig placenta. II. Changes in the Trophoblast of the labyrinth. *Acta Anat.*, III, 359-366.
- Venable, T.H. and R.E. Coggeshall. (1965). A simplified lead citrated stain for use in electron microscopy. *J. Cell Biol.* 25, 407.
- Verma, K, (1965). Notes on the biology and anatomy of the Indian tree shrew, *Anathana wroughtoni*. *Mammalia*, 29, 289-330.
- Vladimirsky, F. L. Chen, A. Amsterdam, U. Zu, and H. R. Linder. (1977). Differentiation of decidual cells in culture of rat endometrium. *J. Reprod. Fert.* 49, 61-68.
- Walker, E.P. (1975). Rhizomyidae. In *Mammals of the world*, Vol. II (3rd edn.), pp. 864-868. Johns Hopkins University Press, Baltimore.
- Ward, M.C. (1948). The early development and implantation of the golden hamster (*Cricetus auratus*) and the associated endometrial changes. *Am. J. Anat.* 82, 231-276.
- Weber, M(1928). *Die Saugetiere*. Jena Gustav Fischer Verlag.  
(As cited by Jarvis, 1969b).
- Weibel, E.R. & Knight, B.W. (1964). A morphometric study on the thickness of the pulmonary air-blood barrier. *J. cel. Biol.*, 21, 367-384.
- Weibel, E.R., (1970) Morphometric estimation of pulmonary diffusion capacity. I. Model & Method *Resp. Physiol.* 11, 54
- Weibel, E.R. (1979). *Stereological methods*, vol. I, Practical methods for Biological morphometry. Lond. Academic Press.
- Weir, B.J. (1966). Aspects of reproduction in chinchilla. *J. Reprod. Fert.*, 12, 410-411.

- Weir, B.J. (1971a). The reproductive physiology of the plains viscacha, *Lagostomus maximus*. *J. Reprod. Fert.* 25, 355-363.
- Weir, B.J. (1971b). The reproductive organs of the female plains viscacha, *Lagostomus maximus*. *J. Reprod. Fert.*, 25, 365-373.
- Weir, B.J. (1974). Reproductive characteristics of hystricomorph rodents. In: *The Biology of Hystricomorph Rodents*, ed. I. W. Rowlands and B.J. Weir. *Symp. Zool. Soc. London*, 34, 265-301.
- Weir, B.J. and I.W. Rowlands. (1974). Functional anatomy of the hystricomorph ovary. In: *The biology of Hystricomorph Rodents*, ed. I.W. Rowlands and B.J. Weir. *Symp. Zool. Soc. London*, 34, 303-332.
- Wimsatt, W. A. (1975). Some comparative aspects of implantation. *Biol. Reprod.*, 12, 1-40.
- Wimsatt, W.A. (1958). The allantoic placental barrier in Chiroptera: A new concept of its organization and histochemistry. *Acta. Anat.* 32, 141-186.
- Wimsatt, W.A. and A. Gopalakrishna. (1958). Occurrence of a placental hematoma in the primitive sheath-tailed bats (Emballonuridae) with observations on its structure. *Am. J. Anat.*, 103, 35-67.
- Winge, H. (1924). *Pattedyr-Slaegter*. Vol. II: Rodentia, Carnivora, Primates.  
(As cited by Jarvis, 1969).
- Wislocki, G.B. (1935). The Placentation of the manatee (*Trichechus latirostris*). *Mess. Mus. Comp. Zool.*, Harvard Univ. 54, 159-178  
(As cited by Mossman, 1987).
- Wislocki, G.B. and E.W. Dempsey (1955). Electron microscopy of the placenta of the rat. *Anat. Rec.* 123, 33-63.

- Wislocki, G.B., and H. A. Padykula. (1953). Reichert's membrane and the yolk sac of the rat investigated by histochemical means. *Am. J. Anat.*, 92, 117-151.
- Wynn, R. M. and E.C. Amoroso. (1964). Placentation in the spotted hyena (*Crocuta crocuta* Ecleben), with particular reference to the circulation. *Am. J. Anat.* 115, 327-362.